THE ASTROPHYSICAL JOURNAL SUPPLEMENT SERIES, 108:301–337, 1997 January

A LINE SURVEY OF ORION KL FROM 325 TO 360 GHz

P. SCHILKE,[1] T. D. GROESBECK, G. A. BLAKE, AND T. G. PHILLIPS
Department of Physics, California Institute of Technology, 320-47, Pasadena, CA 91125
Received 1995 July 31; accepted 1996 June 27

ABSTRACT

We present a high-sensitivity spectral line survey of the high-mass star-forming region Orion KL in the 325–360 GHz frequency band. The survey was conducted at the Caltech Submillimeter Observatory on Mauna Kea, Hawaii. The sensitivity achieved is typically 0.1–0.5 K and is limited mostly by the sideband separation method utilized. We find 717 resolvable features consisting of 1004 lines, among which 60 are unidentified. The identified lines are due to 34 species and various isotopomers. Most of the unidentified lines are weak, and many of them most likely due to isotopomers or vibrationally or torsionally excited states of known species with unknown line frequencies, but a few reach the 2–5 K level. No new species have been identified, but we were able to strengthen evidence for the identification of ethanol in Orion and found the first nitrogen sulfide line in this source. The molecule dominating the integrated line emission is SO_2, which emits twice the intensity of CO, followed by SO, which is only slightly stronger than CO. In contrast, the largest number of lines is emitted from heavy organic rotors like $HCOOCH_3$, CH_3CH_2CN, and CH_3OCH_3, but their contribution to the total flux is unimportant. CH_3OH is also very prominent, both in the number of lines and in integrated flux. An interesting detail of this survey is the first detection of vibrationally excited HCN in the $v_2 = 2$ state, 2000 K above ground. Clearly this is a glimpse into the very inner part of the Orion hot core.

Subject headings: ISM: abundances — ISM: individual (Orion Kleinmann-Low) — line: identification — radio lines: ISM

1. INTRODUCTION

Hot cores are the formation sites of massive young stars. They display a multitude of strong molecular lines from many species. The study of these lines provides insights into the physical conditions of massive star-forming regions and into the interactions between the stars and the remnants of their parent clouds. Unbiased spectral line surveys offer the unique opportunity to investigate their complete chemical composition. The most prominent member of this group is the Orion hot core. It is the richest known source of molecular lines, in part due to its proximity ($\approx$500 pc). It has also the advantage that the lines are not as wide as in Sgr B2 and not as confused by absorption features. Hence, it serves as a reference source for molecular hot cores.

There have been a number of Orion line surveys at millimeter wavelengths: Johansson et al. (1984, hereafter J84) surveyed Orion KL and IRC +10216 from 72 to 91 GHz with the 20 m Onsala telescope; Turner (1989) surveyed Orion A and Sgr B2(OH) from 70 to 115 GHz with the NRAO 12 m telescope; Ziurys & McGonagle (1993, hereafter ZM93) surveyed in KL from 150 to 160 GHz with the FCRAO 14 m telescope; Sutton et al. (1985, hereafter S85) surveyed Orion KL from 215 to 247 GHz and Blake et al. (1986, hereafter B86) from 247 to 263 GHz, both with an Owens Valley 10.4 m telescope; Greaves & White (1991) surveyed Orion KL from 257 to 273 GHz with the 15 m James Clerk Maxwell Telescope (JCMT); Jewell et al. (1989) surveyed Orion KL from 330 to 360 GHz with the NRAO 12 m, and Sutton et al. (1994, hereafter S94) surveyed five positions in the Orion KL vicinity from 334 to 343 GHz with the JCMT. The spectral range from 607 to 725 GHz has been surveyed by Schilke et al. (1996a). Serabyn & Weisstein (1995) conducted a low spectral resolution (200 MHz) line survey of Orion, covering the range 190–900 GHz, using a Fourier transform spectrometer at the CSO. That survey complements existing surveys and extends the range to previously unsurveyed frequency ranges, but it is not suited for investigation of weak lines, due to the low spectral resolution.

The surveys find about 2200 lines in the range 70–343 GHz. Most of the lines are identified, but to a lesser degree in the 3 mm and 2 mm band, due to the high sensitivity of these surveys. The interpretation of the line survey data led to column density determinations for the various molecules, using mostly LTE analyses (Blake et al. 1987, hereafter B87; Turner 1991a, hereafter T91; J84, ZM93, and S94 also give column densities).

Our survey covers the range 325–360 GHz, extending only slightly the range of Jewell et al. (1989), but with much higher sensitivity and a single-sideband (SSB) presentation that makes it useful for future reference. It overlaps partly with the S94 survey. The new survey has also been used for estimating the line contribution to the broadband measurements of the continuum (Groesbeck, Phillips, & Blake 1996).

Since the line width, which is fixed in velocity coordinates, rises in frequency coordinates proportionately to the line frequency, blending problems become increasingly severe for high frequencies. Deep integrations (Mauersberger, Henkel, & Wilson 1988) show that the confusion limit (i.e., the point at which the identification of a line is no longer hampered by the system noise, but by the large number of weak lines) is reached easily. Most lines are due to only a few species: SO_2, CH_3OH, $HCOOCH_3$, and CH_3OCH_3. We find many unidentified lines: 60 out of 717 lines in total. However, in accord with prior survey experience, the majority of the unidentified lines are expected to be due to as yet poorly known transitions of the molecules

[1] Present address: Universität Köln, I. Physikalisches Institut, Zülpicher Strasse 77, D-50937 Köln, Germany; schilke@zeus.ph1.uni-koeln.de.

listed above, their isomers, and isotopomers. This, too, is a problem that becomes more severe at higher frequencies, since laboratory data are also increasingly sparse. Hence, apart from enlarging the database, the present line survey serves as a reference source for observations of other regions and as a motivation for laboratory spectroscopists to study the molecules in question.

Since all surveys have been performed with telescopes of similar size, resulting in larger beam sizes at lower frequencies, and since lines observed at lower frequencies tend to be lower in energy and are excited more easily than high-frequency lines, there is a systematic tendency for higher frequency surveys to pick up smaller, hotter, and denser regions than surveys at lower frequencies. While all information is obviously needed to get a consistent picture of the whole region, for the purposes of this paper we compare mostly with surveys of similar (S94) or adjacent frequencies (S85; B86). A more detailed analysis of the physical and chemical implications of our data, in combination with the results from the 607–725 GHz survey, is planned for a future paper.

2. OBSERVATION AND DATA REDUCTION

The observations of Orion KL were made during a total of four periods between 1990 January and 1991 January at the 10.4 m CSO telescope on Mauna Kea, Hawaii. Table 1 gives a summary of the observing dates and the approximate frequency ranges covered during each period. The overlapping nature of the observations resulted in many frequencies being observed at more than one epoch. The telescope had an FWHM beamwidth of 20″ averaged over the range of frequencies in the survey. Absolute pointing was checked frequently by observing planets; we also used the strong emission from SO_2 lines throughout the survey to optimize consistently our pointing on the source itself. Throughout the observations, the pointing was found to be accurate to better than 5″.

We used the facility single-channel, linear polarization SIS receiver (Ellison et al. 1989) for all observations, obtaining receiver temperatures of typically 200–250 K (SSB) and system temperatures ranging from 700 to 2000 K (SSB). Careful tuning of the receiver for each frequency setting produced double-sideband performance with sideband ratios varying by no more than $\approx$20% across the survey. For spectra containing the ^{12}CO(3–2) emission line, or any of its isotopomers, position switching with an offset position of 1800″ in azimuth was used. For other spectra, it was found that position switching in azimuth by 600″ was sufficient.

The atmospheric opacity, monitored at the CSO by a 227 GHz tipping radiometer, was usually less than 0.25, reaching 0.8 on occasion and even higher for the observations near the H_2O transition at 325 GHz. At the edges of the survey, the atmospheric opacity varies rapidly enough across the receiver sidebands that additional corrections to the calibration procedure, described below, are required. For these local oscillator settings, telescope "sky dips" were performed to measure the mean atmospheric opacity, and atmospheric models were used to determine the individual upper and lower sideband opacities. This procedure also enables the hot spillover efficiency to be measured.

TABLE 1

SUMMARY OF OBSERVING DATES AND FREQUENCIES

Dates	Frequencies[a] (GHz)
1990 Jan 12–18	342–349.5
1990 Feb 14–16	349–355
1990 Mar 13–19.....	330–344, 346.5–357.5
1991 Jan 11–18	325–333, 336–337, 338.5–345.5, 350–351, 353–354, 354, 355–360

[a] Approximate frequency ranges covered during each observing session.

The facility back end (an acousto-optical spectrometer) was used, which had a bandwidth of 500 MHz and a nominal channel width of 0.49 MHz. The SSB spectrum is reconstructed with a channel width of 1.0 MHz, which corresponds to the actual resolution of the back end as determined from frequency calibration measurements. The sensitivity over most of the band is sufficient to identify reliably lines with strengths of 0.1–0.5 K. This includes the effects of deconvolution.

The chopper-wheel method (Penzias & Burrus 1973) was used to calibrate the data as the observations were made, and low-order polynomial baselines were removed from the double-sideband (DSB) spectra. This calibration corrects for atmospheric absorption and telescope losses resulting from ambient temperature effects such as spillover and blockage of the beam, but it does not account for effects such as cold spillover, beam coupling to the source, and sideband gain ratios. The cold spillover term at the CSO is quite small; coupling efficiencies are determined from observations of astronomical standards. The main-beam efficiency was found to be $\eta_{\rm MB} = 0.6 \pm 0.1$ from planetary measurements, while the correction for extended sources has been determined to be $\eta_{\rm fss} = 0.76 \pm 0.03$ from observations of the Moon. This factor is essentially independent of elevation for the CSO telescope, at these frequencies, since the telescope is designed to operate up to 900 GHz.

The complicated nature of the Orion KL region, with different molecules and transitions being emitted from several subsources of different sizes, makes it difficult for a single correction to yield accurate line brightness temperatures in all cases. In this paper, we have used the correction for an extended source and quote T_R^*-values. Line intensities for lines emitted from compact sources, for which the main-beam brightness temperature would be more appropriate, have to be multiplied by a factor of 1.3. In many cases, the majority of the spectrum was occupied by emission lines, making it possible to remove only a constant or possibly linear baseline. The removed baselines have been used to evaluate the continuum emission from Orion KL, giving results consistent with published values (170 Jy at 870 μm in a 20″ beam).

The deconvolution method used has been described previously (Groesbeck, Phillips, & Blake 1994) with a detailed analysis of its performance and limitations given by Groesbeck (1994), so that we present only a brief summary here. The method used is a modification of the CLEAN algorithm for deconvolving aperture synthesis maps. The DSB observations are combined first, with no effort made to assign detected lines to either sideband. (Estimates of the relative sideband gains, which can be made by considering the survey as a whole but not for individual local oscillator [LO] settings, are made by hand, based upon the appearance of the strongest lines; apart from scaling based upon these gains, the DSB spectra are added as though the signal

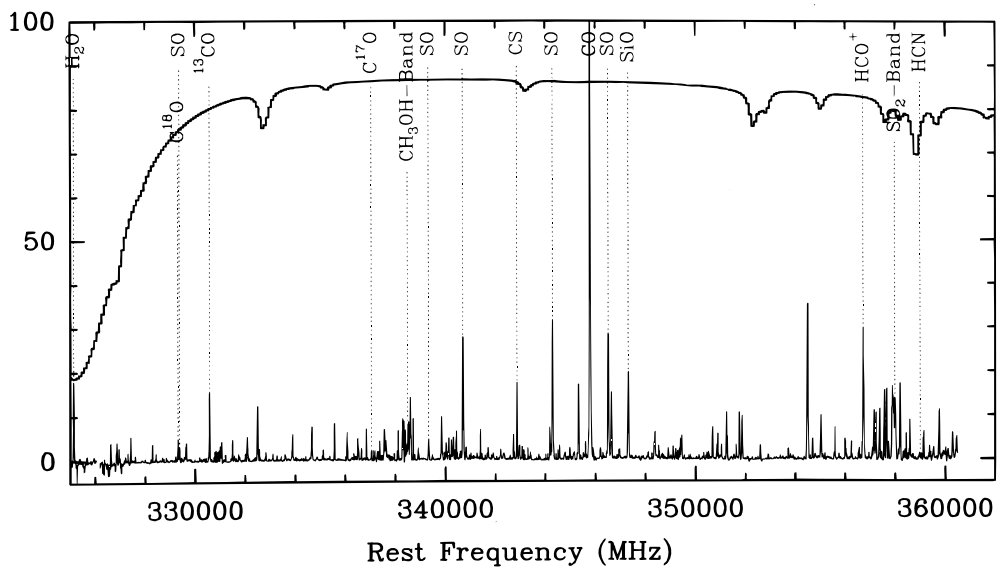

FIG. 1.—Composite spectrum of the whole line survey. The strongest lines are marked, and the atmospheric transmission is plotted on top of the spectrum.

were present in both sidebands.) The resulting spectrum consists of the true underlying spectrum with "ghost" images of the lines superposed at the frequencies corresponding to the image sideband frequencies. An iterative subtraction is then performed to remove the ghosts, found by assuming that the strongest lines represent real detections. A "clean" spectrum is built up that consists of the subtracted amounts at the frequencies of the detected lines, with the final SSB spectrum obtained by adding the residuals to the clean spectrum. Sideband deconvolution using the maximum entropy approach (see S94 for a description), developed for the 650 GHz survey (Schilke et al. 1996), gives a very similar result.

The CLEAN method requires (as does any spectral deconvolution method) a redundant set of observations at different LO settings, so that a given line has images at several frequencies. Following Blake et al. (1986), we made observations centered at intervals of 250 MHz, or half the back-end width. In this way, each frequency could be observed twice in each sideband as we stepped through the range of the survey. We also took several spectra with LO shifts of 10 or 20 MHz, as well as an increased number of settings near the CO (3–2) line, which effectively prevents detection of lines in the opposite sideband because of its strength. These smaller shifts allowed us to estimate better the sideband gains by aiding in the identification of individual lines in the DSB spectra, and they also provided additional redundancy at frequencies near the ends of the survey, at which the coverage included only one sideband. Using correct sideband gain ratios also minimizes the number and strength of ghosts.

Some ghosts are not eliminated completely. One common source of error is the pointing offset between observations of the same spectral feature in different sidebands. For a structured source, like Orion, these offsets will result in nonidentical spectral line shapes for the two positions. Also, the line strength of different lines in one spectrum relative to each other may vary, if different lines peak at different positions. The atmospheric water absorption line at 325 GHz caused the spectrum in this range to be very noisy. Here, as at the upper edge of the observed band, the data were observed with less redundancy. This resulted in imperfect reconstruction and gaps in the spectrum, e.g., between 326 and 327.5 GHz.

3. RESULTS

3.1. *Line Identifications*

The obtained spectrum is displayed in Figures 1 and 2, and a full list of identified lines is shown in Table 2. The line identification was performed on the basis of the JPL catalog (Poynter & Pickett 1985),[2] a list of frequencies compiled by F. J. Lovas (see Lovas 1992 and references therein), the papers by Anderson et al. (1988), Anderson, Herbst, & De Lucia (1992, 1993) on methanol, and the paper of Pearson et al. (1994) on CH_3CH_2CN. The frequencies for the $^{33}SO_2$ and $SO^{18}O$ species were calculated on the basis of measurements in the Cologne submillimeter spectroscopy laboratory and kindly provided by E. Klisch and G. Winnewisser. The observed line intensities and peak temperatures for the various species are displayed in Tables 3–25.

We claim a line as identified if it passes a by-eye inspection of the original double-sideband spectra. For this, a low identification threshold was used, i.e., we only claim a line as real if it shows up as a 3 σ feature in more than one different frequency setting, which also establishes unambiguously the sideband. Some lines of known molecules were also claimed as identified on the basis of an approximate estimated strength for the transition obtained from other transitions already identified. This method, of course, applies only to species with many transitions. Some unidentified lines are questionable in the sense that they may be ghosts. They are indicated in the tables by question marks. The errors of the determined line amplitudes and integrated intensities are dependent on the degree of contamination from the other sideband, which could not be

[2] Now available online on the World Wide Web, ⟨http://spec.jpl.nasa.gov⟩.

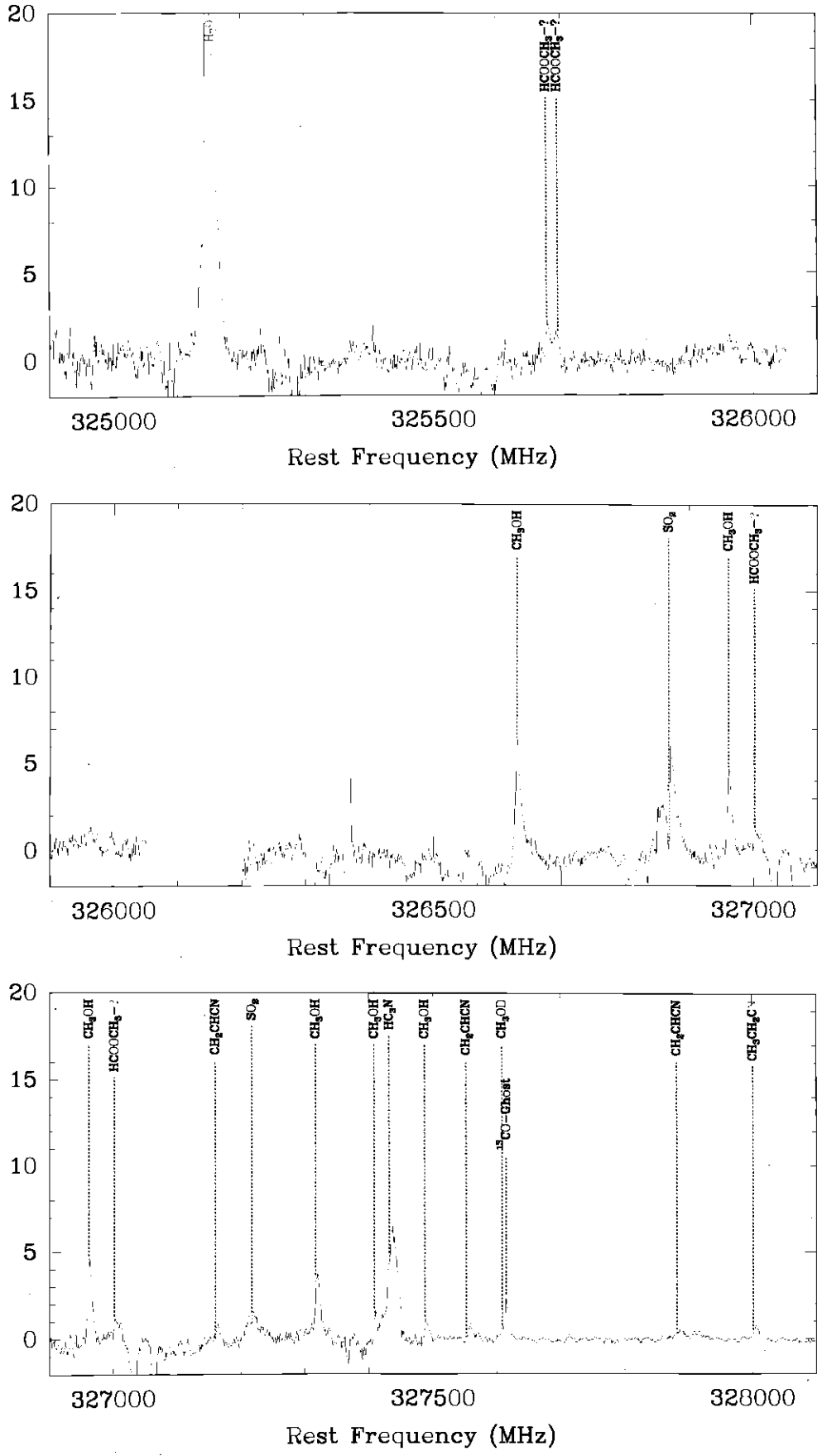

FIG. 2.—Line survey from 325 to 360 GHz. All observed lines are marked. The adopted source velocity is 9 km s^{-1}.

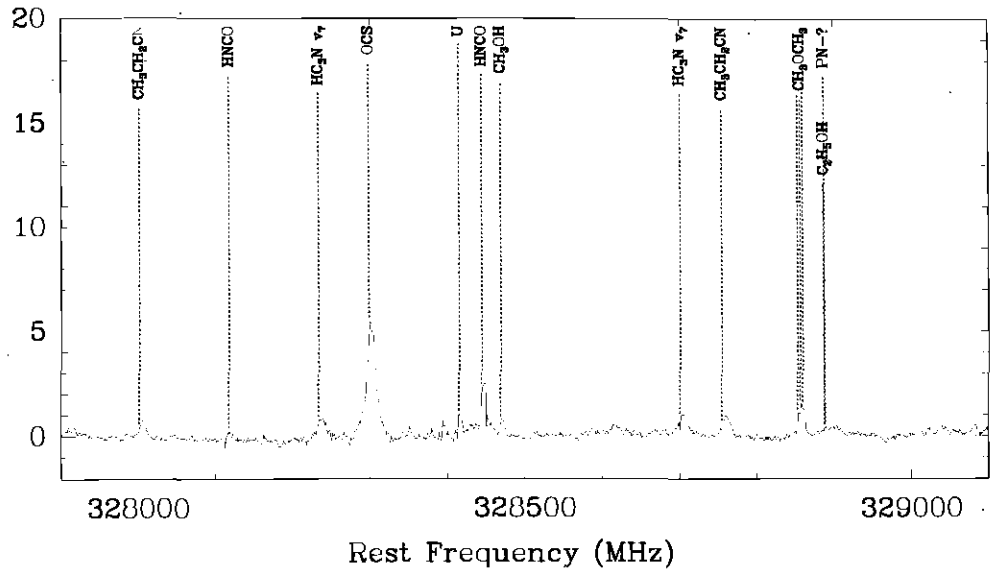

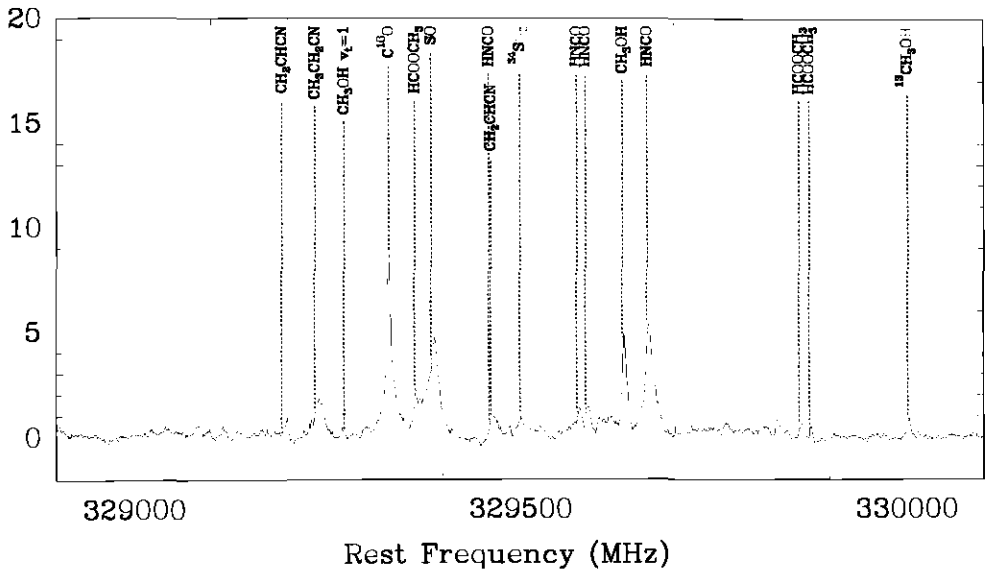

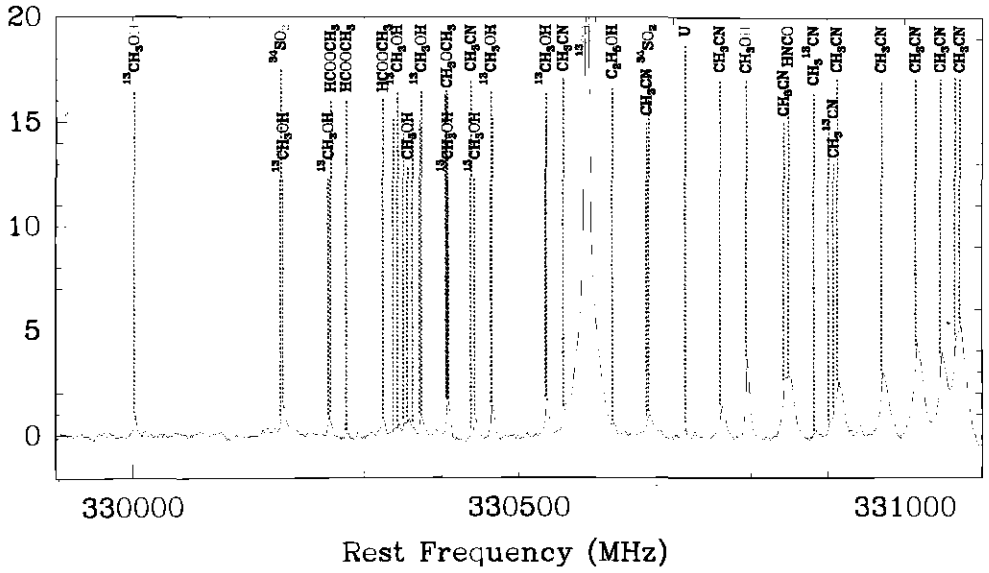

FIG. 2—*Continued*

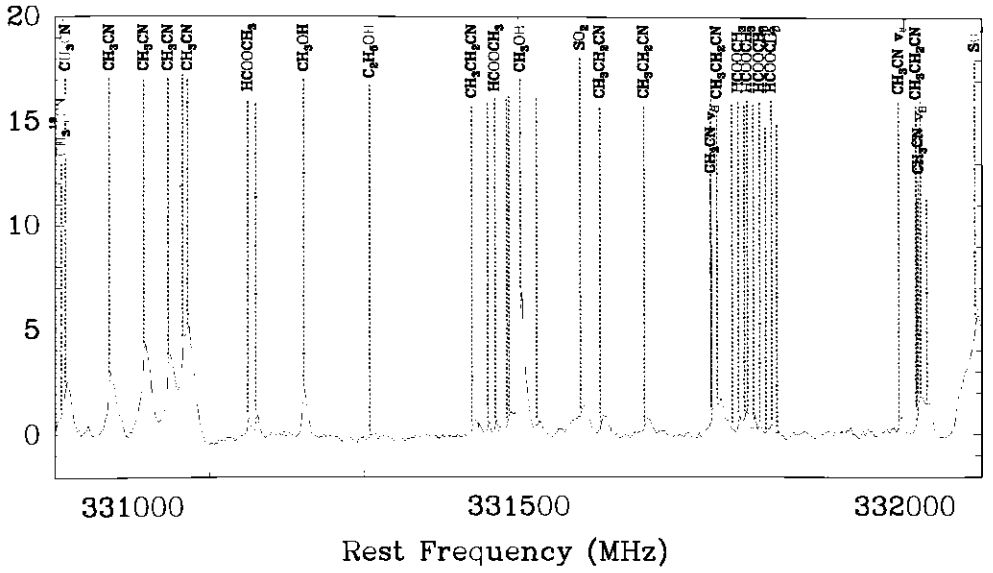

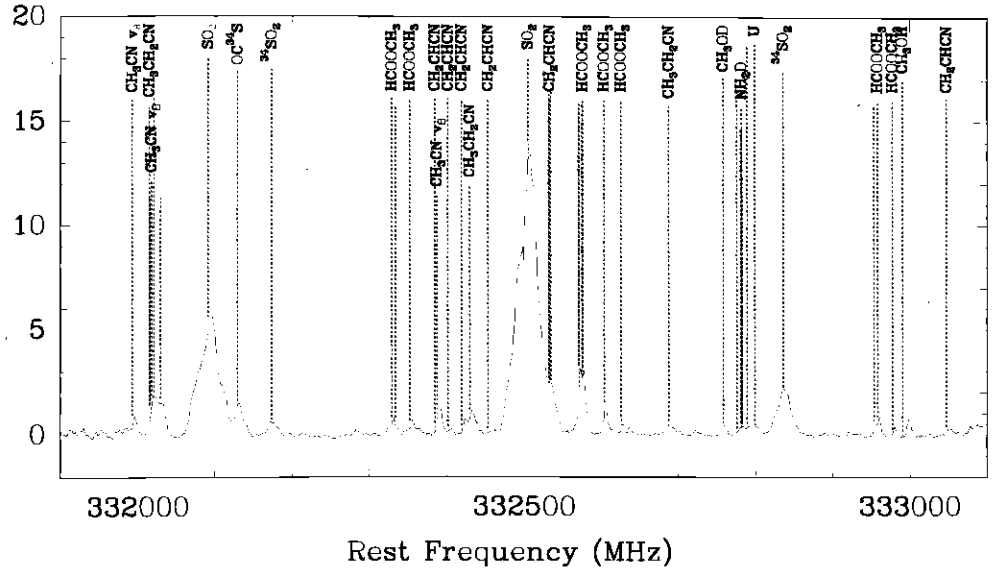

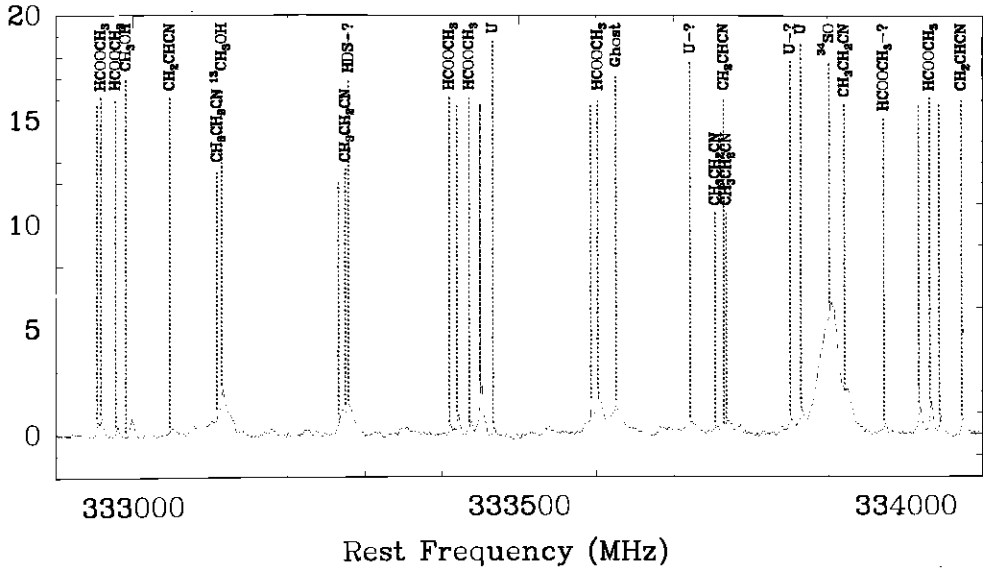

FIG. 2—*Continued*

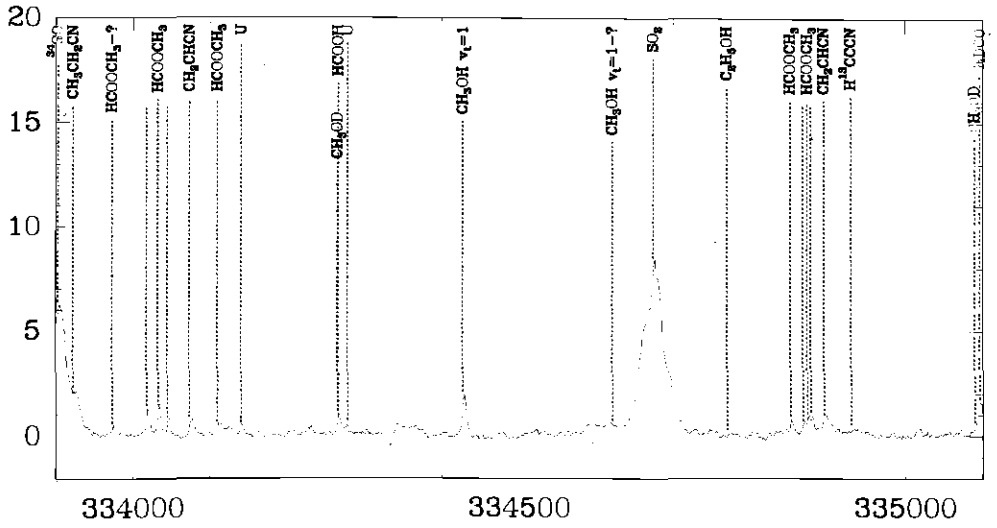

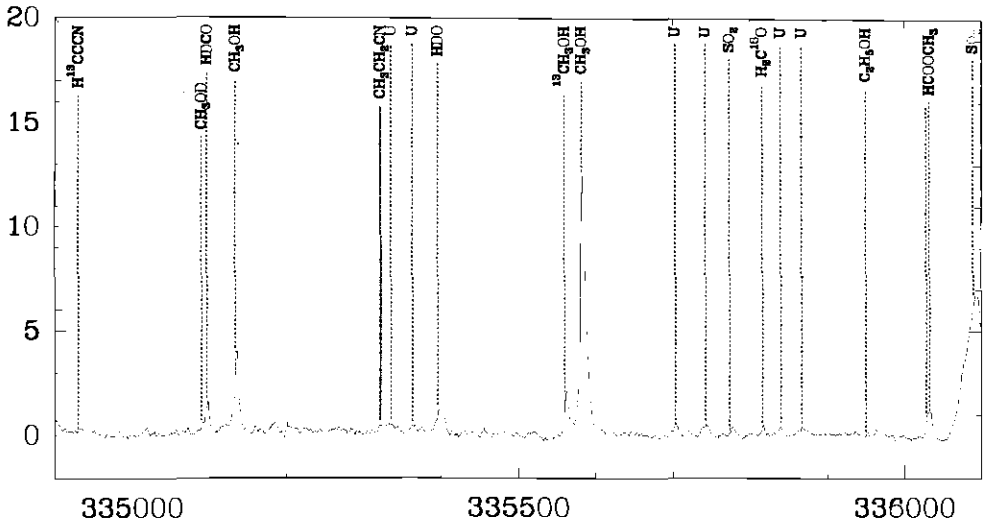

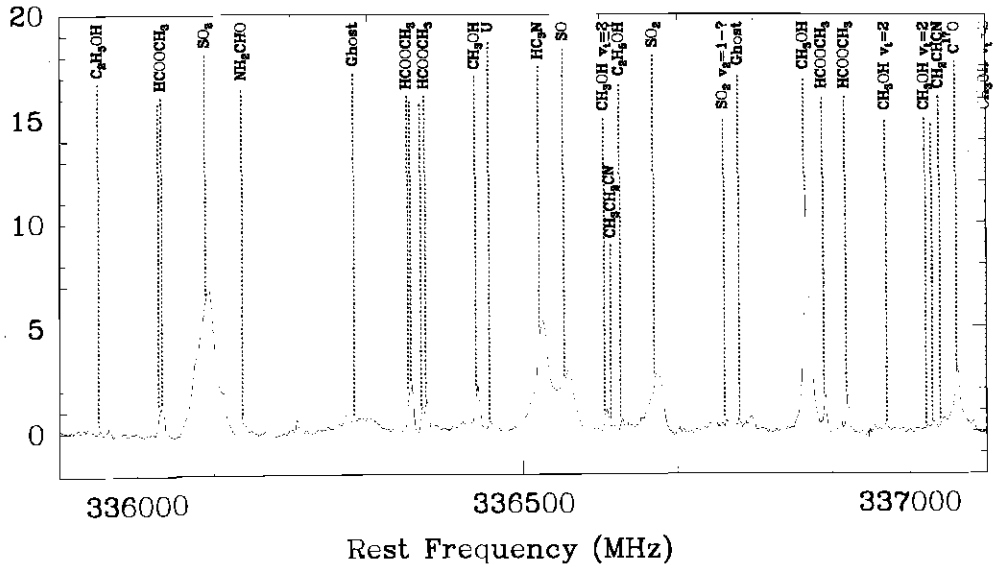

FIG. 2—*Continued*

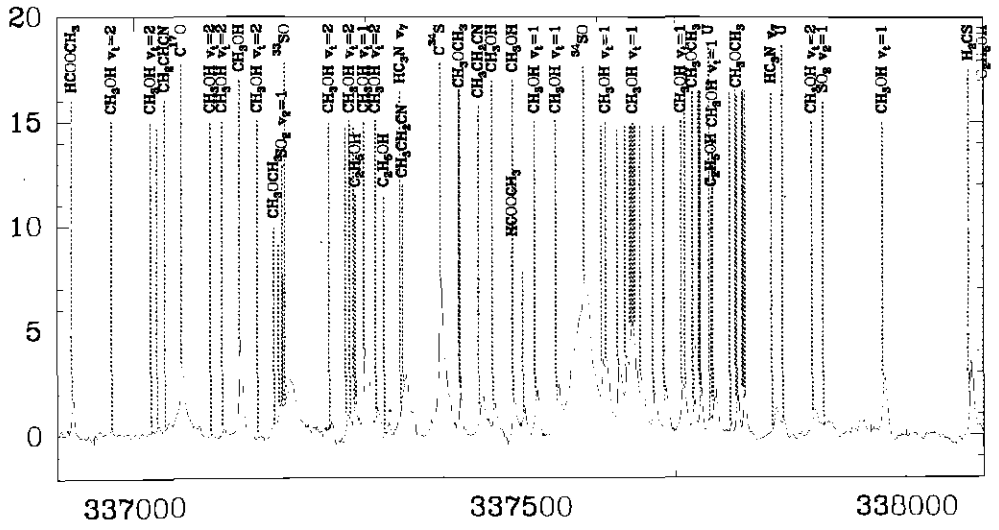

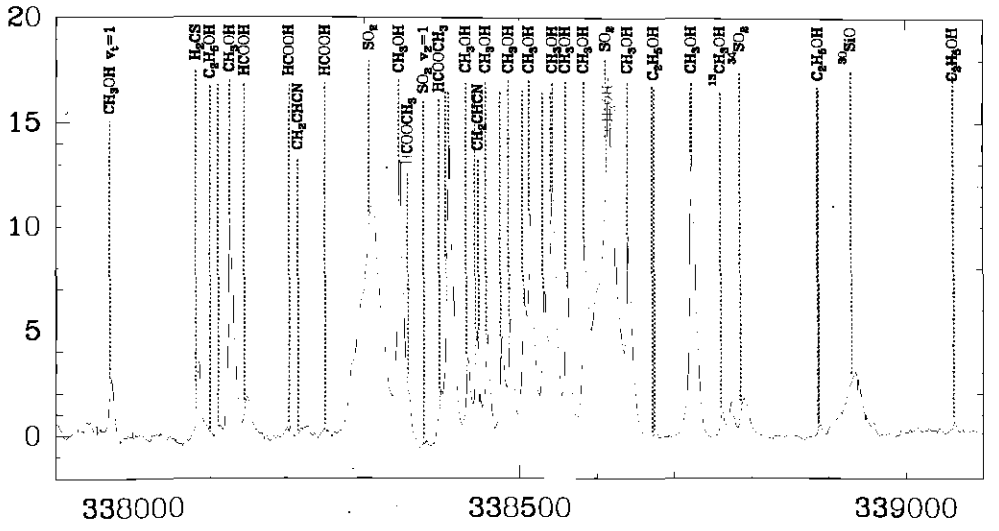

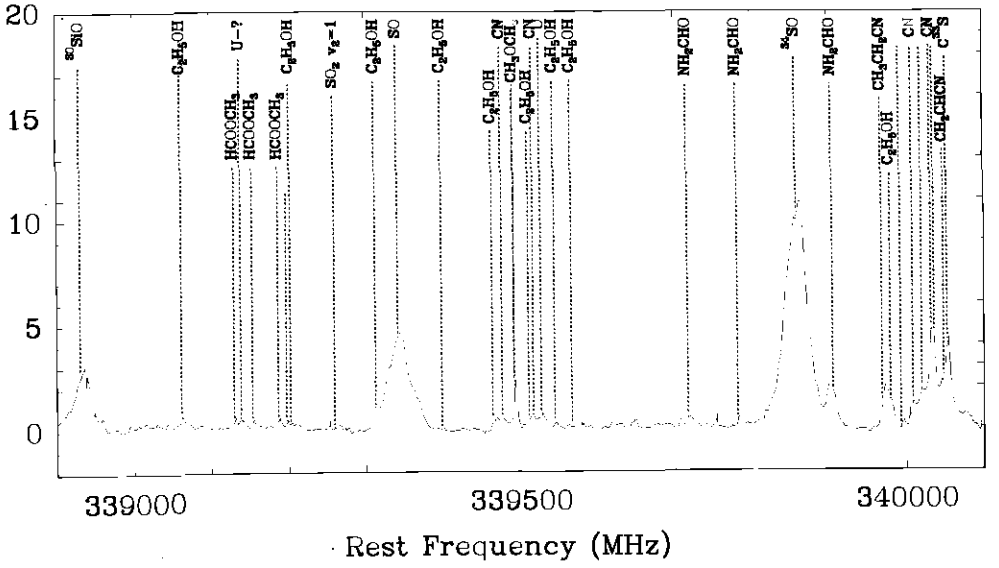

FIG. 2—*Continued*

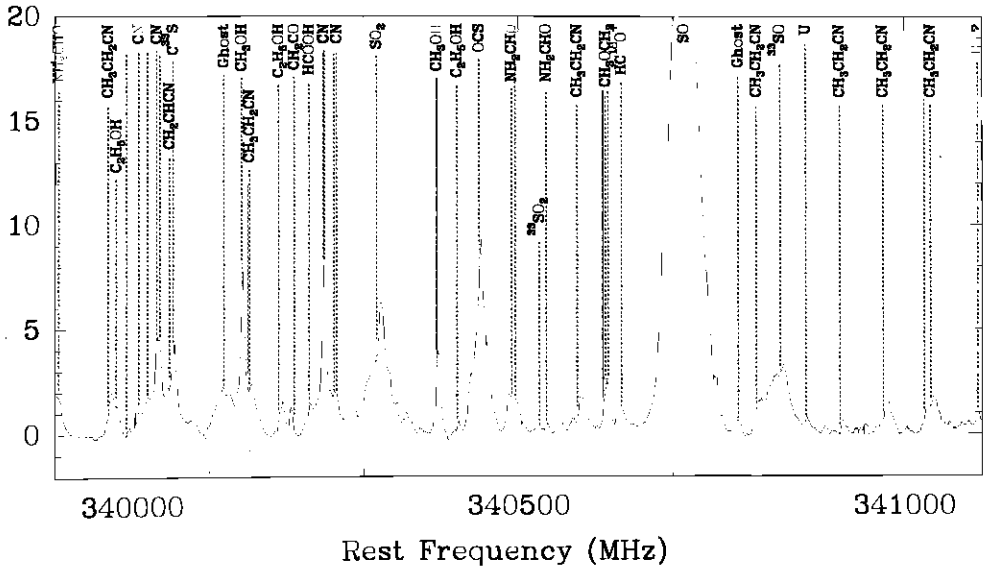

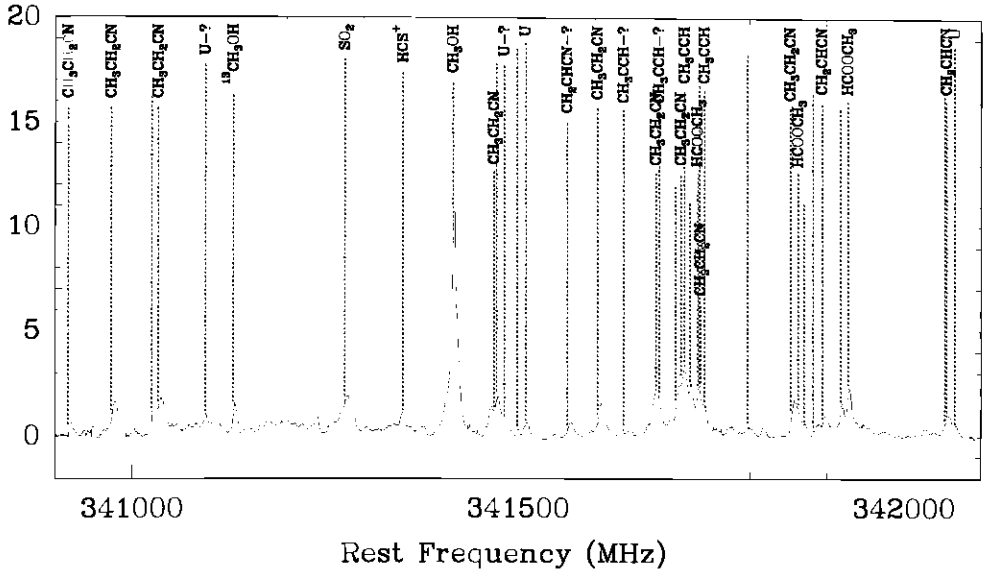

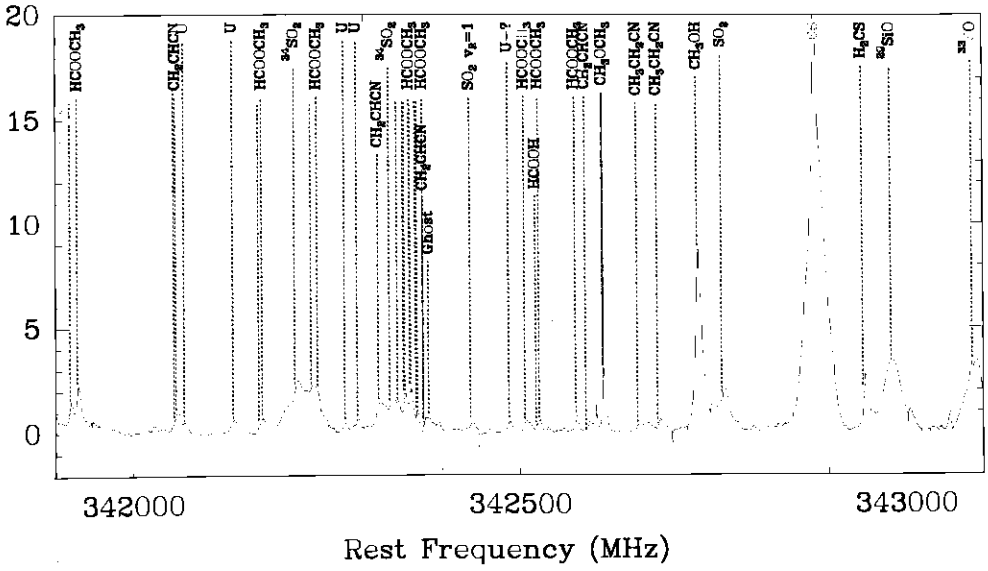

FIG. 2—*Continued*

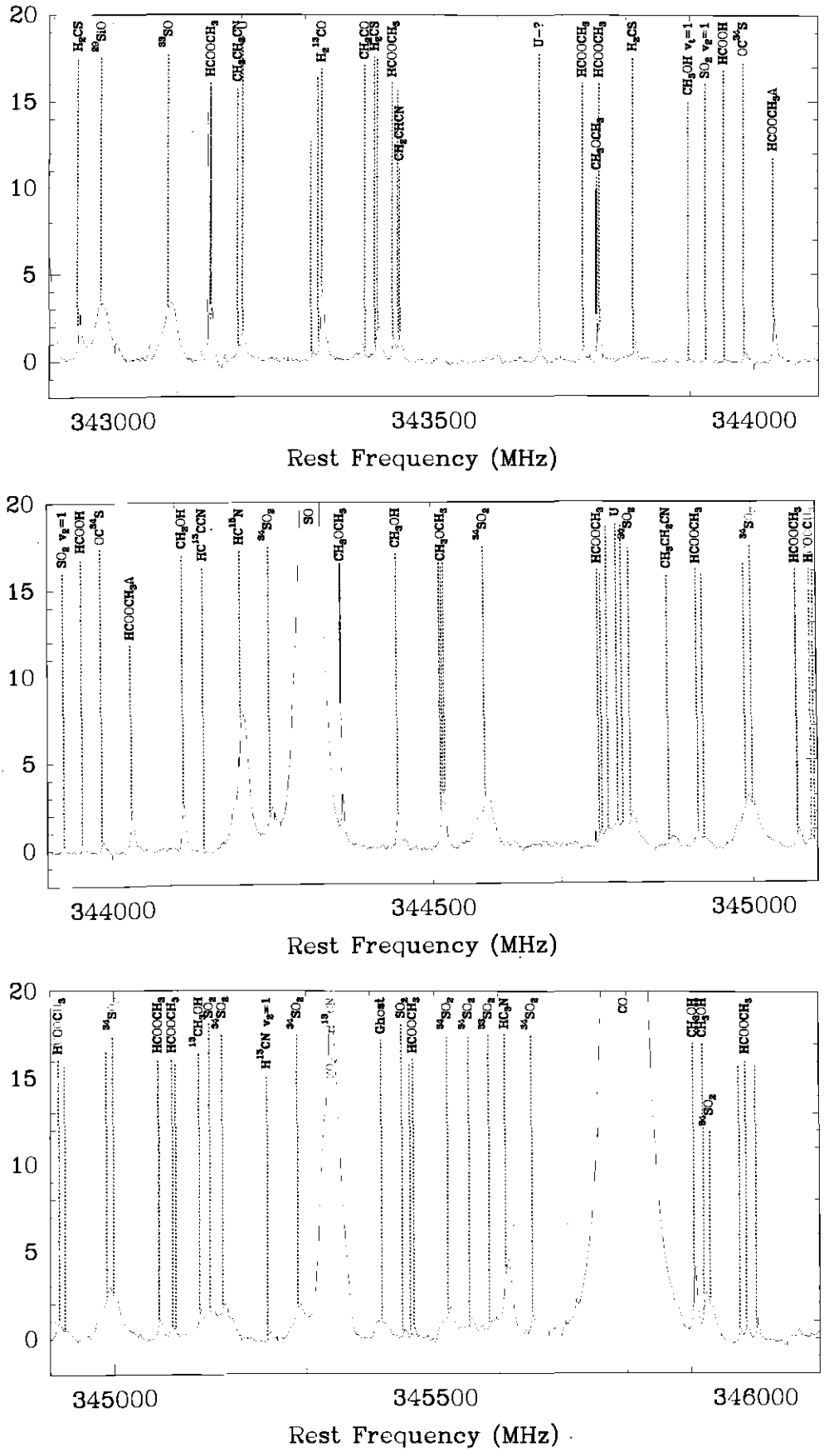

FIG. 2—*Continued*

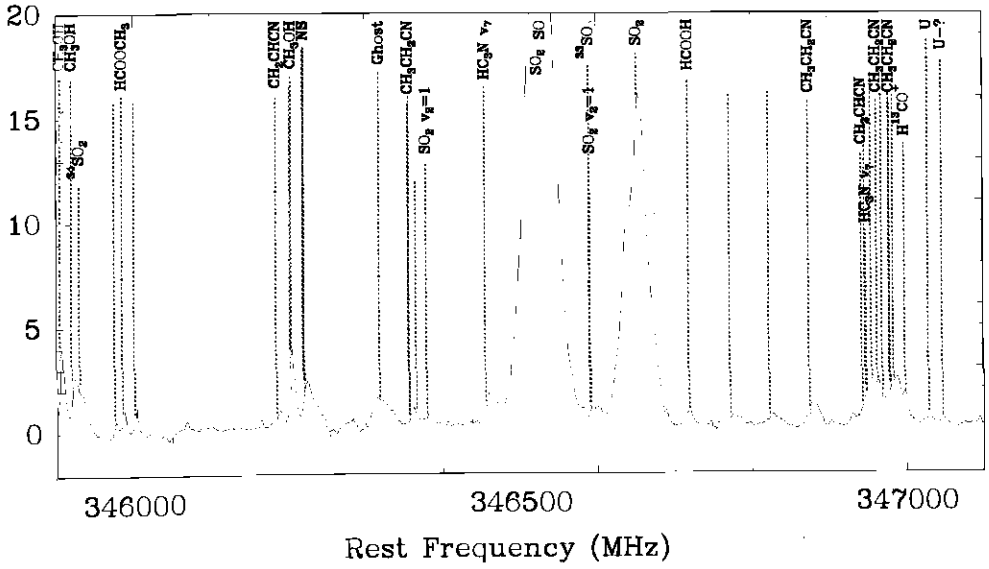

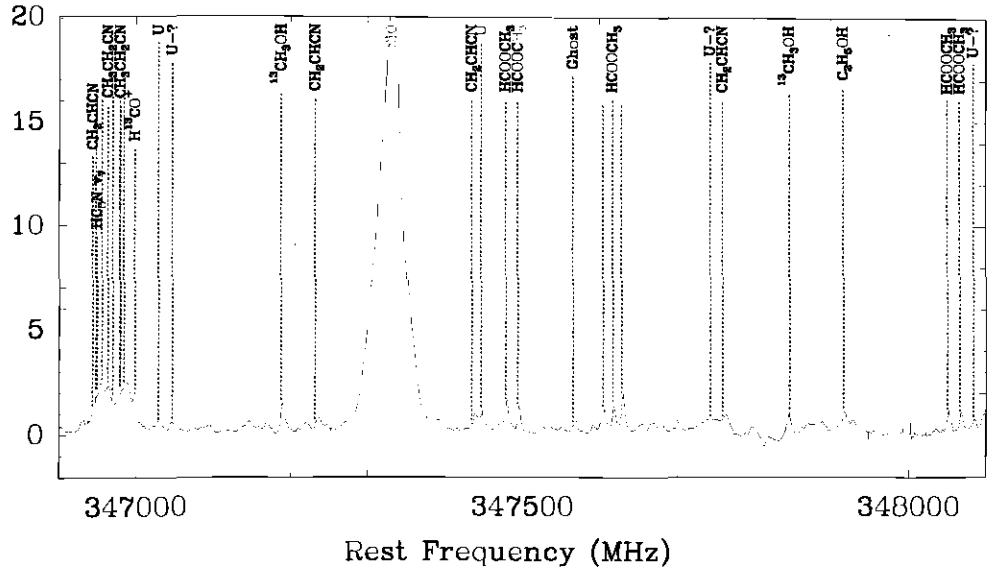

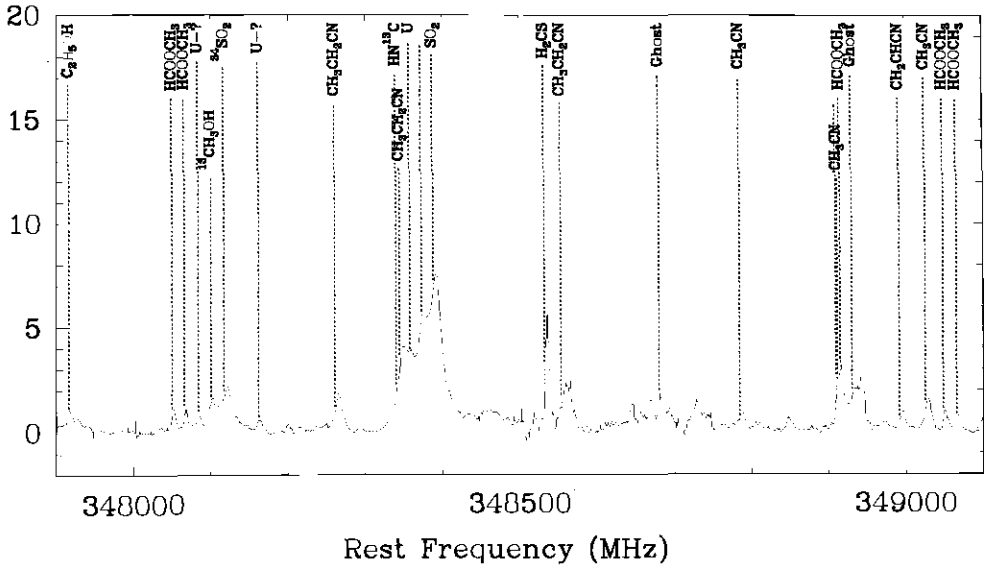

FIG. 2—*Continued*

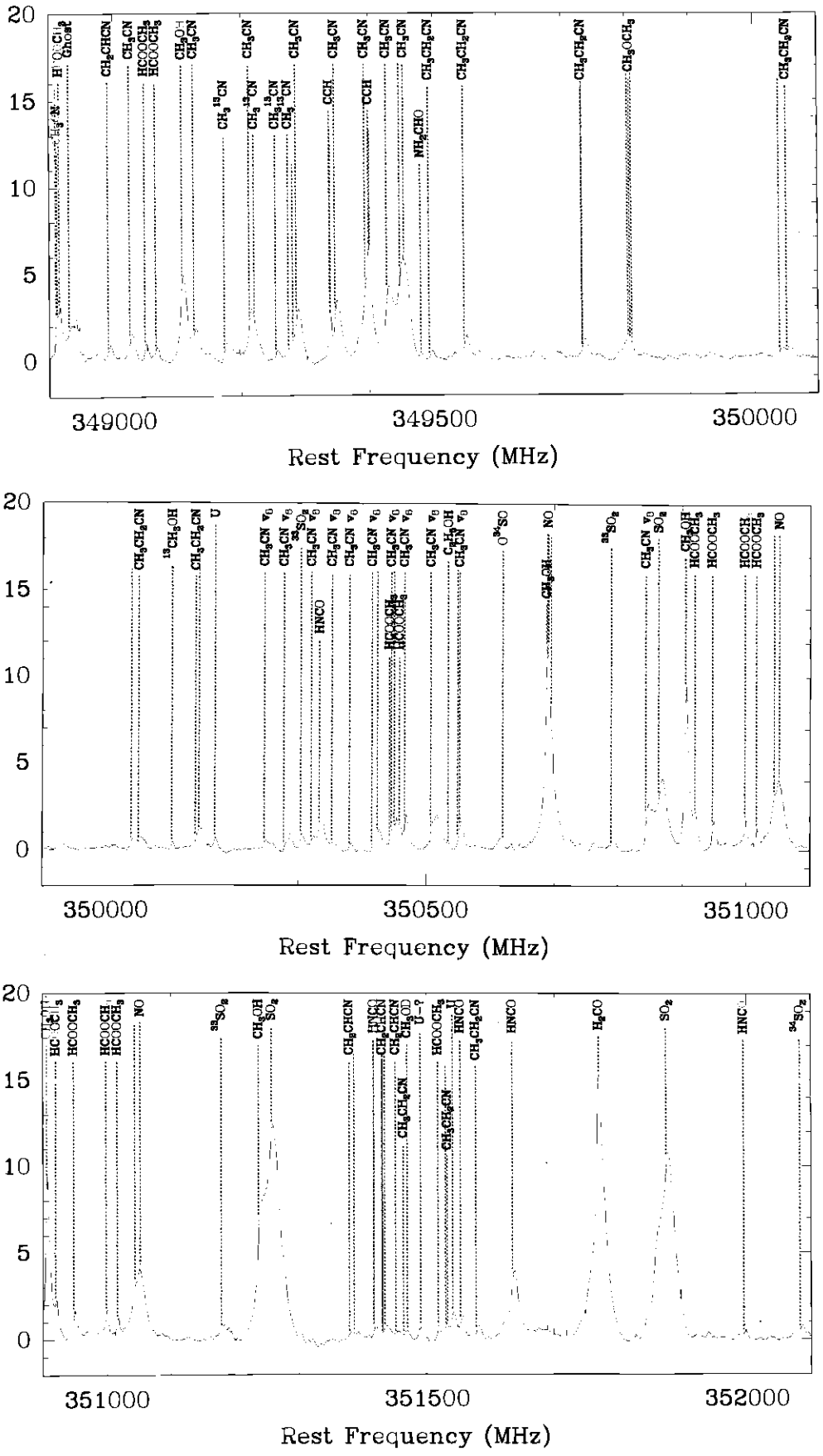

FIG. 2—*Continued*

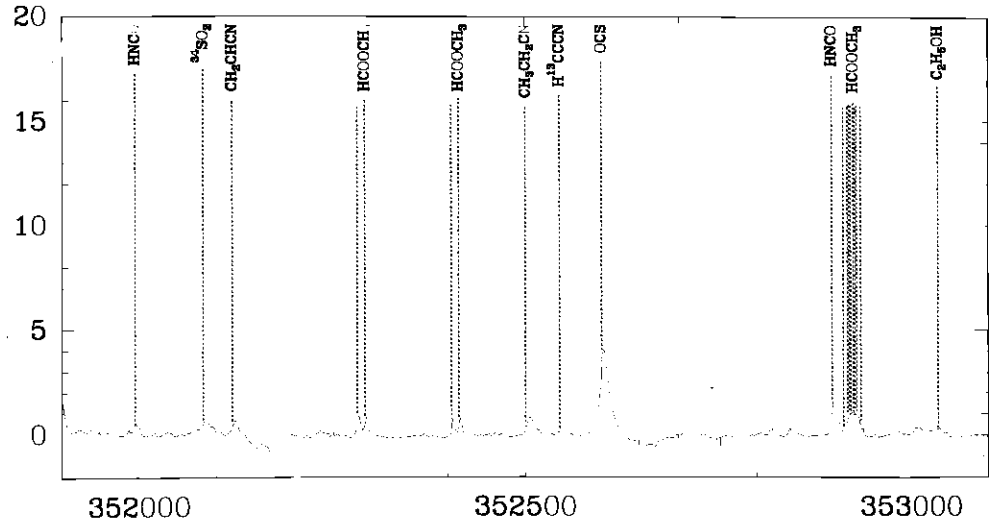

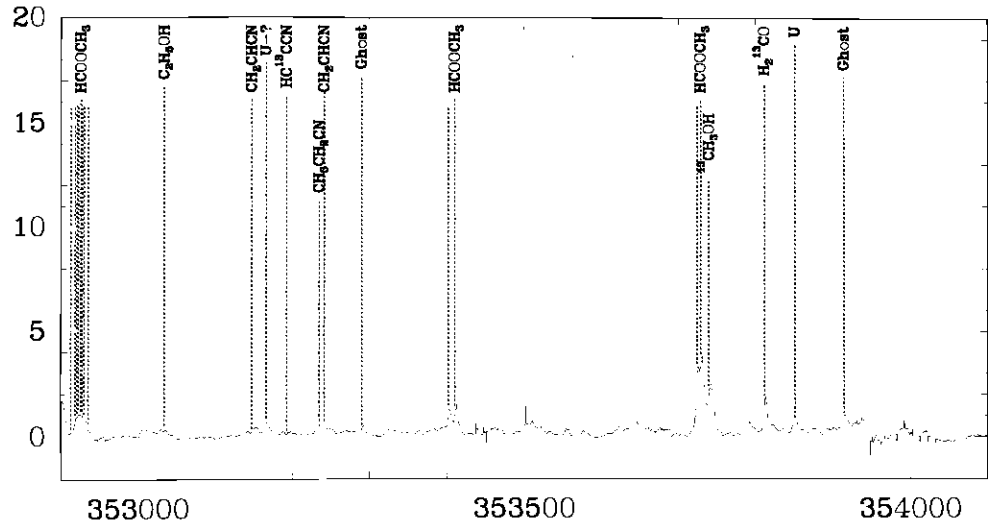

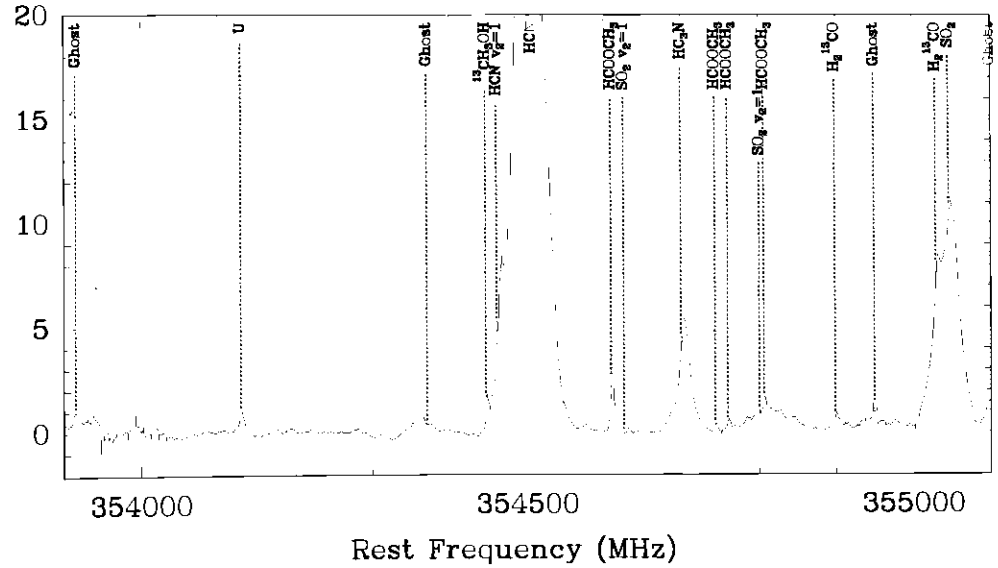

FIG. 2—*Continued*

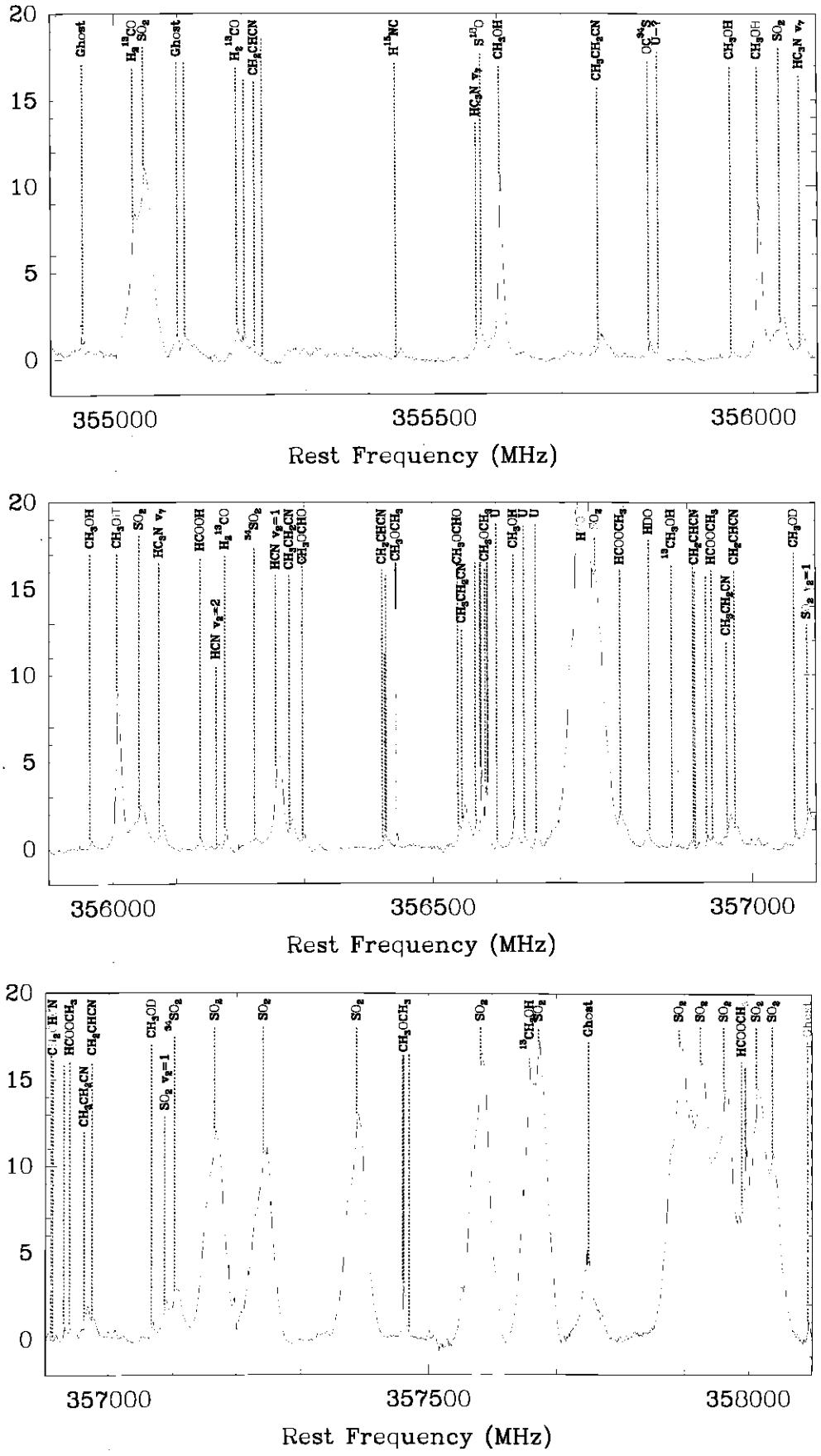

FIG. 2—*Continued*

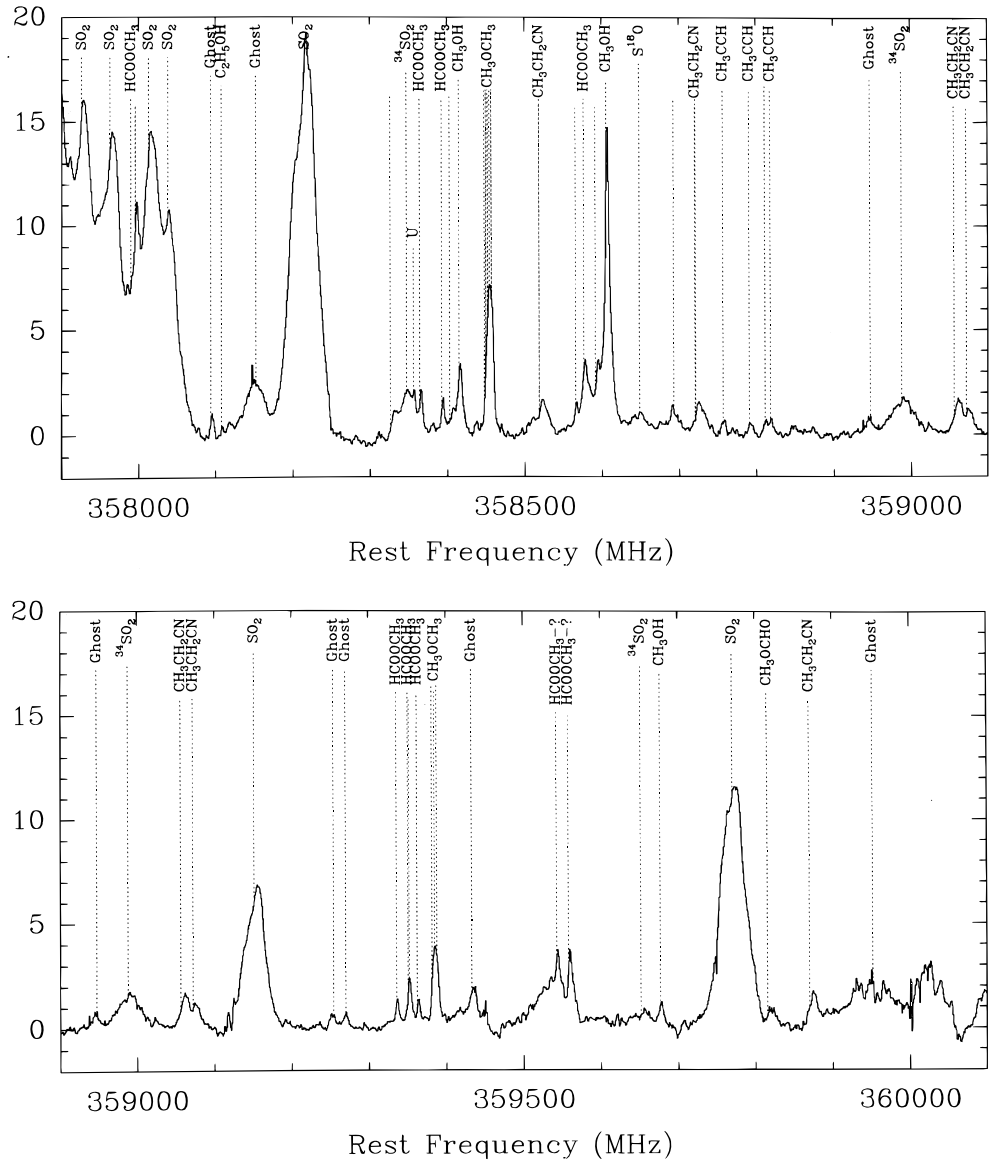

FIG. 2—*Continued*

cleaned completely. In line-crowded regions, the baseline is difficult to determine, and undetected blends with other lines are always possible. Uncertain assignments are referred to in the text.

As noted earlier in J84 and B87, the different species show very distinct line shapes due to different contributions from the four velocity components present in the spectra: extended ($v_{LSR} \approx 9$ km s^{-1}, $\Delta v \approx 4$ km s^{-1}) and compact ridge ($v_{LSR} \approx 8$ km s^{-1}, $\Delta v \approx 3$ km s^{-1}), plateau ($v_{LSR} \approx$ 6–10 km s^{-1}, $\Delta v \gtrsim 20$ km s^{-1}), and hot core ($v_{LSR} \approx 3$–6 km s^{-1}, $\Delta v \approx 5$–10 km s^{-1}). The extended ridge represents the ambient gas in OMC-1; the compact ridge corresponds to a clump about 10″ southwest of the hot core; the plateau is identified with the outflow, and the hot core component itself comes from the dense hot core close to IRc2. Most species show all four components to some degree, but some are dominated by one; the sulphur-bearing molecules and SiO show mostly plateau emission, resulting in broad wings and almost triangular line shapes, while the complex organic molecules, which are emitted mostly from the compact ridge, display much narrower lines at a higher velocity. Some species, like HDO, exist exclusively in the hot core, and the same is true for lines from vibrationally excited transitions. Radicals and ions are most abundant in the quiescent extended ridge.

3.2. *Comments on Individual Species*

3.2.1. *Diatomic Molecules without Electronic Momentum*

CO.—The (3–2) lines of carbon monoxide ^{12}CO, ^{13}CO, C^{18}O, and C^{17}O are clearly detected, the ^{12}CO line being the strongest in the spectrum. The main isotopic line shows broad wings, which are also seen in ^{13}CO and, more weakly, in C^{18}O and C^{17}O. Assuming that C^{18}O is optically thin (as justified by the C^{18}O/C^{17}O line ratio) and that ^{12}C/^{13}C = 60 and ^{16}O/^{18}O = 500, we derive optical depths of 40 for ^{12}CO and 3 for ^{13}CO at the position of the line peak. The technique clearly has its limitations, as demonstrated here by producing inconsistent values: the optical depth of ^{12}CO(3–2) should be 180 based on the ^{13}CO(3–2) optical depth, and not 40. This is partly due to the various components (compact and extended ridge, hot core, and

TABLE 2

ALL OBSERVED FEATURES

ν (MHz)	Molecule
325152.9.....	H_2O
325677.1.....	$HCOOCH_3$-E
325694.4.....	$HCOOCH_3$-A
326630.6.....	CH_3OH-A
326867.5.....	SO_2
326961.2.....	CH_3OH-E
327001.9.....	$HCOOCH_3$-E
327160.1.....	CH_2CHCN
327216.8.....	SO_2
327317.2.....	CH_3OH-A
327408.2.....	CH_3OH-A
327431.4.....	HC_3N
327487.2.....	CH_3OH-E
327552.4.....	CH_2CHCN
327608.7.....	CH_3OD-A
327614.9.....	^{13}CO-Ghost
327882.0.....	CH_2CHCN
328001.1.....	CH_3CH_2CN
328117.5.....	HNCO
328232.8.....	$HC_3N(v_7)$
328298.1.....	OCS
328415.0.....	U
328444.3.....	HNCO
328468.8.....	CH_3OH-A
328700.6.....	$HC_3N(v_7)$
328754.8.....	CH_3CH_2CN
328853.3.....	CH_3OCH_3
328853.4.....	CH_3OCH_3
328856.7.....	CH_3OCH_3
328860.0.....	CH_3OCH_3
328887.1.....	C_2H_5OH
328887.9.....	PN?
329191.7.....	CH_2CHCN
329234.8.....	CH_3CH_2CN
329272.6.....	CH_3OH-$E(v_t = 1)$
329330.6.....	$C^{18}O$
329364.2.....	$HCOOCH_3$-E
329385.5.....	SO
329459.9.....	HNCO
329462.3.....	CH_2CHCN
329499.7.....	$^{34}SO_2$
329573.5.....	HNCO
329585.1.....	HNCO
329632.9.....	CH_3OH-A
329664.5.....	HNCO
329861.6.....	$HCOOCH_3$-E
329874.9.....	$HCOOCH_3$-A
330001.8.....	$^{13}CH_3OH$-E
330191.2.....	$^{34}SO_2$
330194.0.....	$^{13}CH_3OH$-E
330252.8.....	$^{13}CH_3OH$-A
330256.0.....	$HCOOCH_3$-E
330276.4.....	$HCOOCH_3$-E
330323.9.....	$HCOOCH_3$-A
330336.9.....	$^{13}CH_3OH$-E
330342.5.....	$^{13}CH_3OH$-A
330350.0.....	$^{13}CH_3OH$-A
330355.3.....	CH_3OH-A
330362.0.....	$^{13}CH_3OH$-E
330371.3.....	$^{13}CH_3OH$-A
330373.4.....	$^{13}CH_3OH$-A
330405.4.....	CH_3OCH_3
330406.5.....	CH_3OCH_3
330407.6.....	CH_3OCH_3
330408.4.....	$^{13}CH_3OH$-A
330437.4.....	CH_3CN
330442.4.....	$^{13}CH_3OH$-E
330463.6.....	$^{13}CH_3OH$-A
330464.9.....	$^{13}CH_3OH$-A
330535.2.....	$^{13}CH_3OH$-E
330535.9.....	$^{13}CH_3OH$-E

TABLE 2—*Continued*

ν (MHz)	Molecule
330557.6.....	CH_3CN
330588.1.....	^{13}CO
330621.1.....	C_2H_5OH
330665.2.....	CH_3CN
330667.6.....	$^{34}SO_2$
330715.0.....	U
330760.2.....	CH_3CN
330793.9.....	CH_3OH-E
330842.6.....	CH_3CN
330848.8.....	HNCO
330881.9.....	$CH_3{}^{13}CN$
330901.0.....	$CH_3{}^{13}CN$
330907.3.....	$CH_3{}^{13}CN$
330912.5.....	CH_3CN
330969.6.....	CH_3CN
331014.1.....	CH_3CN
331045.9.....	CH_3CN
331065.0.....	CH_3CN
331071.3.....	CH_3CN
331149.3.....	$HCOOCH_3$-E
331159.6.....	$HCOOCH_3$-A
331221.6.....	CH_3OH-E
331307.1.....	C_2H_5OH
331439.5.....	CH_3CH_2CN
331460.0.....	$HCOOCH_3$-E
331469.5.....	$HCOOCH_3$-A
331484.5.....	CH_3CH_2CN
331487.3.....	CH_3CH_2CN
331502.4.....	CH_3OH-A
331523.3.....	CH_3CH_2CN
331580.2.....	SO_2
331605.6.....	CH_3CH_2CN
331662.3.....	CH_3CH_2CN
331748.5.....	$CH_3CN(v_8)$
331748.5.....	CH_3CH_2CN
331756.4.....	CH_3CH_2CN
331775.9.....	$HCOOCH_3$-A
331784.2.....	$HCOOCH_3$-E
331792.1.....	$HCOOCH_3$-A
331795.9.....	$HCOOCH_3$-E
331803.8.....	$HCOOCH_3$-A
331812.2.....	$HCOOCH_3$-E
331819.9.....	$HCOOCH_3$-A
331827.7.....	$HCOOCH_3$-E
331834.5.....	$HCOOCH_3$-E
331992.3.....	$CH_3CN(v_8)$
332014.7.....	CH_3CH_2CN
332015.8.....	$CH_3CN(v_8)$
332017.8.....	$CH_3CN(v_8)$
332020.6.....	CH_3CH_2CN
332028.8.....	$CH_3CN(v_8)$
332091.4.....	SO_2
332129.7.....	$OC^{34}S$
332173.7.....	$^{34}SO_2$
332329.2.....	$HCOOCH_3$-A
332334.0.....	$HCOOCH_3$-E
332352.6.....	$HCOOCH_3$-E
332385.0.....	CH_2CHCN
332387.8.....	$CH_3CN(v_8)$
332401.7.....	CH_2CHCN
332419.0.....	CH_2CHCN
332429.7.....	CH_3CH_2CN
332453.6.....	CH_2CHCN
332505.2.....	SO_2
332532.3.....	CH_2CHCN
332533.2.....	CH_2CHCN
332534.8.....	CH_2CHCN
332570.9.....	$HCOOCH_3$-E
332571.2.....	$HCOOCH_3$-E
332571.4.....	$HCOOCH_3$-E
332571.7.....	$HCOOCH_3$-E

TABLE 2—*Continued*

ν (MHz)	Molecule
332575.6.....	$HCOOCH_3$-*A*
332575.9.....	$HCOOCH_3$-*A*
332576.2.....	$HCOOCH_3$-*A*
332576.4.....	$HCOOCH_3$-*A*
332604.4.....	$HCOOCH_3$-*A*
332626.0.....	$HCOOCH_3$-*E*
332687.7.....	CH_3CH_2CN
332758.3.....	CH_3OD-*E*
332775.7.....	CH_2CHCN
332780.9.....	NH_2D
332781.8.....	NH_2D
332782.4.....	NH_2D
332789.0.....	*U*
332799.0.....	*U*
332836.3.....	$^{34}SO_2$
332953.3.....	$HCOOCH_3$-*E*
332958.2.....	$HCOOCH_3$-*A*
332977.4.....	$HCOOCH_3$-*E*
332990.6.....	CH_3OH-*E*
333047.3.....	CH_2CHCN
333108.8.....	CH_3CH_2CN
333114.8.....	$^{13}CH_3OH$-*A*
333265.9.....	CH_3CH_2CN
333274.7.....	CH_3CH_2CN
333278.5.....	HDS
333409.4.....	$HCOOCH_3$-*E*
333419.2.....	$HCOOCH_3$-*A*
333435.2.....	$HCOOCH_3$-*E*
333449.3.....	$HCOOCH_3$-*A*
333449.4.....	$HCOOCH_3$-*E*
333466.0.....	*U*
333593.2.....	$HCOOCH_3$-*E*
333602.0.....	$HCOOCH_3$-*A*
333625.5.....	Ghost
333721.0.....	*U*
333753.4.....	CH_3CH_2CN
333764.6.....	CH_2CHCN
333767.7.....	CH_3CH_2CN
333851.0.....	*U*?
333865.0.....	*U*
333902.1.....	^{34}SO
333921.6.....	CH_3CH_2CN
333972.4.....	$HCOOCH_3$-*E*
334017.2.....	$HCOOCH_3$-*E*
334031.5.....	$HCOOCH_3$-*A*
334031.8.....	$HCOOCH_3$-*A*
334044.0.....	$HCOOCH_3$-*E*
334073.1.....	CH_2CHCN
334109.2.....	$HCOOCH_3$-*A*
334140.0.....	*U*
334264.9.....	CH_3OD-*E*
334265.8.....	HCOOH
334278.0.....	*U*
334426.6.....	CH_3OH-$E(v_t = 1)$
334620.7.....	CH_3OH-$E(v_t = 1)$
334673.3.....	SO_2
334769.0.....	C_2H_5OH
334851.0.....	$HCOOCH_3$-*E*
334867.0.....	$HCOOCH_3$-*A*
334872.8.....	$HCOOCH_3$-*A*
334877.5.....	$HCOOCH_3$-*E*
334894.5.....	CH_2CHCN
334929.5.....	$H^{13}CCCN$
335089.7.....	CH_3OD-*A*
335096.5.....	HDCO
335133.5.....	CH_3OH-*A*
335321.4.....	CH_3CH_2CN
335321.4.....	CH_3CH_2CN
335335.0.....	*U*
335363.0.....	*U*
335395.5.....	HDO

TABLE 2—*Continued*

ν (MHz)	Molecule
335559.9.....	$^{13}CH_3OH$-*A*
335582.0.....	CH_3OH-*A*
335703.0.....	*U*
335742.0.....	*U*
335773.2.....	SO_2
335816.0.....	$H_2C^{18}O$
335840.0.....	*U*
335867.0.....	*U*
335949.7.....	C_2H_5OH
336028.1.....	$HCOOCH_3$-*A*
336032.4.....	$HCOOCH_3$-*E*
336089.2.....	SO_2
336136.9.....	NH_2CHO
336281.8.....	Ghost
336351.5.....	$HCOOCH_3$-*E*
336354.9.....	$HCOOCH_3$-*E*
336368.2.....	$HCOOCH_3$-*A*
336373.8.....	$HCOOCH_3$-*A*
336438.3.....	CH_3OH-*A*
336456.0.....	*U*
336521.0.....	HC_3N
336553.3.....	SO
336605.9.....	CH_3OH-$A(v_t = 2)$
336613.9.....	CH_3CH_2CN
336626.4.....	C_2H_5OH
336669.6.....	SO_2
336760.7.....	$SO_2(v_2 = 1)$
336780.0.....	Ghost
336865.1.....	CH_3OH-*A*
336889.2.....	$HCOOCH_3$-*E*
336918.1.....	$HCOOCH_3$-*A*
336970.4.....	CH_3OH-$A(v_t = 2)$
337021.4.....	CH_3OH-$E(v_t = 2)$
337029.6.....	CH_3OH-$A(v_t = 2)$
337039.7.....	CH_2CHCN
337061.1.....	$C^{17}O$
337098.6.....	CH_3OH-$A(v_t = 2)$
337113.9.....	CH_3OH-$E(v_t = 2)$
337135.9.....	CH_3OH-*E*
337159.2.....	CH_3OH-$E(v_t = 2)$
337180.8.....	CH_3OCH_3
337186.7.....	CH_3OCH_3
337191.5.....	$SO_2(v_2 = 1)$
337192.6.....	CH_3OCH_3
337195.0.....	^{33}SO
337252.2.....	CH_3OH-$A(v_t = 2)$
337273.5.....	CH_3OH-$A(v_t = 2)$
337279.1.....	CH_3OH-$E(v_t = 2)$
337284.2.....	CH_3OH-$A(v_t = 2)$
337286.5.....	C_2H_5OH
337297.4.....	CH_3OH-$A(v_t = 1)$
337312.3.....	CH_3OH-$A(v_t = 2)$
337323.1.....	C_2H_5OH
337344.3.....	$HC_3N(v_7)$
337347.6.....	CH_3CH_2CN
337396.7.....	$C^{34}S$
337420.9.....	CH_3OCH_3
337421.3.....	CH_3OCH_3
337421.8.....	CH_3OCH_3
337445.9.....	CH_3CH_2CN
337463.7.....	CH_3OH-*A*
337489.7.....	$HCOOCH_3$-*E*
337490.5.....	CH_3OH-*E*
337503.4.....	$HCOOCH_3$-*A*
337519.1.....	CH_3OH-$E(v_t = 1)$
337546.1.....	CH_3OH-$A(v_t = 1)$
337582.2.....	^{34}SO
337605.2.....	CH_3OH-$E(v_t = 1)$
337610.6.....	CH_3OH-$E(v_t = 1)$
337625.7.....	CH_3OH-$A(v_t = 1)$
337635.7.....	CH_3OH-$A(v_t = 1)$

TABLE 2—*Continued*

ν (MHz)	Molecule
337642.4.....	CH_3OH-$E(v_t = 1)$
337643.9.....	CH_3OH-$E(v_t = 1)$
337646.0.....	CH_3OH-$E(v_t = 1)$
337648.2.....	CH_3OH-$E(v_t = 1)$
337655.2.....	CH_3OH-$A(v_t = 1)$
337671.2.....	CH_3OH-$E(v_t = 1)$
337685.3.....	CH_3OH-$E(v_t = 1)$
337685.8.....	CH_3OH-$A(v_t = 1)$
337707.6.....	CH_3OH-$E(v_t = 1)$
337712.4.....	CH_3OCH_3
337722.3.....	CH_3OCH_3
337723.0.....	CH_3OCH_3
337730.7.....	CH_3OCH_3
337731.9.....	CH_3OCH_3
337732.2.....	CH_3OCH_3
337744.0.....	*U*
337747.0.....	C_2H_5OH
337748.7.....	CH_3OH-$A(v_t = 1)$
337770.6.....	CH_3OCH_3
337778.0.....	CH_3OCH_3
337779.5.....	CH_3OCH_3
337787.2.....	CH_3OCH_3
337787.9.....	CH_3OCH_3
337790.1.....	CH_3OCH_3
337824.9.....	$HC_3N(v_7)$
337839.0.....	*U*
337877.5.....	CH_3OH-$A(v_t = 1)$
337892.1.....	$SO_2(v_2 = 1)$
337969.4.....	CH_3OH-$A(v_t = 1)$
338080.8.....	H_2CS
338099.2.....	C_2H_5OH
338109.7.....	C_2H_5OH
338124.5.....	CH_3OH-*E*
338143.7.....	HCOOH
338201.8.....	HCOOH
338213.5.....	CH_2CHCN
338248.7.....	HCOOH
338306.0.....	SO_2
338344.6.....	CH_3OH-*E*
338355.8.....	$HCOOCH_3$-*E*
338376.3.....	$SO_2(v_2 = 1)$
338396.4.....	$HCOOCH_3$-*E*
338404.6.....	CH_3OH-*E*
338408.7.....	CH_3OH-*A*
338430.9.....	CH_3OH-*E*
338442.3.....	CH_3OH-*A*
338446.6.....	CH_2CHCN
338456.5.....	CH_3OH-*E*
338475.3.....	CH_3OH-*E*
338486.3.....	CH_3OH-*A*
338504.1.....	CH_3OH-*E*
338512.6.....	CH_3OH-*A*
338512.9.....	CH_3OH-*A*
338530.2.....	CH_3OH-*E*
338540.8.....	CH_3OH-*A*
338543.2.....	CH_3OH-*A*
338559.9.....	CH_3OH-*E*
338583.2.....	CH_3OH-*E*
338611.8.....	SO_2
338615.0.....	CH_3OH-*E*
338639.9.....	CH_3OH-*A*
338671.8.....	C_2H_5OH
338674.2.....	C_2H_5OH
338721.6.....	CH_3OH-*E*
338722.9.....	CH_3OH-*E*
338760.4.....	$^{13}CH_3OH$-*A*
338785.8.....	$^{34}SO_2$
338886.2.....	C_2H_5OH
338887.3.....	C_2H_5OH
338929.5.....	^{30}SiO
339061.0.....	*U*

TABLE 2—*Continued*

ν (MHz)	Molecule
339061.2.....	C_2H_5OH
339129.3.....	$HCOOCH_3$-*E*
339138.0.....	*U*
339152.8.....	$HCOOCH_3$-*E*
339186.0.....	$HCOOCH_3$-*A*
339196.4.....	$HCOOCH_3$-*A*
339201.7.....	C_2H_5OH
339259.1.....	$SO_2(v_2 = 1)$
339312.6.....	C_2H_5OH
339341.5.....	SO
339398.4.....	C_2H_5OH
339463.3.....	C_2H_5OH
339475.9.....	CN
339491.7.....	CH_3OCH_3
339491.8.....	CH_3OCH_3
339510.8.....	C_2H_5OH
339516.7.....	CN
339527.0.....	*U*
339544.1.....	C_2H_5OH
339566.3.....	C_2H_5OH
339715.8.....	NH_2CHO
339780.8.....	NH_2CHO
339857.6.....	^{34}SO
339904.1.....	NH_2CHO
339968.2.....	CH_3CH_2CN
339978.9.....	C_2H_5OH
339992.3.....	CN
340008.1.....	CN
340019.6.....	CN
340031.5.....	CN
340035.4.....	CN
340047.9.....	CH_2CHCN
340052.7.....	$C^{33}S$
340118.5.....	Ghost
340141.2.....	CH_3OH-*A*
340149.1.....	CH_3CH_2CN
340151.2.....	CH_3CH_2CN
340189.2.....	C_2H_5OH
340189.2.....	C_2H_5OH
340209.7.....	CH_2CO
340229.0.....	HCOOH
340247.8.....	CN
340248.6.....	CN
340261.8.....	CN
340265.0.....	CN
340316.4.....	SO_2
340394.2.....	CH_3OH-*A*
340394.2.....	CH_3OH-*A*
340420.4.....	C_2H_5OH
340449.2.....	OCS
340491.1.....	NH_2CHO
340496.0.....	*U*
340527.0.....	$^{33}SO_2$
340536.0.....	NH_2CHO
340576.0.....	CH_3CH_2CN
340609.2.....	CH_3OCH_3
340609.3.....	CH_3OCH_3
340612.6.....	CH_3OCH_3
340615.9.....	CH_3OCH_3
340633.0.....	$HC^{18}O^+$
340714.2.....	SO
340784.6.....	Ghost
340803.3.....	CH_3CH_2CN
340839.0.....	^{33}SO
340872.0.....	*U*
340916.5.....	CH_3CH_2CN
340972.7.....	CH_3CH_2CN
341025.6.....	CH_3CH_2CN
341033.9.....	CH_3CH_2CN
341095.0.....	*U*
341131.2.....	$^{13}CH_3OH$-*A*

TABLE 2—*Continued*

ν (MHz)	Molecule
341275.5.....	SO_2
341350.8.....	HCS^+
341415.6.....	CH_3OH-*A*
341468.7.....	CH_3CH_2CN
341472.0.....	*U*
341482.0.....	*U*
341499.0.....	*U*
341510.0.....	*U*
341563.8.....	CH_2CHCN
341603.2.....	CH_3CH_2CN
341637.0.....	CH_3CCH
341678.5.....	CH_3CH_2CN
341682.6.....	CH_3CCH
341703.7.....	CH_3CH_2CN
341710.6.....	CH_3CH_2CN
341715.1.....	CH_3CCH
341722.4.....	$HCOOCH_3$-*E*
341732.3.....	$HCOOCH_3$-*A*
341734.6.....	CH_3CCH
341735.9.....	CH_3CH_2CN
341741.1.....	CH_3CCH
341796.6.....	*U*
341852.7.....	CH_3CH_2CN
341862.6.....	$HCOOCH_3$-*A*
341870.3.....	$HCOOCH_3$-*A*
341882.0.....	CH_2CHCN
341894.2.....	CH_2CHCN
341918.1.....	$HCOOCH_3$-*E*
341927.5.....	$HCOOCH_3$-*A*
342052.9.....	CH_2CHCN
342055.2.....	CH_2CHCN
342066.0.....	*U*
342129.0.....	*U*
342162.5.....	$HCOOCH_3$-*E*
342166.8.....	$HCOOCH_3$-*E*
342208.9.....	$^{34}SO_2$
342230.1.....	$HCOOCH_3$-*E*
342238.5.....	$HCOOCH_3$-*A*
342274.0.....	*U*
342290.0.....	*U*
342317.6.....	CH_2CHCN
342332.1.....	$^{34}SO_2$
342342.3.....	$HCOOCH_3$-*E*
342350.1.....	$HCOOCH_3$-*A*
342351.7.....	$HCOOCH_3$-*E*
342358.5.....	$HCOOCH_3$-*E*
342359.4.....	$HCOOCH_3$-*A*
342366.2.....	$HCOOCH_3$-*A*
342367.9.....	$HCOOCH_3$-*E*
342375.6.....	CH_2CHCN
342375.6.....	$HCOOCH_3$-*A*
342382.7.....	Ghost
342436.3.....	$SO_2(v_2 = 1)$
342486.0.....	*U*
342506.7.....	$HCOOCH_3$-*E*
342521.2.....	HCOOH
342525.3.....	$HCOOCH_3$-*E*
342572.4.....	$HCOOCH_3$-*A*
342585.5.....	CH_2CHCN
342608.1.....	CH_3OCH_3
342608.1.....	CH_3OCH_3
342608.2.....	CH_3OCH_3
342652.0.....	CH_3CH_2CN
342677.7.....	CH_3CH_2CN
342729.8.....	CH_3OH-*A*
342761.6.....	SO_2
342883.0.....	CS
342944.4.....	H_2CS
342981.1.....	^{29}SiO
343086.0.....	^{33}SO
343148.2.....	$HCOOCH_3$-*E*
343148.4.....	$HCOOCH_3$-*E*

TABLE 2—*Continued*

ν (MHz)	Molecule
343148.5.....	$HCOOCH_3$-*E*
343148.7.....	$HCOOCH_3$-*E*
343152.8.....	$HCOOCH_3$-*A*
343153.0.....	$HCOOCH_3$-*A*
343153.1.....	$HCOOCH_3$-*A*
343153.3.....	$HCOOCH_3$-*A*
343194.6.....	CH_3CH_2CN
343202.0.....	*U*
343308.5.....	H_2CS
343319.6.....	H_2CS
343325.7.....	$H_2{}^{13}CO$
343392.9.....	CH_2CO
343408.1.....	H_2CS
343412.3.....	H_2CS
343435.4.....	$HCOOCH_3$-*E*
343443.9.....	$HCOOCH_3$-*A*
343446.5.....	CH_2CHCN
343665.0.....	*U*?
343731.8.....	$HCOOCH_3$-*E*
343753.3.....	CH_3OCH_3
343753.3.....	CH_3OCH_3
343754.2.....	CH_3OCH_3
343755.1.....	CH_3OCH_3
343757.9.....	$HCOOCH_3$-*A*
343810.8.....	H_2CS
343897.2.....	CH_3OH-$E(v_t = 1)$
343923.8.....	$SO_2(v_2 = 1)$
343952.4.....	HCOOH
343983.3.....	$OC^{34}S$
344029.6.....	$HCOOCH_3$-*EA*
344110.4.....	CH_2OH-*E*
344142.5.....	$HC^{13}CCN$
344200.3.....	$HC^{15}N$
344245.4.....	$^{34}SO_2$
344310.6.....	SO
344358.0.....	CH_3OCH_3
344358.0.....	CH_3OCH_3
344358.1.....	CH_3OCH_3
344358.2.....	CH_3OCH_3
344444.7.....	CH_3OH-*A*
344512.2.....	CH_3OCH_3
344512.2.....	CH_3OCH_3
344515.4.....	CH_3OCH_3
344518.6.....	CH_3OCH_3
344581.1.....	$^{34}SO_2$
344759.0.....	$HCOOCH_3$-*A*
344763.6.....	$HCOOCH_3$-*E*
344773.0.....	*U*
344788.0.....	*U*
344796.0.....	*U*
344808.0.....	$^{34}SO_2$
344867.3.....	CH_3CH_2CN
344913.3.....	$HCOOCH_3$-*E*
344922.2.....	$HCOOCH_3$-*E*
344987.6.....	$^{34}SO_2$
344998.2.....	$^{34}SO_2$
345068.6.....	$HCOOCH_3$-*E*
345069.0.....	$HCOOCH_3$-*A*
345090.3.....	$HCOOCH_3$-*E*
345095.3.....	$HCOOCH_3$-*E*
345132.6.....	$^{13}CH_3OH$-*E*
345149.0.....	SO_2
345168.8.....	$^{34}SO_2$
345238.7.....	$H^{13}CN(v_2 = 1)$
345285.7.....	$^{34}SO_2$
345338.5.....	SO_2
345339.8.....	$H^{13}CN$
345416.9.....	Ghost
345448.8.....	SO_2
345461.6.....	$HCOOCH_3$-*E*
345466.9.....	$HCOOCH_3$-*A*
345519.8.....	$^{34}SO_2$

TABLE 2—*Continued*

ν (MHz)	Molecule
345553.2.....	$^{34}SO_2$
345584.6.....	$^{33}SO_2$
345610.1.....	HC_3N
345651.4.....	$^{34}SO_2$
345796.0.....	CO
345901.2.....	CH_3OH-*A*
345919.2.....	CH_3OH-*E*
345929.4.....	$^{34}SO_2$
345975.1.....	$HCOOCH_3$-*E*
345985.3.....	$HCOOCH_3$-*A*
346000.9.....	$HCOOCH_3$-*E*
346184.9.....	CH_2CHCN
346202.8.....	CH_3OH-*A*
346204.4.....	CH_3OH-*A*
346220.1.....	NS
346221.2.....	NS
346221.2.....	NS
346318.7.....	Ghost
346356.2.....	CH_3CH_2CN
346356.9.....	CH_3CH_2CN
346365.6.....	$SO_2(v_2 = 1)$
346379.0.....	$SO_2(v_2 = 1)$
346455.3.....	$HC_3N(v_7)$
346523.9.....	SO_2
346528.5.....	SO
346590.5.....	$^{33}SO_2$
346591.8.....	$SO_2(v_2 = 1)$
346652.2.....	SO_2
346718.9.....	HCOOH
346772.1.....	CH_3CH_2CN
346822.6.....	CH_3CH_2CN
346874.3.....	CH_3CH_2CN
346943.1.....	CH_2CHCN
346947.3.....	CH_3CH_2CN
346948.7.....	$HC_3N(v_7)$
346955.4.....	CH_3CH_2CN
346962.8.....	CH_3CH_2CN
346969.2.....	CH_3CH_2CN
346978.7.....	CH_3CH_2CN
346979.3.....	CH_3CH_2CN
346983.8.....	CH_3CH_2CN
346998.5.....	$H^{13}CO^+$
347029.0.....	*U*
347047.0.....	*U*?
347187.7.....	$^{13}CH_3OH$-*A*
347232.0.....	CH_2CHCN
347330.6.....	SiO
347434.2.....	CH_2CHCN
347446.0.....	*U*
347478.4.....	$HCOOCH_3$-*E*
347494.0.....	$HCOOCH_3$-*A*
347565.9.....	Ghost
347604.6.....	$HCOOCH_3$-*E*
347617.0.....	$HCOOCH_3$-*A*
347628.4.....	$HCOOCH_3$-*A*
347743.0.....	*U*
347759.0.....	CH_2CHCN
347845.8.....	$^{13}CH_3OH$-*A*
347915.8.....	C_2H_5OH
348050.0.....	$HCOOCH_3$-*E*
348066.0.....	$HCOOCH_3$-*A*
348084.0.....	*U*?
348100.6.....	$^{13}CH_3OH$-*E*
348117.6.....	$^{34}SO_2$
348162.0.....	*U*?
348260.6.....	CH_3CH_2CN
348340.3.....	$HN^{13}C$
348344.5.....	CH_3CH_2CN
348358.0.....	*U*
348373.0.....	*U*
348387.8.....	SO_2
348531.9.....	H_2CS

TABLE 2—*Continued*

ν (MHz)	Molecule
348553.3.....	CH_3CH_2CN
348680.0.....	Ghost
348784.6.....	CH_3CN
348909.5.....	$HCOOCH_3$-*E*
348911.4.....	CH_3CN
348915.0.....	$HCOOCH_3$-*A*
348930.0.....	Ghost
348991.4.....	CH_2CHCN
349025.0.....	CH_3CN
349048.5.....	$HCOOCH_3$-*E*
349065.7.....	$HCOOCH_3$-*A*
349107.0.....	CH_3OH-*A*
349125.3.....	CH_3CN
349173.2.....	$CH_3{}^{13}CN$
349212.1.....	$CH_3{}^{13}CN$
349220.0.....	$CH_3{}^{13}CN$
349253.5.....	$CH_3{}^{13}CN$
349273.3.....	$CH_3{}^{13}CN$
349280.3.....	$CH_3{}^{13}CN$
349285.8.....	CH_3CN
349337.9.....	CCH
349338.7.....	CCH
349346.1.....	CH_3CN
349393.0.....	CH_3CN
349398.9.....	CCH
349400.3.....	CCH
349426.6.....	CH_3CN
349446.7.....	CH_3CN
349453.4.....	CH_3CN
349479.5.....	NH_2CHO
349492.6.....	CH_3CH_2CN
349547.0.....	CH_3CH_2CN
349730.8.....	CH_3CH_2CN
349731.3.....	CH_3CH_2CN
349803.0.....	CH_3OCH_3
349806.1.....	CH_3OCH_3
349809.2.....	CH_3OCH_3
350039.4.....	CH_3CH_2CN
350050.9.....	CH_3CH_2CN
350103.1.....	$^{13}CH_3OH$-*A*
350139.7.....	CH_3CH_2CN
350145.2.....	CH_3CH_2CN
350170.0.....	*U*
350247.2.....	$CH_3CN(v_8)$
350277.9.....	$CH_3CN(v_8)$
350304.0.....	$^{33}SO_2$
350320.6.....	$CH_3CN(v_8)$
350333.3.....	HNCO
350352.7.....	$CH_3CN(v_8)$
350379.8.....	$CH_3CN(v_8)$
350415.1.....	$CH_3CN(v_8)$
350423.5.....	$CH_3CN(v_8)$
350442.2.....	$HCOOCH_3$-*E*
350444.9.....	$CH_3CN(v_8)$
350449.6.....	$CH_3CN(v_8)$
350457.6.....	$HCOOCH_3$-*A*
350465.6.....	$CH_3CN(v_8)$
350507.1.....	$CH_3CN(v_8)$
350534.3.....	C_2H_5OH
350549.5.....	$CH_3CN(v_8)$
350552.2.....	$CH_3CN(v_8)$
350619.6.....	$^{34}SO_2$
350687.7.....	CH_3OH-*E*
350689.5.....	NO
350690.8.....	NO
350694.8.....	NO
350788.7.....	$^{33}SO_2$
350842.7.....	$CH_3CN(v_8)$
350862.7.....	SO_2
350905.1.....	CH_3OH-*A*
350919.6.....	$HCOOCH_3$-*E*
350947.2.....	$HCOOCH_3$-*A*

TABLE 2—*Continued*

ν (MHz)	Molecule
350998.1.....	$HCOOCH_3$-*E*
351015.8.....	$HCOOCH_3$-*A*
351043.5.....	NO
351051.7.....	NO
351178.5.....	$^{33}SO_2$
351236.7.....	CH_3OH-*E*
351257.2.....	SO_2
351379.0.....	CH_2CHCN
351386.3.....	CH_2CHCN
351417.1.....	HNCO
351417.2.....	HNCO
351430.1.....	CH_2CHCN
351430.2.....	CH_2CHCN
351434.0.....	CH_2CHCN
351450.9.....	CH_2CHCN
351462.9.....	CH_3CH_2CN
351469.2.....	CH_3OD-*A*
351490.0.....	*U*
351517.2.....	$HCOOCH_3$-*E*
351529.1.....	$HCOOCH_3$-*A*
351531.6.....	CH_3CH_2CN
351540.0.....	*U*
351551.9.....	HNCO
351575.9.....	CH_3CH_2CN
351633.5.....	HNCO
351768.7.....	H_2CO
351873.9.....	SO_2
351994.8.....	HNCO
352082.9.....	$^{34}SO_2$
352120.6.....	CH_2CHCN
352283.0.....	$HCOOCH_3$-*E*
352292.6.....	$HCOOCH_3$-*A*
352404.9.....	$HCOOCH_3$-*E*
352414.2.....	$HCOOCH_3$-*A*
352500.7.....	CH_3CH_2CN
352544.6.....	$H^{13}CCCN$
352599.6.....	OCS
352897.9.....	HNCO
352912.6.....	$HCOOCH_3$-*E*
352918.0.....	$HCOOCH_3$-*E*
352920.2.....	$HCOOCH_3$-*A*
352922.0.....	$HCOOCH_3$-*E*
352925.6.....	$HCOOCH_3$-*A*
352927.4.....	$HCOOCH_3$-*E*
352929.6.....	$HCOOCH_3$-*A*
352935.0.....	$HCOOCH_3$-*A*
353034.5.....	C_2H_5OH
353147.2.....	CH_2CHCN
353166.0.....	*U*
353192.4.....	$HC^{13}CCN$
353234.9.....	CH_3CH_2CN
353234.9.....	CH_3CH_2CN
353241.5.....	CH_2CHCN
353241.6.....	CH_2CHCN
353290.0.....	Ghost
353402.0.....	$HCOOCH_3$-*E*
353410.6.....	$HCOOCH_3$-*A*
353724.1.....	$HCOOCH_3$-*E*
353728.5.....	$HCOOCH_3$-*A*
353739.3.....	$^{13}CH_3OH$-*A*
353811.9.....	$H_2{}^{13}CO$
353851.0.....	*U*
353914.6.....	Ghost
354129.0.....	*U*
354370.0.....	Ghost
354445.9.....	$^{13}CH_3OH$-*E*
354460.6.....	HCN($v_2 = 1$)
354505.5.....	HCN
354608.0.....	$HCOOCH_3$-*A*
354608.4.....	$HCOOCH_3$-*E*
354624.8.....	SO_2($v_2 = 1$)
354698.7.....	HC_3N

TABLE 2—*Continued*

ν (MHz)	Molecule
354742.4.....	$HCOOCH_3$-*E*
354759.1.....	$HCOOCH_3$-*E*
354800.0.....	SO_2($v_2 = 1$)
354805.7.....	$HCOOCH_3$-*A*
354898.7.....	$H_2{}^{13}CO$
354949.5.....	Ghost
355028.7.....	$H_2{}^{13}CO$
355028.7.....	$H_2{}^{13}CO$
355045.5.....	SO_2
355098.5.....	Ghost
355109.8.....	Ghost
355190.9.....	$H_2{}^{13}CO$
355202.6.....	$H_2{}^{13}CO$
355218.9.....	CH_2CHCN
355231.0.....	*U*
355439.5.....	$H^{15}NC$
355565.8.....	$HC_3N(v_7)$
355573.6.....	$S^{18}O$
355603.0.....	CH_3OH-*A*
355755.9.....	CH_3CH_2CN
355836.0.....	$OC^{34}S$
355851.0.....	*U*
355964.3.....	CH_3OH-*E*
356006.6.....	CH_3OH-*A*
356040.6.....	SO_2
356072.1.....	$HC_3N(v_7)$
356137.2.....	HCOOH
356162.7.....	HCN($v_2 = 2$)
356176.1.....	$H_2{}^{13}CO$
356222.4.....	$^{34}SO_2$
356255.6.....	HCN($v_2 = 1$)
356276.7.....	CH_3CH_2CN
356297.1.....	CH_3OCHO-*A*
356301.3.....	HCN($v_2 = 2$)
356421.7.....	CH_2CHCN
356426.0.....	CH_3OCHO-*E*
356427.4.....	CH_3OCHO-*E*
356442.9.....	CH_3OCH_3
356442.9.....	CH_3OCH_3
356443.2.....	CH_3OCH_3
356443.6.....	CH_3OCH_3
356539.8.....	CH_3OCHO-*A*
356546.1.....	CH_3CH_2CN
356567.2.....	CH_3OCH_3
356575.2.....	CH_3OCH_3
356576.0.....	CH_3OCH_3
356582.8.....	CH_3OCH_3
356586.8.....	CH_3OCH_3
356587.0.....	CH_3OCH_3
356601.0.....	*U*
356627.3.....	CH_3OH-*E*
356644.0.....	*U*
356662.0.....	*U*
356734.3.....	HCO^+
356755.2.....	SO_2
356794.0.....	$HCOOCH_3$-*E*
356839.6.....	HDO
356874.9.....	$^{13}CH_3OH$-*A*
356908.6.....	CH_2CHCN
356911.1.....	CH_2CHCN
356928.6.....	$HCOOCH_3$-*A*
356937.7.....	$HCOOCH_3$-*E*
356960.4.....	CH_3CH_2CN
356973.1.....	CH_2CHCN
357066.2.....	CH_3OD-*A*
357087.0.....	SO_2($v_2 = 1$)
357102.2.....	$^{34}SO_2$
357165.4.....	SO_2
357241.2.....	SO_2
357387.6.....	SO_2
357459.4.....	CH_3OCH_3
357460.2.....	CH_3OCH_3

TABLE 2—*Continued*

ν (MHz)	Molecule
357461.0.....	CH_3OCH_3
357469.4.....	CH_3OCH_3
357581.4.....	SO_2
357657.9.....	$^{13}CH_3OH$-*E*
357671.8.....	SO_2
357750.0.....	Ghost
357892.4.....	SO_2
357926.0.....	SO_2
357962.9.....	SO_2
357989.8.....	$HCOOCH_3$-*E*
357995.6.....	$HCOOCH_3$-*A*
357995.9.....	$HCOOCH_3$-*E*
358013.1.....	SO_2
358038.1.....	SO_2
358093.7.....	Ghost
358107.5.....	C_2H_5OH
358152.4.....	Ghost
358215.6.....	SO_2
358326.2.....	CH_3CH_2CN
358347.3.....	$^{34}SO_2$
358356.0.....	*U*
358364.2.....	$HCOOCH_3$-*E*
358392.3.....	$HCOOCH_3$-*A*
358402.6.....	CH_3CH_2CN
358414.9.....	CH_3OH-*E*
358447.4.....	CH_3OCH_3
358449.4.....	CH_3OCH_3
358449.4.....	CH_3OCH_3
358451.4.....	CH_3OCH_3
358451.9.....	CH_3OCH_3
358454.0.....	CH_3OCH_3
358456.5.....	CH_3OCH_3
358456.5.....	CH_3OCH_3
358518.6.....	CH_3CH_2CN
358518.7.....	CH_3CH_2CN
358565.8.....	$HCOOCH_3$-*E*
358576.6.....	$HCOOCH_3$-*A*
358591.6.....	$HCOOCH_3$-*E*
358605.8.....	CH_3OH-*E*
358648.8.....	$S^{18}O$
358692.5.....	CH_3CH_2CN
358720.4.....	CH_3CH_2CN
358721.2.....	CH_3CH_2CN
358756.6.....	CH_3CCH
358790.8.....	CH_3CCH
358811.2.....	CH_3CCH
358818.1.....	CH_3CCH
358947.2.....	Ghost
358988.0.....	$^{34}SO_2$
359056.1.....	CH_3CH_2CN
359071.9.....	CH_3CH_2CN
359151.2.....	SO_2
359254.0.....	Ghost
359270.0.....	Ghost
359335.6.....	$HCOOCH_3$-*E*
359350.6.....	$HCOOCH_3$-*A*
359352.0.....	$HCOOCH_3$-*A*
359362.3.....	$HCOOCH_3$-*E*
359381.6.....	CH_3OCH_3
359381.6.....	CH_3OCH_3
359384.6.....	CH_3OCH_3
359387.7.....	CH_3OCH_3
359432.7.....	Ghost
359543.0.....	$HCOOCH_3$-*E*
359558.0.....	$HCOOCH_3$-*A*
359651.8.....	$^{34}SO_2$
359676.9.....	CH_3OH-*E*
359770.7.....	SO_2
359815.4.....	CH_3OCHO-*A*
359870.1.....	CH_3CH_2CN
359952.1.....	Ghost

TABLE 3

TRANSITIONS OF CO, CS, AND SiO

Molecule	ν (MHz)	J	T_R^* (K)	$\int T_R^* dv$ (K km s^{-1})	Notes
CO	345796.0	3–2	144.5	5497.4	
^{13}CO	330588.1	3–2	34.9	415.8	
C^{18}O	329330.6	3–2	11.7	115.1	
C^{17}O	337061.1	3–2	4.5	52.2	
CS	342883.0	7–6	28.9	513.2	
C^{34}S.....	337396.7	7–6	9.9	93.9	
C^{33}S.....	340052.7	7–6	5.8	<46.1	1
SiO	347330.6	8–7	34.5	917.1	
^{29}SiO.....	342981.1	8–7	4.6	117.1	
^{30}SiO.....	338929.5	8–7	4.1	99.5	
PN	328887.9	7–6	0.4	1.6	2

NOTES.—(1) Blend with CN at 340035.4 and CH_2CHCN at 340047.4. (2) Blended with a broad feature.

plateau), which contribute differently to the isotopomeric line temperatures, and partly to the very high optical depth differences between the isotopomers and temperature gradients along the line of sight. Nonetheless, it gives an approximate idea of the optical depths and should be more reliable for other molecules with smaller optical depths. It is noteworthy that neither C^{18}O nor C^{17}O shows a noticeable contribution from the hot core velocity component, while the other three velocity components are present. Vibrationally excited CO at 342.647494 GHz was not found at the level of $\approx$0.2 K.

CS.—The (7–6) lines of carbon monosulfide C^{32}S, C^{34}S, and C^{33}S are present, while ^{13}CS is outside the band. The CS lines show broad wings from the plateau emission. All four velocity components are present in these transitions. Assuming a ^{32}S/^{34}S ratio of 22.5, we determine the peak optical depth of ^{12}CS to be 9. The line of vibrationally excited CS at 333.9713 GHz is very close to an $HCOOCH_3$ line at 333.9723 GHz, which probably accounts for most of the flux in this feature.

SiO.—The (8–7) lines of silicon monoxide are observed in its ^{28}SiO, ^{29}SiO, and ^{30}SiO isotopomers. As noted by previous studies, the lines have only contributions from the hot

TABLE 4

TRANSITIONS OF HCN, HNC, AND OCS

Molecule	ν (MHz)	J	T_R^* (K)	$\int T_R^* dv$ (K km s^{-1})	Notes
HCN	354505.5	4–3	50.0	1744.7	
HCN(0, 1^{1c}, 0)	354460.5	4–3	<11.2	<102.0	1
HCN(0, 1^{1d}, 0)	356255.6	4–3	7.1	90.7	
HCN(0, 2^{2e}, 0)	356162.7	4–3	0.4	1.4	
HCN(0, 2^0, 0)	356301.3	4–3	...	...	2
H^{13}CN.....	345339.8	4–3	<27.6	<682.5	3
H^{13}CN(0, 1^{1c}, 0).....	345238.7	4–3	0.7	2.6	
HC^{15}N.....	344200.3	4–3	10.5	205.0	4
HN^{13}C.....	348340.3	4–3	<5.5	<66.1	5
H^{15}NC.....	355439.5	4–3	0.9	7.8	
OCS.....	328298.1	27–26	7.4	92.1	
	340449.2	28–27	12.2	170.8	6
	352599.6	29–28	5.5	71.1	
OC^{34}S	332129.7	28–27	2.1	23.2	
	343983.3	29–28	0.8	4.7	
	355836.0	30–29	1.2	<10.8	7

NOTES.—(1) Blend with HCN at 354505.5. (2) Blend with $HCOOCH_3$ at 356297.1. (3) Blend with SO_2 at 345338.5 and $^{34}SO_2$ at 345285.7. (4) Blend with $^{34}SO_2$ at 344245.4. (5) Blend with CH_3CH_2CN at 348344.5. (6) Too strong; possible blend with *U* line. (7) Blend with *U* line at 355851.

TABLE 5

TRANSITIONS OF HC_3N

ν (MHz)	J	T_R^* (K)	$\int T_R^* dv$ (K km s^{-1})	Notes
HC_3N:				
327431.4.....	36–35	<7.9	<105.0	
336521.0.....	37–36	6.6	<127.1	
345610.1.....	38–37	5.7	85.0	
354698.7.....	39–38	6.7	120.3	1
$HC_3N(v_7^1)$:				
328232.8.....	36*e*–35*e*	1.4	7.9	
328700.6.....	36*f*–35*f*	1.2	12.2	
337344.3.....	37*e*–36*e*	<3.6	<36.3	2
337824.0.....	37*f*–36*f*	1.4	8.9	
346455.3.....	38*e*–37*e*	2.1	17.9	
346948.7.....	38*f*–37*f*	<3.2	<33.8	3
355565.8.....	39*e*–38*e*	<2.2	<30.5	4
356072.0.....	39*f*–38*f*	1.7	13.7	
$H^{13}CCCN$:				
334929.5.....	38–37	0.5	2.5	
352544.6.....	40–39	0.3	2.4	
$HC^{13}CCN$:				
344142.5.....	38–37	0.1	1.1	
353192.4.....	39–38	0.3	3.3	

NOTES.—(1) Blend with CH_3CH_2CN at 348344. (2) Blend with CH_3CH_2CN at 337347.6. (3) Blend with CH_3CH_2CN at 346947.3. (4) Blend with wing of $S^{18}O$ at 355573.6.

core and plateau velocity components and show no trace of the compact and extended ridge. The line ratios are consistent with a ^{28}SiO optical depth of about 2, if a $^{28}SiO/^{29}SiO$ ratio of 20 is assumed. Given that the peak intensity of ^{28}SiO is similar to CS and the line is twice as broad, this indicates clearly that the SiO abundance is enhanced greatly in the plateau gas, as known from previous studies. One explanation for this and other observations of SiO abundance enhancements in shocked gas is that SiO is produced by destruction of grain cores in shocks (Martín-Pintado, Bachiller, & Fuente 1992; Schilke et al. 1996b). Another possibility is that SiO is embedded in icy grain mantles, which are evaporated (Turner 1991b). There is also a hint that vibrationally excited SiO may be present, but the line is blended with an $HCOOCH_3$ transition, and hence the evidence is not conclusive.

SiS.—Two lines of silicon monosulfide fall into our band: the (18–17) line at 326.6 GHz and the (19–18) line at 344.8 GHz. The first frequency is very noisy due to the atmospheric water line at 325 GHz, and, moreover, the data are contaminated by line emission from the other sideband. Hence, no statement about the presence of this line is possible. The other line happens to lie inside a group of $HCOOCH_3$ lines and other features. No distinct feature is visible if the line velocity is assumed to be 8 km s^{-1}. However, if one follows Dickinson & Rodriguez Kuiper (1981) and uses a velocity of 14 km s^{-1}, as do Sutton et al. (1985), one finds a spectral feature that corresponds to the line. Turner (1989) claims two of the three SiS lines in his survey range as detected, but he does not further comment on the line velocities. The SiS line in the band of Blake et al. (1986) falls in one of the gaps in their data. The conclusion has to be that the existence of SiS in Orion is still questionable.

TABLE 6

TRANSITIONS OF HCO^+ AND HCS^+

Molecule	ν (MHz)	J	T_R^* (K)	$\int T_R^* dv$ (K km s^{-1})	Notes
HCO^+	356734.3	4–3	47.0	<1026.3	1
$H^{13}CO^+$.....	346998.5	4–3	<2.0	<18.4	2
$HC^{18}O^+$.....	340633.0	4–3	1.3	22.4	
HCS^+	341350.8	8–7	1.2	9.9	

NOTES.—(1) Blend with SO_2 line at 356755.2. (2) Blend with CH_3CH_2CN at 346983.8.

TABLE 7

TRANSITIONS OF SO, NO, AND NS

ν (MHz)	N_J; J, F	T_R^* (K)	$\int T_R^* dv$ (K km s^{-1})	Notes
SO:				
329385.5.....	2_1–1_0	6.3	91.2	1
336553.3.....	11_{10}–10_{10}	3.9	71.1	
339341.5.....	3_3–2_3	6.3	172.6	2
340714.2.....	8_7–7_6	37.8	1382.9	
344310.6.....	8_8–7_7	43.3	1398.0	
346528.5.....	8_9–7_8	40.4	<1407.6	3
^{34}SO:				
333902.1.....	8_7–7_6	8.4	<203.4	4
337582.2.....	8_8–7_7	10.3	<220.1	5
339857.6.....	8_9–7_8	14.3	418.0	
^{33}SO:				
337195.0	8_7–7_6	3.7	57.1	6
340839.0.....	8_8–7_7	4.5	<77.2	7
343086.0.....	8_9–7_8	4.6	105.7	
$S^{18}O$:				
355573.6.....	9_8–8_7	2.2	30.5	
358648.8.....	9_9–8_8	1.1	12.8	
NO:				
350689.5.....	$\frac{7}{2}, \frac{9}{2}$–$\frac{5}{2}, \frac{7}{2}f$	<14.6	<204.7	8
350690.8.....	$\frac{7}{2}, \frac{7}{2}$–$\frac{5}{2}, \frac{5}{2}f$			
350694.8.....	$\frac{7}{2}, \frac{5}{2}$–$\frac{5}{2}, \frac{3}{2}f$			
351043.5.....	$\frac{7}{2}, \frac{9}{2}$–$\frac{5}{2}, \frac{7}{2}e$	5.8	108.7	
351051.7.....	$\frac{7}{2}, \frac{7}{2}$–$\frac{5}{2}, \frac{5}{2}e$			
351051.7.....	$\frac{7}{2}, \frac{5}{2}$–$\frac{5}{2}, \frac{3}{2}e$			
NS:				
346220.1.....	$\frac{15}{2}, \frac{17}{2}$–$\frac{13}{2}, \frac{15}{2}f$	3.2	32.1	
346221.2.....	$\frac{15}{2}, \frac{13}{2}$–$\frac{13}{2}, \frac{11}{2}f$			
346221.2.....	$\frac{15}{2}, \frac{15}{2}$–$\frac{13}{2}, \frac{13}{2}f$			

NOTES.—(1) Blend with $HCOOCH_3$ at 329364.2. (2) Blend with C_2H_5OH at 339312.6. (3) Blend with SO_2 at 346523.9. (4) Blend with CH_3CH_2CN at 331921.6 (5) Blend with $CH_3OH(v_t = 1)$ at 337546.1, 337605.3, and 337610.6. (6) Blend with CH_3OCH_3 lines from 337180 to 337192. (7) Blend with CH_2CH_3CN at 340808.3. (8) Blend with CH_3OH at 350687.7 and with the other *f* components.

SiC *and* SiC_2.—ZM93 see a weak feature at the frequency of the SiC(4–3, $\Omega = 2$) line. In our survey, a weak feature ($\approx$0.2 K) close to the SiC (9–8, $\Omega = 2$) line is also present, but we do not consider this as sufficient evidence for the detection of SiC in Orion. We see no lines at the many silicon dicarbide frequencies. T91 claims the tentative detection of SiC_2, but no lines of this species are seen in ZM93 or S94.

PN.—The (7–6) at 326.8879 GHz line of phosphorous nitride has been detected tentatively. This species was identified tentatively by Sutton et al. (1985) and later confirmed by Ziurys (1987) and Turner & Bally (1987), who observed several transitions. Since the line seems to be blended with a broad underlying feature, no analysis of the velocity components is possible.

3.2.2. *Polyatomic Linear Molecules and Ions without Electronic Angular Momentum*

HCN *and* HNC.—The (4–3) transition of hydrogen

TABLE 8

TRANSITIONS OF CN AND CCH

ν (MHz)	N, J, F	T_R^* (K)	$\int T_R^* dv$ (K km s^{-1})	Notes
CN:				
339475.9.....	$3, \frac{5}{2}, \frac{5}{2}-2, \frac{5}{2}, \frac{5}{2}$	0.9	<5.7	1
339516.7.....	$3, \frac{5}{2}, \frac{7}{2}-2, \frac{5}{2}, \frac{7}{2}$	1.2	8.2	
339992.3.....	$3, \frac{5}{2}, \frac{3}{2}-2, \frac{3}{2}, \frac{5}{2}$	0.3	0.7	
340008.1.....	$3, \frac{5}{2}, \frac{5}{2}-2, \frac{3}{2}, \frac{5}{2}$	1.8	14.2	
340019.6.....	$3, \frac{5}{2}, \frac{3}{2}-2, \frac{3}{2}, \frac{3}{2}$	2.5	15.7	
340031.5.....	$3, \frac{5}{2}, \frac{7}{2}-2, \frac{3}{2}, \frac{5}{2}$	6.1	36.6	
340035.4.....	$3, \frac{5}{2}, \frac{3}{2}-2, \frac{3}{2}, \frac{1}{2}$	6.3	28.6	2
340035.4.....	$3, \frac{5}{2}, \frac{5}{2}-2, \frac{3}{2}, \frac{3}{2}$			
340247.7.....	$3, \frac{7}{2}, \frac{9}{2}-2, \frac{5}{2}, \frac{7}{2}$	10.8	62.5	3
340247.8.....	$3, \frac{7}{2}, \frac{7}{2}-2, \frac{5}{2}, \frac{5}{2}$			
340248.6.....	$3, \frac{7}{2}, \frac{5}{2}-2, \frac{5}{2}, \frac{3}{2}$			
340261.8.....	$3, \frac{7}{2}, \frac{5}{2}-2, \frac{5}{2}, \frac{5}{2}$	2.8	21.4	4
340265.0.....	$3, \frac{7}{2}, \frac{7}{2}-2, \frac{5}{2}, \frac{7}{2}$			
CCH:				
349337.9.....	$4, \frac{9}{2}, \frac{9}{2}-3, \frac{7}{2}, \frac{7}{2}$	3.9	19.5	
349338.7.....	$4, \frac{9}{2}, \frac{7}{2}-3, \frac{7}{2}, \frac{5}{2}$			
349398.9.....	$4, \frac{7}{2}, \frac{7}{2}-3, \frac{5}{2}, \frac{5}{2}$	<8.6	<80.0	5
349400.3.....	$4, \frac{7}{2}, \frac{5}{2}-3, \frac{5}{2}, \frac{3}{2}$			

NOTES.—(1) Blend with U line at 339468. (2) Blend with $C^{33}S$ at 340052.7. (3) Blend with HCOOH at 340229.0. (4) Blend with broad underlying feature. (5) Blend with CH_3CN at 349393.0.

cyanide is detected in its isotopomers HCN, $H^{13}CN$, and $HC^{15}N$. All these lines show broad wings. Assuming a $^{14}N/^{15}N$ ratio of 300 (Wilson & Matteucci 1992) and a $^{12}C/^{13}C$ ratio of 60, one derives optical depths of 70 for HCN and of 2 for $H^{13}CN$ at the position of the line maximum. We also find evidence for the (4–3) lines of hydrogen isocyanide $HN^{13}C$ and $H^{15}NC$. The $HN^{13}C$ line is blended with CH_3CH_2CN, and its strength cannot be determined reliably, but the expected $HN^{13}C/H^{15}NC$ ratio of 5 is consistent with the data. The $HC^{15}N/H^{15}NC$ integrated intensity line ratio is 26, in good agreement with a study of Schilke et al. (1992a), who determine the HCN/HNC ratio to be 80 in the plateau and about 13 in the spike component toward Orion KL. None of the lines of DCN or DNC are present in our frequency band.

Vibrationally excited HCN is found in the (4–3) lines of the bending vibration (0, 1^{1c}, 0), (0, 1^{1d}, 0), (0, 2^{2c}, 0), and, tentatively, (0, 2^0, 0) states. The (0, 2^{2d}, 0) line is blended with HCOOH. No lines in the stretching vibration modes (1, 0, 0) and (0, 0, 1) were found. The $H^{13}CN$ (0, 1^{1c}, 0) line is detected, but the (0, 1^{1d}, 0) line is blended with CH_3CH_2CN. While the ground-state lines show all four velocity components, they are dominated by hot core and plateau. The vibrationally excited lines show exclusively the hot core component.

HC_3N.—We detect cyanoacetylene in the (36–35), (37–36), (38–37), and (39–38) transitions. Most of the lines are blended with other features, which makes a rotation temperature estimate difficult. Some very weak ^{13}C isotopomer features, but no DC_3N transitions, were detected. The ratios of the HC_3N lines to the ^{13}C isotopomer lines are consistent with optically thin emission. The rotation temperature and hence the column density are very uncertain. Transitions of HC_3N in the v_7^1 state, 350 K above ground, were

TABLE 9

TRANSITIONS OF CH_3CN

ν (MHz)	J_K	T_R^* (K)	$\int T_R^* dv$ (K km s^{-1})	Notes
CH_3CN:				
330437.4	$18_{10}-17_{10}$	1.1	<5.7	1
330557.6	18_9-17_9	...	...	2
330665.2	18_8-17_8	1.4	12.1	3
330760.2	18_7-17_7	2.1	15.5	
330842.6	18_6-17_6	3.8	54.6	4
330912.5	18_5-17_5	3.4	35.5	5
330969.6	18_4-17_4	4.1	48.7	
331014.1	18_3-17_3	6.1	76.6	
331045.9	18_2-17_2	5.4	61.8	
331065.0	18_1-17_1	6.3	108.4	
331071.3	18_0-17_0	6.8		
348784.6	$19_{10}-18_{10}$	1.1	11.3	
348911.4	19_9-18_9	...	...	6
349025.0	19_8-18_8	2.1	19.7	
349125.3	19_7-18_7	2.5	27.4	7
349212.1	19_6-18_6	3.8	54.6	
349285.8	19_5-18_5	3.9	46.2	8
349346.1	19_4-18_4	4.6	50.7	
349393.0	19_3-18_3	<8.6	<79.6	9
349426.6	19_2-18_2	5.5	76.8	
349446.7	19_1-18_1	7.8	67.9	
349453.4	19_0-18_0			
$CH_3CN(v_8=1)$:				
331748.5	18_1-17_1	2.2	18.8	
331992.3	$18_{-2}-17_{-2}$	1.3	9.2	
332015.8	18_0-17_0	2.5	26.1	10
332017.8	$18_{-1}-17_{-1}$			
332028.8	18_4-17_4	2.2	18.9	
332387.8	18_1-17_1	2.0	15.1	11
350168.1	19_1-18_1	1.1	7.2	
350247.3	$19_{-5}-18_{-5}$	0.7	4.3	
350277.9	19_7-18_7	1.7	13.2	
350320.6	$19_{-4}-18_{-4}$	1.2	9.6	
350352.7	19_6-18_6	0.8	5.8	
350379.7	$19_{-3}-18_{-3}$	0.7	5.0	
350315.1	19_5-18_5	1.8	18.2	
350423.5	$19_{-2}-18_{-2}$			
350444.9	19_0-18_0	2.4	15.1	
350449.6	$19_{-1}-18_{-1}$			
350465.7	19_4-18_4	2.9	24.5	
350507.2	19_3-18_3	2.5	37.1	
350552.2	19_2-18_2	2.1	15.4	
350842.7	19_1-18_1	3.4	32.0	
$CH_3{}^{13}CN$:				
330881.9	18_2-17_2	0.4	2.2	12
330901.0	18_1-17_1	1.1	6.4	13
330907.3	18_0-17_0			
349173.2	19_4-18_4	1.4	12.5	
349220.0	19_3-18_3	...	...	14
349253.5	19_2-18_2	0.8	5.5	
349273.3	19_1-18_1	1.3	10.5	15
349280.3	19_0-18_0			

NOTES.—(1) Blend with $^{13}CH_3OH$ at 330442.4. (2) Blend with ^{13}CO at 330588.1. (3) Blend with $^{34}SO_2$ at 330667.6. (4) Blend with HNCO at 330848.8. (5) Blend with $CH_3{}^{13}CN$ at 330901.0 and 330907.3. (6) Blend with $HCOOCH_3$ at 348909.5 and 348915. (7) Blend with $CH_3{}^{13}CN$ at 349220.0. (8) Blend with $CH_3{}^{13}CN$ at 349273.6 and 349280.3. (9) Blend with CCH at 349398 and 349400.3. (10) Blend with CH_3CH_2CN at 332014.7 and 332020.6. (11) Blend with CH_2CHCN at 332385.0. (12) Blend with SO_2 at 350862.7. (13) Blend with CH_3CN at 330912.5. (14) Blend with CH_3CN at 349212.1. (15) Blend with CH_3CN at 349285.8.

TABLE 10

TRANSITIONS OF CH_3CCH

ν (MHz)	J_K	T_R^* (K)	$\int T_R^* dv$ (K km s^{-1})	Notes
341637.0.....	20_4–19_4	0.3	0.9	
341682.6.....	20_3–19_3	2.8	18.4	1
341715.1.....	20_2–19_2	4.3	29.6	2
341734.6.....	20_1–19_1	3.3	20.5	3
341741.1.....	20_0–19_0	2.1	13.3	4
358756.6.....	21_3–20_3	1.1	6.4	
358790.9.....	21_2–20_2	0.9	6.3	
358811.2.....	21_1–20_1	1.1	5.4	
358818.1.....	21_0–20_0	1.1	6.8	

NOTES.—(1) Blend with CH_3CH_2CN at 331678.4. (2) Blend with $HCOOCH_3$ at 341722.4 and CH_2CHCN at 341703.7 and 341710.6. (3) Blend with $HCOOCH_3$ at 341732.3 and CH_3CCH at 341741.1. (4) Blend with CH_3CCH at 341734.6.

observed. No heavier cyanopolyynes were detected, as expected at our sensitivity level and observing frequency. Both ground-state and vibrationally excited state transitions are dominated by the hot core velocity component. The ground-state line also shows some contribution from the plateau component, while signs of compact and extended ridge components are absent in both. The isotopomers are too weak to determine the origin.

OCS.—We detect the (27–26), (28–27), and (29–28) transitions of carbonyl sulfide and the (28–27), (29–28), and (30–29) transitions of $OC^{34}S$. We see no convincing evidence for $O^{13}CS$ lines. From the only unblended pair of isotopomeric transitions, the (29–28), we calculate an optical depth of about 3.5 for OCS, again assuming a $^{33}S/^{34}S$ ratio of 22.5. The rotation temperature, based on only two unblended lines, is 82 K. The $OC^{34}S$ data are too noisy to allow the determination of a rotation temperature. No vibrationally excited OCS was found. All velocity components except extended ridge are found for the main isotopomer, while $OC^{34}S$ is dominated by the hot core.

HCO^+.—The formyl ion (4–3) transition was detected in the HCO^+, $H^{13}CO^+$, and $HC^{18}O^+$ isotopomers. The comparison of the HCO^+ and $HC^{18}O^+$ line intensities gives an optical depth of 15 in the HCO^+(4–3) line. $H^{13}CO^+$ is blended with $HCOOCH_3$ lines, which make quantitative statements unreliable. Blending makes statements about the velocity structure unreliable, but all isotopomers show an extended ridge component, with an additional contribution by the plateau to the main isotopomeric line. The hot core contribution, if present, is not prominent. The vibrationally excited lines of HCO^+ at 356.5487 GHz and 358.2425 GHz are blended with CH_3CH_2CN and SO_2, respectively, and thus their presence cannot be established.

HCS^+.—We detect HCS^+ in the (8–7) transition of the main isotopomer. The line velocity and width seem to indicate an origin in the extended ridge.

3.2.3. *Linear Molecules with Electronic Angular Momentum*

SO.—Sulphur monoxide ($^3\Sigma^-$) is observed in five lines of the ^{32}SO, in three lines of the ^{34}SO and ^{33}SO isotopomers, and in two $S^{18}O$ lines. The main isotopomer lines are very broad, comparable to CO. From SO, we derive a rotation temperature of 27 K and a column density of $(3.8 \pm 0.4) \times 10^{16}$ cm^{-2}, which are of course both affected by optical thickness effects. Serabyn & Weisstein (1995) find about a similar rotation temperature for low-excitation SO; however, if a correction for optical thickness is applied, their

TABLE 11

TRANSITIONS OF SO_2

ν (MHz)	J_{K_-,K_+}	T_R^* (K)	$\int T_R^* dv$ (K km s^{-1})	Notes
SO_2:				
326867.5.....	$20_{4,16}$–$20_{3,17}$	8.3	115.0	1
327216.8.....	$38_{5,33}$–$38_{4,34}$	2.2	39.3	1
331580.2.....	$11_{6,6}$–$12_{5,7}$	2.1	33.2	
332091.4.....	$21_{2,20}$–$21_{1,21}$	7.6	191.8	
332505.2.....	$4_{3,1}$–$3_{2,2}$	18.7	482.1	
334673.3.....	$8_{2,6}$–$7_{1,7}$	11.3	302.2	
335773.2.....	$29_{5,25}$–$30_{2,28}$	0.5	1.7	
336089.2.....	$23_{3,21}$–$23_{2,22}$	9.2	221.3	
336669.6.....	$16_{7,9}$–$17_{6,12}$	4.1	65.3	
338306.0.....	$18_{4,14}$–$18_{3,15}$	14.9	391.8	
338611.8.....	$20_{1,19}$–$19_{2,18}$	<22.9	<395.5	2
340316.4.....	$28_{2,26}$–$28_{1,27}$	8.4	169.5	
341275.5.....	$21_{8,14}$–$22_{7,15}$	2.6	41.6	
342761.6.....	$34_{3,31}$–$34_{2,32}$	2.9	37.4	
345149.0.....	$5_{5,1}$–$6_{4,2}$	2.5	28.3	3
345338.5.....	$13_{2,12}$–$12_{1,11}$	<27.6	<682.5	4
345448.8.....	$26_{9,17}$–$27_{8,20}$	0.8	5.1	
346523.9.....	$16_{4,12}$–$16_{3,13}$	<40.4	<1407.6	5
346652.2.....	$19_{1,19}$–$18_{0,18}$	20.7	601.1	
348387.8.....	$24_{2,22}$–$23_{3,21}$	10.0	<200.0	6
350862.7.....	$10_{6,4}$–$11_{5,7}$	5.5	11.6	7
351257.2.....	$5_{3,3}$–$4_{2,2}$	16.4	<466.4	8
351873.9.....	$14_{4,10}$–$14_{3,11}$	14.5	372.1	
355045.5.....	$12_{4,8}$–$12_{3,9}$	15.0	<438.8	9
356040.6.....	$15_{7,9}$–$16_{6,10}$	3.4	<45.8	
356755.2.....	$10_{4,6}$–$10_{3,7}$	<21.3	<127.2	10
357165.4.....	$13_{4,10}$–$13_{3,11}$	16.1	470.0	
357241.2.....	$15_{4,12}$–$15_{3,13}$	14.6	429.5	
357387.6.....	$11_{4,8}$–$11_{3,9}$	17.2	490.8	
357581.4.....	$8_{4,4}$–$8_{3,5}$	21.8	605.3	
357671.8.....	$9_{4,6}$–$9_{3,7}$	22.8	<733.0	11
357892.4.....	$7_{4,4}$–$7_{3,5}$	23.2	623.0	12
357926.0.....	$6_{4,2}$–$6_{3,3}$	20.0	468.3	12
357962.9.....	$17_{4,14}$–$17_{3,15}$	19.5	466.6	12
358013.1.....	$5_{4,2}$–$5_{3,3}$	19.2	381.7	13, 14
358038.1.....	$4_{4,0}$–$4_{3,1}$	14.5	250.8	14
358215.6.....	$20_{0,20}$–$19_{1,19}$	25.5	753.3	
359151.2.....	$25_{3,23}$–$25_{2,24}$	9.3	238.4	
359770.7.....	$19_{4,16}$–$19_{3,17}$	15.5	501.6	
$SO_2(v_2 = 1)$:				
336760.7.....	$20_{1,19}$–$19_{2,18}$	0.8	10.4	15
337191.5.....	$12_{2,11}$–$11_{1,10}$	...	...	16
337892.2.....	$21_{2,20}$–$21_{1,21}$	1.1	7.2	17
338376.3.....	$8_{2,6}$–$7_{1,7}$	0.4	5.5	
330259.1.....	$19_{0,19}$–$18_{1,18}$	0.4	1.1	
342436.4.....	$23_{3,21}$–$23_{2,22}$	0.7	5.1	
343923.8.....	$24_{2,22}$–$23_{3,21}$	0.1	1.1	
346365.6.....	$34_{3,31}$–$34_{2,32}$	0.5	2.8	
346379.2.....	$19_{1,19}$–$18_{0,18}$	0.8	5.0	
346591.8.....	$18_{4,14}$–$18_{3,15}$	<1.2	<7.5	18
354624.8.....	$46_{5,41}$–$46_{4,42}$	0.4	1.3	
354800.0.....	$16_{4,12}$–$16_{3,13}$	...	...	19
357087.0.....	$5_{3,3}$–$4_{2,2}$	2.6	28.7	

NOTES.—(1) Lower limits for line intensity and integrated area due to high atmospheric noise and improper sideband cleaning. (2) Blend with CH_3OH at 338615.0. (3) Blend with $^{13}CH_3OH$ at 345132.6 and $^{34}SO_2$ at 345168.8. (4) Blend with $H^{13}CN$ at 345339.8. (5) Blend with SO at 346528.5. (6) Blend with *U* line at 348373. (7) Blend with $CH_3CN(v_8 = 1)$ at 350842.7. (8) Blend with CH_3OH at 351236.7. (9) Blend with $H_2{}^{13}CO$ at 355028.7. (10) Blend with HCO^+ at 356734.3. (11) Blend with $^{13}CH_3OH$ at 357657.9. (12) Blend of SO_2 lines at 357892.4, 357926.0, and 357962.9. (13) Blend with $HCOOCH_3$ lines at 357989.8 and 357995.6. (14) Blend of SO_2 lines at 358013.1 and 358038.1. (15) Questionable identification. (16) Blend with ^{33}SO at 337195.0. (17) Blend with $CH_3OH(v_t = 2)$ at 337877.5. (18) Blend with $^{33}SO_2$ at 3465590.5. (19) Blended with ghost.

TABLE 12

TRANSITIONS OF $^{34}SO_2$ AND $^{33}SO_2$

ν (MHz)	$J_{K-,K+}$	T_R^* (K)	$\int T_R^* d\nu$ (K km s^{-1})	Notes
$^{34}SO_2$:				
329499.7.....	$5_{5,1}$–$6_{4,2}$	0.7	6.4	
330191.2.....	$8_{2,6}$–$7_{1,7}$	1.8	17.4	1
330667.6.....	$21_{2,20}$–$21_{1,21}$	1.6	16.2	2
332173.7.....	$23_{3,21}$–$23_{2,22}$	1.1	12.6	
332836.3.....	$16_{4,12}$–$16_{3,13}$	3.0	59.2	
338785.8.....	$14_{4,10}$–$14_{3,1}$	2.5	31.8	
342208.9.....	$5_{3,3}$–$4_{2,2}$	<3.4	<50.5	3
342332.1.....	$12_{4,8}$–$12_{3,9}$	<2.4	<28.2	4
344245.4.....	$10_{4,6}$–$10_{3,7}$	<3.6	<52.8	5
344581.1.....	$19_{1,19}$–$18_{0,18}$	5.1	114.9	
344808.0.....	$13_{4,10}$–$13_{3,11}$	3.0	51.7	6
344987.6.....	$15_{4,12}$–$15_{3,13}$	4.2	126.7	
344998.2.....	$11_{4,8}$–$11_{3,9}$	3.8		
345168.8.....	$8_{4,4}$–$8_{3,5}$	2.9	61.1	7
345285.7.....	$9_{4,6}$–$9_{3,7}$	2.8	55.7	8
345519.7.....	$7_{4,4}$–$7_{3,5}$	1.7	14.5	
345553.2.....	$6_{4,2}$–$6_{3,3}$	0.8	3.7	
345651.4.....	$5_{4,2}$–$5_{3,3}$	1.4	12.8	
345929.4.....	$17_{4,14}$–$17_{3,15}$	3.7	59.3	9
348117.6.....	$19_{4,16}$–$19_{3,17}$	2.6	35.8	10
350619.6.....	$34_{4,30}$–$33_{5,29}$	1.1	11.1	
352082.9.....	$21_{4,18}$–$21_{3,19}$	0.9	5.4	
356222.4.....	$25_{3,23}$–$25_{2,24}$	0.9	12.0	
357102.2.....	$20_{0,20}$–$19_{1,19}$	3.7	51.8	
358347.3.....	$23_{4,20}$–$23_{3,21}$	2.9	31.7	
358988.0.....	$15_{2,14}$–$14_{1,13}$	2.2	58.4	
359651.8.....	$24_{2,22}$–$23_{3,21}$	0.9	7.6	
$^{33}SO_2$:				
340527.0.....	$20_{1,19}$–$19_{2,18}$	0.3	4.5	
345584.6.....	$19_{1,19}$–$18_{0,18}$	0.8	5.4	
346590.5.....	$5_{3,3}$–$4_{2,2}$	0.5	<3.9	11
350304.0.....	$10_{4,6}$–$10_{3,7}$	0.9	4.9	
350788.7.....	$14_{4,10}$–$14_{3,11}$	0.7	4.9	
351178.5.....	$8_{4,4}$–$8_{3,5}$	1.1	4.9	

NOTES.—(1) Blend with $^{13}CH_3OH$ at 330194.0. (2) Blend with CH_3CN at 330665.2. (3) Blend with $HCOOCH_3$ at 342230.1 and 342238.5. (4) Blend with $HCOOCH_3$ at 342342.3. (5) Blend with $HC^{15}N$ at 344200.3 and SO at 344310.6. (6) Blend with *U* line at 344796. (7) Blend with SO_2 at 345149.0. (8) Blend with SO_2 at 345338.5 and $H^{13}CN$ at 345339.8. (9) Blend with wing of CO(3–2) at 345796.0 and CH_3OH at 345919.2. (10) Blend with $^{13}CH_3OH$ at 348100.6. (11) Blend with SO_2 ($v_2 = 1$) at 346591.8.

SO rotation temperature increases to 83 K. In fact, the $^{32}SO/^{34}SO$ line ratio suggests an optical depth of 5–6 at the peak. The derived rotation temperatures and column densities are consistent with the results of J84, B87, T91, and S94. Since all line shapes are vastly dominated by the wings, the existence or absence of the other velocity components is

TABLE 13

TRANSITIONS OF H_2O, HDO, HDS, AND NH_2D

Molecule	ν (MHz)	$J_{K-,K+}(, v_F)$	T_R^* (K)	$\int T_R^* d\nu$ (K km s^{-1})	Notes
H_2O.....	325152.9	$5_{1,5}$–$4_{2,2}$	32.8	701.4	
HDO.....	335395.5	$3_{3,1}$–$4_{2,2}$	1.8	17.1	
	356839.6	$5_{3,2}$–$6_{1,5}$	1.2	8.7	
HDS	333278.5	$2_{0,2}$–$1_{1,1}$	2.0	17.1	1
NH_2D.....	332780.9	$1_{0,1}$, 1_0–$0_{0,0}$, 0_1			
	332781.8	$1_{0,1}$, 1_2–$0_{0,0}$, 0_1	0.7	5.8	2
	332782.4	$1_{0,1}$, 1_1–$0_{0,0}$, 0_1			

NOTES.—(1) Blend with CH_3CH_2CN at 333274.7, questionable identification. (2) Blend of $F = 0$–1, 2–1, and 1–1 lines with CH_3CH_2CN at 332775 and *U* line at 332789.

TABLE 14

TRANSITIONS OF CH_3OH

ν (MHz)	$J_{K-,K+}$	T_R^* (K)	$\int T_R^* d\nu$ (K km s^{-1})	Notes
CH_3OH:				
326630.6.....	$10_{6,5}A^-$–$10_{5,5}A^+$	9.9	52.4	1
326961.2.....	$10_{5,6}E$–$9_{5,5}E$	6.4	36.4	
327317.2.....	$12_{7,5}A^-$–$11_{7,4}A^-$	5.3	48.6	1
327408.2.....	$17_{11,6}A^+$–$18_{11,7}A^+$	2.4	10.5	1
327487.2.....	$13_{9,5}E$–$14_{9,6}E$	1.8	11.2	1
328468.8.....	$20_{12,9}A^+$–$19_{12,8}A^+$	1.4	9.9	
329632.9.....	$12_{7,5}A^+$–$11_{7,4}A^+$	6.1	37.0	
330355.3.....	$20_{12,9}A^-$–$19_{12,8}A^-$	1.1	<6.6	2
330793.9.....	$8_{3,6}E$–$9_{4,6}E$	4.9	27.4	
331221.6.....	$16_{8,9}E$–$15_{7,9}E$	3.0	20.1	
331502.4.....	$11_{6,5}A^-$–$11_{6,6}A^+$	9.1	76.6	3
332990.6.....	$22_{10,12}E$–$21_{9,12}E$	1.2	5.9	
335133.5.....	$2_{2,0}A^-$–$3_{2,1}A^+$	5.5	37.6	
335582.0.....	$7_{4,3}A^+$–$6_{4,3}A^+$	16.8	132.2	
336438.3.....	$14_{11,4}A^\pm$–$15_{11,5}A^\pm$	2.8	15.3	
336865.1.....	$12_{7,6}A^-$–$12_{6,6}A^+$	15.0	123.2	
337135.9.....	$3_{3,0}E$–$4_{3,1}E$	5.9	28.9	
337463.7.....	$7_{7,1}A^+$–$6_{6,0}A^+$	2.1	13.6	
337490.5.....	$7_{1,7}E$–$6_{0,6}E$	<2.6	<14.6	4
338124.5.....	$7_{4,4}E$–$6_{3,3}E$	13.6	102.1	
338344.6.....	$3_{4,0}E$–$6_{3,4}E$	17.4	<141.2	5
338404.6.....	$7_{7,1}E$–$6_{6,0}E$	18.2	<149.3	6
338408.7.....	$7_{4,4}A^+$–$6_{3,3}A^+$			
338431.0.....	$7_{1,7}E$–$6_{0,6}E$	4.6	29.9	
338442.3.....	$7_{7,1}A^\pm$–$6_{0,0}A^\pm$	6.2	35.9	
338456.5.....	$7_{1,6}E$–$6_{1,6}E$	6.2	41.6	
338475.3.....	$7_{6,1}E$–$6_{6,1}E$	6.1	39.2	
338486.3.....	$7_{6,1}A^\pm$–$6_{6,1}A^\pm$	7.0	46.3	
338504.1.....	$7_{2,6}E$–$6_{1,5}E$	9.3	49.7	
338512.6.....	$7_{6,2}A^\mp$–$6_{5,1}A^\mp$	13.9	105.7	
338512.9.....	$7_{5,3}A^-$–$6_{4,2}A^-$			
338530.3.....	$7_{6,2}E$–$6_{5,1}E$	9.1	59.6	
338540.8.....	$7_{5,2}A^+$–$6_{5,2}A^+$	15.8	127.0	
338543.2.....	$7_{5,2}A^-$–$6_{5,2}A^-$			
338559.9.....	$7_{2,5}E$–$6_{2,5}E$	10.3	69.5	
338583.2.....	$7_{5,2}E$–$6_{5,2}E$	12.5	<99.9	7
338615.0.....	$7_{4,3}E$–$6_{4,3}E$	<22.5	<169.3	7
338639.9.....	$7_{5,3}A^+$–$6_{4,2}A^+$	12.6	<100.1	7
338721.6.....	$7_{5,3}E$–$6_{4,2}E$	17.8	35.3	
338722.9.....	$7_{3,5}E$–$6_{2,4}E$			
340141.2.....	$2_{2,0}A^+$–$3_{2,1}A^+$	<10.8	<35.7	8
340394.2.....	$16_{11,5}A^-$–$17_{11,6}A^-$	5.1	27.8	
340394.3.....	$16_{11,5}A^+$–$17_{11,6}A^+$			
341415.6.....	$7_{4,3}A^-$–$6_{4,3}A^-$	14.2	119.1	
342729.8.....	$13_{7,6}A^-$–$13_{7,7}A^+$	11.4	107.4	
344110.4.....	$18_{10,8}E$–$17_{10,7}E$	3.6	20.8	
344444.7.....	$19_{10,9}A^+$–$18_{10,8}A^+$	2.9	18.3	
345904.2.....	$16_{9,8}A^-$–$15_{9,7}A^-$	<5.9	<46.7	9
345919.2.....	$18_{8,11}E$–$17_{7,11}E$	...	...	9, 10
346202.8.....	$5_{5,1}A^-$–$6_{5,2}A^-$	4.9	30.7	
346204.4.....	$5_{5,1}A^+$–$6_{5,2}A^+$			
349107.0.....	$14_{8,7}A^-$–$14_{7,7}A^+$	5.9	55.7	
350687.7.....	$4_{2,2}E$–$3_{1,2}E$	14.7	<135.1	11
350905.1.....	$1_{1,0}A^+$–$0_{0,0}A^+$	12.1	84.5	12
351236.7.....	$9_{7,2}E$–$10_{7,3}E$	<10.1	<58.7	13
355603.0.....	$13_{7,7}A^+$–$12_{7,6}A^+$	13.9	114.3	
356006.6.....	$15_{8,7}A^-$–$15_{8,8}A^+$	11.7	106.6	
356627.3.....	$23_{10,14}E$–$22_{9,14}E$	2.5	19.2	
358414.9.....	$10_{8,2}E$–$11_{8,3}E$	4.6	30.8	
358605.8.....	$4_{3,2}E$–$3_{2,2}E$	<18.7	<130.3	14
$CH_3OH(v_t = 1)$:				
329272.6.....	$23_{13,10}E$–$23_{13,11}E$	0.8	3.3	
334426.6.....	$3_{2,2}A^-$–$2_{1,1}A^+$	2.5	11.4	
334620.7.....	$22_{13,10}E$–$22_{12,10}E$	0.3	1.6	
337297.4.....	$7_{4,3}A^+$–$6_{4,3}A^+$	5.5	40.4	

TABLE 14—*Continued*

ν (MHz)	$J_{K-,K+}$	T_R^* (K)	$\int T_R^* dv$ (K km s^{-1})	Notes
337284.3.....	$7_{4,4}\,A^-$–$6_{3,3}\,A^-$	0.5	3.0	
337519.1.....	$7_{5,2}\,A^+$–$6_{5,2}\,A^+$	2.9	16.6	
337546.1.....	$7_{6,1}\,A^\pm$–$6_{6,1}\,A^\pm$	<3.2	<22.4	15
337605.3.....	$7_{3,5}\,E$–$6_{2,4}\,E$	<4.9	<21.1	15, 16
337610.6.....	$7_{2,5}E$–$6_{2,5}\,E$	<4.9	<25.8	16
337625.6.....	$7_{5,3}\,A^+$–$6_{4,2}\,A^+$	4.9	<31.6	16
337635.6.....	$7_{5,3}\,A^-$–$6_{4,2}\,A^-$	<5.1	<21.3	16
337642.4.....	$7_{4,3}\,E$–$6_{4,3}\,E$	<7.1	<54.2	16
337643.8.....	$7_{4,4}\,E$–$6_{3,3}\,E$			
337646.0.....	$7_{2,6}\,E$–$6_{1,5}\,E$			
337648.2.....	$7_{1,6}\,E$–$6_{1,6}\,E$			
337655.2.....	$7_{5,2}\,A^\mp$–$6_{5,2}\,A^\mp$	<4.1	<80.4	16
337671.2.....	$7_{5,3}\,E$–$6_{4,2}\,E$	2.8	16.8	
337685.3.....	$7_{6,1}\,E$–$6_{6,1}\,E$	3.0	18.9	
337685.8.....	$7_{6,2}\,A^\mp$–$6_{5,1}\,A^\mp$			
337707.6.....	$7_{3,4}\,E$–$6_{3,4}\,E$	<3.3	<25.9	17
337748.8.....	$7_{4,4}\,A^+$–$6_{3,3}\,A^+$	2.8	7.8	
337969.4.....	$7_{4,3}\,A^-$–$6_{4,3}\,A^-$	3.3	18.0	
343897.2.....	$10_{4,6}\,E$–$11_{4,7}\,E$	0.3	2.6	
359676.9.....	$14_{9,6}\,E$–$14_{8,6}\,E$	1.7	13.6	
355964.3.....	$16_{10,7}\,E$–$16_{9,7}\,E$	0.8	5.5	
$CH_3OH(v_t = 2)$:				
336605.9.....	$7_{4,3}\,A^+$–$6_{4,3}\,A^+$	<1.4	<8.3	18
336970.4.....	$7_{7,1}\,A^\pm$–$6_{6,0}\,A^\pm$	0.3	0.7	
337021.4.....	$7_{2,5}\,E$–$6_{2,5}\,E$	0.3	0.5	
337029.6.....	$7_{5,3}\,A^\mp$–$6_{4,2}\,A^\mp$	0.5	2.2	
337098.6.....	$7_{6,1}\,A^\mp$–$6_{6,1}\,A^\mp$	0.3	0.7	
337113.9.....	$7_{4,3}\,E$–$6_{4,3}\,E$	0.5	1.8	
337159.2.....	$7_{7,1}\,E$–$6_{6,0}\,E$	0.3	0.9	
337252.2.....	$7_{5,2}\,A^\mp$–$6_{5,2}\,A^\mp$	0.5	1.8	
337273.5.....	$7_{6,2}\,A^\pm$–$6_{5,1}\,A^\pm$	0.9	4.5	
337279.1.....	$7_{3,5}\,E$–$6_{2,4}\,E$			
337284.3.....	$7_{4,4}\,A^+$–$6_{3,3}\,A^+$	2.0	8.8	
337312.3.....	$7_{3,4}\,E$–$6_{3,4}\,E$	1.6	7.4	
337877.5.....	$7_{4,3}\,A^-$–$6_{4,3}\,A^-$	1.4	8.0	19

NOTES.—(1) Noisy part of the spectrum, parameters not reliable. (2) Blend with $^{13}CH_3OH$ at 330350.0 and 330362.0. (3) Blend with CH_3CH_2CN at 331487.3. (4) Blend with $HCOOCH_3$ at 337489.7. (5) Blend with wing of SO_2 at 338306.0 and $HCOOCH_3$ at 338355.0. (6) Blend with $HCOOCH_3$ at 338396.4. (7) Blend with SO_2 at 338611.8. (8) Blend with ghost at 340118.5 and CH_3CH_2CN at 340151.3. (9) Blend with the wing of CO at 345796.0. (10) Blend with $^{34}SO_2$ at 345929.4. (11) Blend with NO at 350698.5, 350690.8, and 350694.8. (12) Blend with $HCOOCH_3$ at 350919.6. (13) Blend with SO_2 at 351257.2. (14) Blend with $HCOOCH_3$ at 358591.6. (15) Blend with ^{34}SO at 337582.2. (16) Band of partly blended CH_3OH lines. Due to blending, individual line strengths are hard to estimate. (17) Blend with CH_3OCH_3 at 337712.4. (18) Blend with CH_3CH_2CN at 336613.9. (19) Blend with $SO_2(v_2 = 1)$ at 337892.2.

hard to establish, even for $S^{18}O$. The plateau component here, as for SO_2, is best fitted by two components with large line widths (20–30 km s^{-1}) and center velocities of $\approx$4 and $\approx$11 km s^{-1}, respectively.

NO.—The existence of nitric oxide ($^2\Pi_{1/2}$) in the hot core was established tentatively by Wootten, Loren, & Bally (1984) and in the earlier line survey of Blake et al. (1986), where it was blended with a CH_2CH_3CN line. It was shown to be present in the Orion hot core spectra of Gérin et al. (1992). In our band, we find two hyperfine split Λ doubling components of the $J = 7/2$–$5/2$ transition. Unfortunately, the strongest hyperfine components of one of the Λ doubling components (the $F = 9/2$–$7/2$, $7/2$–$5/2$, and $5/2$–$3/2$ f transitions) are blended with CH_3OH, but the $F = 9/2$–$7/2$, $7/2$–$5/2$, and $5/2$–$3/2$ e transitions show up strongly. The line shape is dominated by the extended ridge velocity component.

TABLE 15

TRANSITIONS OF $^{13}CH_3OH$

ν (MHz)	$J_{K-,K+}$	T_R^* (K)	$\int T_R^* dv$ (K km s^{-1})	Notes
330001.8.....	$7_{4,4}\,E$–$6_{3,3}\,E$	1.1	2.0	
330194.0.....	$7_{3,4}\,E$–$6_{3,4}\,E$	1.8	17.4	1
330252.8.....	$7_{4,4}\,A^+$–$6_{3,3}\,A^+$	<1.1	<3.7	2
330336.9.....	$7_{2,6}\,E$–$6_{1,5}\,E$	0.3	1.1	
330342.5.....	$7_{6,2}\,A^\pm$–$6_{5,1}\,A^\pm$	0.5	4.2	
330350.0.....	$7_{5,3}\,A^-$–$6_{4,2}\,A^-$	0.7	1.4	3
330362.0.....	$7_{6,2}\,E$–$6_{5,1}E$	0.4	1.4	3
330371.3.....	$7_{5,2}\,A^+$–$6_{5,2}\,A^+$	1.1	5.1	
330373.4.....	$7_{5,2}\,A^-$–$6_{5,2}\,A_-$			
330408.4.....	$7_{5,2}\,E$–$6_{5,2}\,E$	<2.0	<8.0	4
330442.4.....	$7_{4,3}\,E$–$6_{4,3}\,E$	0.9	3.3	5
330463.7.....	$11_{6,5}\,A^-$–$11_{6,6}\,A^+$	1.8	6.6	
330464.9.....	$7_{5,3}\,A^+$–$6_{4,2}\,A^+$			
330535.2.....	$7_{5,3}\,E$–$6_{4,2}\,E$	2.1	11.2	
330535.9.....	$7_{3,5}\,E$–$6_{2,4}\,E$			
438308.9.....	$7_{4,3}\,A^-$–$6_{4,3}\,A^-$	2.9	27.4	6
335559.9.....	$12_{7,6}\,A^-$–$12_{6,6}\,A^+$	2.8	16.7	
338760.4.....	$13_{7,7}\,A^+$–$12_{7,6}\,A^+$	1.7	9.5	
341131.2.....	$13_{7,6}\,A^-$–$13_{7,7}\,A^+$	2.2	14.3	
345132.6.....	$4_{2,2}\,E$–$3_{1,2}\,E$	2.4	19.7	7
347187.7.....	$14_{8,7}\,A^-$–$14_{7,7}\,A^-$	2.4	19.9	
347845.8.....	$21_{12,9}\,A^+$–$20_{12,8}\,A^+$	1.4	9.3	
348100.6.....	$11_{6,6}\,E$–$10_{6,5}\,E$	2.2	24.3	
350103.1.....	$1_{1,0}\,A^+$–$0_{0,0}\,A^+$	1.1	1.6	
353739.3.....	$15_{8,7}\,A^-$–$15_{8,8}\,A^+$	3.4	26.1	
354445.9.....	$4_{3,2}\,E$–$3_{2,2}\,E$	<2.6	<12.4	8
356874.9.....	$13_{8,6}\,A^-$–$12_{8,5}\,A^-$	0.9	4.2	
357657.9.....	$7_{5,3}\,E$–$6_{4,3}\,E$	...	...	9

NOTES.—(1) Blend with $^{34}SO_2$ at 330191.2. (2) Blend with $HCOOCH_3$ at 330256.0. (3) Blend with CH_3OH at 330355.3. (4) Blend with CH_3OCH_3 lines at 330405.4, 330406.5, and 330407.6. (5) Blend with CH_3CN at 330437.4. (6) Blend with CH_3CH_2CN at 333108.8. (7) Blend with wing of SO_2 at 345149.0. (8) Blend with wing of HCN(4–3) at 354505.5. (9) Blend with SO_2 at 357671.8.

NS.—Nitrogen sulfide ($^2\Pi_{1/2}$) was detected in the $J = 15/2$–$13/2$ transition. This is the first detection of this molecule in Orion. It was found previously in Sgr B2 by Gottlieb et al. (1975) and Kuiper et al. (1975) and was also present in the line survey of Cummins, Linke, & Thaddeus (1986). The frequencies of NS were in gaps or off the edges of previous, lower frequency surveys in Orion. The line velocity points to a hot core origin of this line, somewhat unusual for a radical.

CN.—The cyanide radical ($^2\Sigma^+$) is present in several hyperfine components of the $N = 3$–2, $J = 7/2$–$5/2$, and $J = 5/2$–$3/2$ transitions. The hyperfine ratios suggest that

TABLE 16

TRANSITIONS OF CH_3OD

ν (MHz)	$J_{K-,K+}$	T_R^* (K)	$\int T_R^* dv$ (K km s^{-1})	Notes
327608.7.....	$4_{3,1}\,A^-$–$4_{3,2}\,A^+$	0.8	3.2	1
332758.3.....	$3_{3,2}\,E$–$2_{2,1}E$	0.7	5.0	
334264.9.....	$7_{3,4}\,E$–$6_{3,3}\,E$	<1.6	<8.7	2
335089.7.....	$6_{4,2}\,A^-$–$6_{4,3}\,A^+$	0.3	2.0	3
351469.3.....	$9_{6,4}\,A^-$–$9_{5,4}\,A^+$	0.8	6.3	
357066.2.....	$8_{5,4}\,A^+$–$7_{4,3}\,A^+$	<1.1	<4.6	4

NOTES.—(1) Blend with ^{13}CO ghost. (2) Blend with HCOOH line at 334265.8. (3) Blend with DNCO at 335096.5. (4) Blend with C_2H_5OH at 357065.6.

TABLE 17

TRANSITIONS OF C_2H_5OH

ν (MHz)	$J_{K-,K+}$	T_R^* (K)	$\int T_R^* dv$ (K km s^{-1})	Notes
328884.5.....	$11_{2,9}$–$10_{1,10}$	...	...	1
330632.9.....	$20_{0,20}$–$19_{1,19}$	...	...	1
331319.3.....	$20_{1,20}$–$19_{0,19}$	...	...	1
331653.5.....	$11_{3,8}$–$10_{2,9}$	...	...	1
334770.2.....	$20_{1,19}$–$19_{2,18}$	...	...	1
335947.8.....	$13_{3,11}$–$12_{2,10}$	...	...	1
336626.4.....	$19_{2,18}$–$18_{1,17}$	0.9	3.4	
337281.9.....	$20_{7,13}$–$20_{6,14}$	...	...	1
337318.9.....	$20_{7,14}$–$20_{6,15}$	<1.6	<7.4	2
337742.9.....	$19_{7,13}$–$19_{6,14}$	<0.9	<3.6	2
338095.1.....	$18_{7,11}$–$18_{6,12}$	...	...	1
338105.7.....	$18_{7,12}$–$18_{6,11}$	...	...	1
338668.3.....	$16_{7,9}$–$16_{6,10}$	0.4	1.8	
332670.8.....	$16_{7,10}$–$16_{6,11}$			
338883.1.....	$15_{7,8}$–$15_{7,9}$	<1.4	<8.0	2
338884.3.....	$15_{7,9}$–$15_{6,10}$			
339058.2.....	$14_{7,7}$–$14_{6,8}$	0.7	4.2	
339058.7.....	$14_{7,8}$–$14_{6,9}$			
339198.9.....	$13_{7,6}$–$13_{6,7}$	0.5	2.8	
339199.1.....	$13_{7,7}$–$13_{6,8}$			
339310.2.....	$12_{7,5}$–$12_{6,6}$	...	...	3
339310.2.....	$12_{7,6}$–$12_{6,7}$			
339396.3.....	$11_{7,4}$–$11_{6,5}$	...	...	1
339396.3.....	$11_{7,5}$–$11_{6,6}$			
339461.3.....	$10_{7,3}$–$10_{6,4}$	0.5	2.9	
339461.3.....	$10_{7,4}$–$10_{6,5}$			
339508.9.....	$9_{7,2}$–$9_{6,3}$	0.3	2.1	
339508.9.....	$9_{7,3}$–$9_{6,4}$			
339542.4.....	$8_{7,1}$–$8_{6,2}$	0.4	3.3	
339542.4.....	$8_{7,1}$–$8_{6,2}$			
339542.4.....	$8_{7,2}$–$8_{6,3}$			
339564.7.....	$7_{7,0}$–$7_{6,1}$	0.3	2.5	
339564.7.....	$7_{7,1}$–$7_{6,2}$			
339977.4.....	$9_{4,6}$–$8_{3,5}$	...	...	4
340188.3.....	$6_{5,2}$–$5_{4,1}$	1.8	11.4	
340188.4.....	$6_{5,1}$–$5_{4,2}$			
340418.9.....	$9_{4,5}$–$8_{3,6}$	0.8	3.6	
347915.8.....	$20_{4,17}$–$19_{4,16}$	1.6	13.2	
350542.3.....	$20_{2,19}$–$19_{1,18}$	...	...	1
353032.3.....	$12_{3,9}$–$11_{2,10}$	...	...	5
357065.6.....	$10_{4,7}$–$9_{3,6}$	<1.1	<4.6	6
358106.2.....	$15_{3,13}$–$14_{2,12}$	0.8	2.6	

NOTES.—(1) Spectral feature is present, but too weak for reliable identification. (2) Intensity too high based on rotation diagram. (3) Blend with wing of SO at 339341.5. (4) Blend with CH_3CH_2CN at 339968.2. (5) Blend with complex structure. (6) Blend with CH_3OD at 357066.2.

the line is somewhat optically thick, but definitive conclusions cannot be drawn because the strength of the low line intensity lines is determined poorly due to low-level line contamination. As for NO, the shape is consistent with the extended ridge component.

CCH.—Ethynyl ($^2\Sigma$) has been observed in the $N = 4$–3 transitions. Both the $J = 9/2$–$7/2$ and the $J = 7/2$–$5/2$ fine-structure components are detected, but the latter is blended with $CH_3CN(19_3$–$18_3)$. Due to this, the hyperfine ratios and thus the optical depth cannot be determined. The line velocity and width are consistent with an extended ridge origin.

C_2S.—Both T91 and ZM93 claim the detection of low-lying transitions of C_2S ($^2\Sigma$). We see no convincing evidence

TABLE 18

TRANSITIONS OF H_2CO, $H_2{}^{13}CO$, $H_2C^{18}O$, AND H_2CS

ν (MHz)	$J_{K-,K+}$	T_R^* (K)	$\int T_R^* dv$ (K km s^{-1})	Notes
H_2CO:				
351768.7.....	$5_{1,5}$–$4_{1,4}$	20.4	364.2	
$H_2{}^{13}CO$:				
343325.7.....	$5_{1,5}$–$4_{1,4}$	<5.7	<48.9	1
353811.9.....	$5_{0,5}$–$4_{0,4}$	2.2	12.1	
354898.7.....	$5_{2,4}$–$4_{2,3}$	0.9	3.3	
355028.7.....	$5_{4,2}$–$4_{4,1}$	...	...	2
355028.7.....	$5_{4,1}$–$4_{4,0}$			
355190.9.....	$5_{3,3}$–$4_{2,2}$	2.4	18.3	
355202.6.....	$5_{3,2}$–$4_{3,1}$	2.0	14.9	
356176.1.....	$5_{2,3}$–$4_{2,2}$	1.7	10.5	
$H_2C^{18}O$:				
335816.0.....	$5_{1,5}$–$4_{1,4}$	0.5	1.4	
HDCO:				
335096.8.....	$5_{1,4}$–$4_{1,3}$	1.8	8.6	3
H_2CS:				
338080.8.....	$10_{1,10}$–$9_{1,9}$	4.5	23.0	
342944.4.....	$10_{0,10}$–$9_{0,9}$	3.6	22.1	
343308.5.....	$10_{4,7}$–$9_{4,6}$	5.5	38.4	
343308.5.....	$10_{4,6}$–$9_{4,5}$			
343319.6.....	$10_{2,9}$–$9_{2,8}$	<5.7	<48.9	4
343408.1.....	$10_{3,8}$–$9_{3,7}$	2.8	23.4	
343412.3.....	$10_{3,7}$–$9_{3,6}$			
343810.8.....	$10_{2,8}$–$9_{2,7}$	1.4	7.1	
348531.9.....	$10_{1,9}$–$9_{1,8}$	7.1	35.3	

NOTES.—(1) Blend with $H_2{}^{13}CO$ line at 343319.6. (2) Blend with SO_2 line at 355045.5. (3) Blend with CH_3OD at 335089.7. (4) Blend with $H_2{}^{13}CO$ line at 343325.7.

TABLE 19

TRANSITIONS OF HNCO AND HCOOH

ν (MHz)	$J_{K-,K+}$	T_R^* (K)	$\int T_R^* dv$ (K km s^{-1})	Notes
HNCO:				
328117.4.....	$24_{1,24}$–$25_{0,25}$	0.5	2.0	
328444.3.....	$15_{1,15}$–$14_{1,14}$	3.0	16.3	
329459.9.....	$15_{3,12}$–$14_{3,11}$	<1.3	<7.2	1
329459.9.....	$15_{3,13}$–$14_{3,13}$			
329573.5.....	$15_{2,14}$–$14_{2,13}$	1.4	13.0	
329585.1.....	$15_{2,13}$–$14_{2,12}$	1.4	9.2	
329664.5.....	$15_{0,15}$–$14_{0,14}$	6.7	79.2	
330848.8.....	$15_{1,14}$–$14_{1,13}$	<3.6	<45.5	2
350333.3.....	$16_{1,16}$–$15_{1,15}$	2.5	23.3	
351417.1.....	$16_{3,14}$–$15_{3,13}$	1.1	7.0	
351417.2.....	$16_{3,13}$–$15_{3,12}$			
351551.9.....	$16_{2,14}$–$15_{2,13}$	1.7	12.0	
351633.5.....	$16_{0,16}$–$15_{0,15}$	5.0	77.8	
351994.8.....	$23_{1,23}$–$24_{0,24}$	0.8	4.5	
352897.9.....	$16_{1,15}$–$15_{1,14}$	2.2	17.6	
HCOOH:				
334265.8.....	$15_{2,14}$–$14_{2,13}$	<1.6	<8.7	3
338143.7.....	$15_{4,12}$–$14_{4,11}$	2.2	17.6	
338201.8.....	$15_{3,13}$–$14_{3,12}$	0.5	3.3	
338248.7.....	$15_{4,11}$–$14_{4,10}$	0.4	2.2	
340229.0.....	$15_{3,12}$–$14_{3,11}$	...	...	4
342521.2.....	$16_{1,16}$–$15_{1,15}$	0.7	1.4	5
343952.4.....	$15_{1,14}$–$14_{1,13}$	0.3	0.8	
346718.8.....	$15_{2,13}$–$14_{2,12}$	0.8	6.3	
356137.2.....	$16_{2,15}$–$15_{2,14}$	0.9	5.7	

NOTES.—(1) Blend with CH_2CHCN at 329461.4. (2) Blend wth CH_3CN at 330842.6. (3) Blend with CH_3OD at 334264.9. (4) Blend with CN at 340247.8. (5) Blend with $HCOOCH_3$ at 342525.3.

TABLE 20

TRANSITIONS OF CH_2CO AND NH_2CHO

ν (MHz)	J_{K_-,K_+}	T_R^* (K)	$\int T_R^* dv$ (K km s^{-1})	Notes
CH_2CO:				
340209.7.....	$17_{1,17}$–$16_{1,16}$	1.7	6.8	
343392.9.....	$17_{2,16}$–$16_{2,15}$	1.3	9.1	
NH_2CHO:				
336136.9.....	$16_{2,15}$–$15_{2,14}$	0.7	5.1	
339715.8.....	$16_{8,8}$–$15_{8,7}$	0.4	1.8	
339715.8.....	$16_{8,9}$–$15_{8,8}$			
339780.8.....	$16_{7,10}$–$15_{7,9}$	0.4	1.4	
339780.8.....	$16_{7,9}$–$15_{7,8}$			
339904.1.....	$16_{6,11}$–$15_{6,10}$	2.6	36.3	1
339904.1.....	$16_{6,10}$–$15_{6,9}$			
340491.1.....	$16_{3,14}$–$15_{3,13}$	2.4	18.4	2
340536.0.....	$16_{4,13}$–$15_{4,12}$	0.7	2.1	
349479.5.....	$16_{2,14}$–$16_{2,13}$	0.5	3.3	

NOTES.—(1) Possible blend with *U* line. (2) Blend with *U* line at 340496.

of this molecule, but our frequency range is unfavorable if the rotation temperature is as low as claimed by T91.

3.2.4. *Symmetric Rotors*

CH_3CN.—Methyl cyanide (acetonitrile) is detected in several *K*-components of the $J = 18$–17 and $J = 19$–18 transitions of both CH_3CN and $CH_3^{13}CN$. The $^{13}CH_3CN$ isotopomeric lines are distributed so unfortunately that they are all blended with other strong features. We detect also 20 lines of vibrationally excited CH_3CN in the $v_8 = 1$ state, 530 K above ground. The isotopomer ratios indicate optical depths of 5 for the $CH_3CN(18_2$–$17_2)$ line and 8 for the $CH_3CN(19_2$–$18_2)$ line. The very high rotation temperature of 445 K is most likely an artifact of these high optical depths. The levels with low excitation energies in our data are dominated by compact ridge and hot core emission, but plateau wings and components due to the extended ridge are also present. High-excitation lines show only the compact ridge and hot core components, and the vibrationally excited lines show exclusively the hot core. The isotopomeric lines are blended heavily and it is difficult to determine the origin, but the hot core component seems to dominate.

CH_3CCH.—Methyl acetylene (propyne) is detected in several *K*-components of the $J = 20$–19 and $J = 21$–20 transitions. The derived rotation temperature is much lower than for CH_3CN: 65 K. No information about the optical depths is available, since the ^{13}C isotopomers are not detected. The line velocity and line width are consistent with an extended ridge origin of the lines. Rotation temperature and column density are consistent with B87.

3.2.5. *Inorganic Asymmetric Rotors*

SO_2.—Sulphur dioxide is observed in the $^{32}SO_2$, $^{34}SO_2$, and $^{33}SO_2$ isotopomers and in some vibrationally excited ($v_2 = 1$) transitions of the main isotopomer. Lines from $SO^{18}O$ have been searched for but not conclusively identified. The ground-state lines clearly show hot core and strong plateau contributions, resulting in triangular line shapes. As for SO, the plateau component is best fitted by two Gaussians with large line widths (20–30 km s^{-1}) and center velocities of $\approx$4 and $\approx$11 km s^{-1}, respectively. The hot core component becomes more pronounced the higher the energy of the transition is, indicating a higher temperature or higher densities in the hot core than in the plateau component. The rotation temperature is 124 K, based on the integrated line intensities. No attempt has been made to separate different velocity components. The line velocities of the vibrationally excited SO_2, like those of other vibrationally excited lines, indicate a pure hot core origin. From the $^{32}SO_2/^{34}SO_2$ line ratio, we estimate peak optical depths of 1–7 for the $^{32}SO_2$ lines. Rotation temperatures and column densities are similar to those observed by the earlier studies.

H_2O *and* HDO.—The water maser line of $H_2^{16}O(5_{1,5}$–$4_{2,2})$ at 325 GHz was detected (see Menten, Melnick, & Phillips 1990 for a discussion). Two lines from high-excitation states of deuterated water are also clearly detected. The line velocity indicates a hot core origin of the line, as predicted by chemical models.

HDS.—One line at the frequency of deuterated hydrogen sulfide is detected. The identification is questionable, since HDS has not been detected before in Orion, although the ground-state line lies in the frequency range covered by S85. If the line is due to HDS, the line velocity is consistent with an extended or compact ridge origin of the line. No detectable lines of H_2S are present in the band.

NH_2D.—Deuterated ammonia has a very complex spectrum: it is an asymmetric rotor with inversion splitting and hyperfine splitting due to the ^{14}N nucleus. We have the ground-state transition in our band, which is split into two inversion transitions. One transition ($v = 1$–1) is detected, and the $v = 0$–0 transition is buried under a $^{34}SO_2$ line. The line is too weak to permit a determination of the origin via the velocity profile.

3.2.6. *Organic Asymmetric Rotors*

CH_3OH.—Methanol is detected in its $^{12}CH_3OH$, $^{13}CH_3OH$, and CH_3OD isotopomers. $^{12}CH_3OH$ shows a band of torsionally excited lines around 337.6 GHz. Another band around 338.5 GHz is blended heavily with the ground-state band of methanol, so that the torsionally excited lines could not be separated out. The rotation temperature of methanol is 155 K, while the rotation temperatures of $^{13}CH_3OH$ and torsionally excited methanol could not be determined because the lines are blended and the integrated line intensity could not be determined reliably. Methanol, like most of the other complex organic molecules, is known to be associated mainly with the compact ridge, but it also present in the hot core. The line velocities and widths we observe support that. Both rotation temperature and column density agree well with earlier studies.

C_2H_5OH.—Ethanol has been identified tentatively in Orion by T91, ZM93, and S94. We seem to find all transitions present in our band, but many of them are so weak that they cannot be identified conclusively. In addition to the $K_- = 7$–6 *Q*-branch transitions observed by S94, we observe other transitions outside their frequency range. Apart from three lines, which appear to be too strong and may be misidentified or blended, the rotation diagram looks sensible and gives a rotation temperature of 65 K. This temperature and the column density are in reasonable agreement with ZM93 and S94. Based on the velocity profile, a compact ridge origin of the lines seems most likely.

H_2CO.—Four isotopomers of formaldehyde are detected, one line each of H_2CO, $H_2C^{18}O$, and HDCO and

TABLE 21

TRANSITIONS OF $HCOOCH_3$

ν (MHz)	J_{K_-,K_+}	T_R^* (K)	$\int T_R^* dv$ (K km s^{-1})	Notes
325677.1.....	$26_{7,20}\,E$–$25_{7,19}\,E$	2.8	18.4	1
325694.4.....	$26_{7,20}\,A$–$25_{7,19}\,A$	2.2	17.2	1
327001.9.....	$12_{7,4}\,E$–$11_{6,5}\,E$	2.0	22.4	1
329364.2.....	$26_{7,19}\,E$–$25_{7,18}\,E$	...	...	2
329861.6.....	$27_{3,24}\,E$–$26_{3,23}\,E$	0.7	2.0	
329874.9.....	$27_{5,23}\,A$–$26_{5,22}\,A$	0.5	0.9	
330256.0.....	$10_{8,3}\,E$–$9_{7,3}\,E$	...	...	3
330276.4.....	$10_{8,2}\,E$–$9_{7,2}\,E$	0.3	0.4	
330323.9.....	$10_{8,3}\,A$–$9_{7,2}\,A$	1.1	6.6	
330323.9.....	$10_{8,2}\,A$–$9_{7,3}\,A$			
331149.3.....	$28_{6,23}\,E$–$27_{6,22}\,E$	1.3	6.2	
331159.6.....	$28_{4,25}\,A$–$27_{4,24}\,A$	1.3	8.4	
331460.0.....	$28_{5,23}\,E$–$27_{5,22}\,E$	0.9	6.1	
331469.5.....	$28_{3,25}\,A$–$27_{3,24}\,A$	0.9	5.0	
331775.9.....	$29_{2,27}\,A$–$28_{3,26}\,A$	0.9	6.7	
331784.2.....	$29_{5,25}\,E$–$28_{5,24}\,E$	1.2	6.6	
331792.1.....	$29_{3,27}\,A$–$28_{3,26}\,A$	1.4	13.8	
331795.9.....	$29_{4,26}\,E$–$28_{4,25}\,E$			
331803.8.....	$29_{2,27}\,A$–$28_{2,26}\,A$	1.3	5.4	
331812.2.....	$29_{5,25}\,E$–$28_{4,25}\,E$	0.7	4.5	
331819.9.....	$29_{3,27}\,A$–$28_{2,26}\,A$	0.5	2.5	
331827.7.....	$27_{18,9}\,E$–$26_{18,8}\,E$	0.8	5.1	
331834.5.....	$27_{18,10}\,E$–$26_{18,9}\,E$	0.3	1.4	
332329.2.....	$27_{15,12}\,A$–$26_{15,11}\,A$	1.1	3.8	4
332329.2.....	$27_{15,13}\,A$–$26_{15,12}\,A$			
332334.0.....	$27_{15,12}\,E$–$26_{15,11}\,E$	0.5	3.9	4
332352.6.....	$27_{15,13}\,E$–$26_{15,12}\,E$	0.9	6.3	
332570.9.....	$30_{3,28}\,E$–$29_{2,27}\,E$	4.2	23.6	
332571.2.....	$30_{4,27}\,E$–$29_{2,27}\,E$			
332571.4.....	$30_{3,28}\,E$–$29_{3,27}\,E$			
332571.7.....	$30_{4,27}\,E$–$29_{3,27}\,E$			
332575.6.....	$30_{1,29}\,A$–$29_{2,28}\,E$	3.9	6.8	
332575.9.....	$30_{2,29}\,A$–$29_{2,28}\,E$			
332576.2.....	$30_{1,29}\,A$–$29_{1,28}\,A$			
332576.4.....	$30_{2,29}\,A$–$29_{1,28}\,A$			
332604.4.....	$27_{14,13}\,E$–$26_{14,12}\,E$	2.1	14.1	
332604.4.....	$27_{14,13}\,A$–$26_{14,12}\,A$			
332604.4.....	$27_{14,14}\,A$–$26_{14,13}\,A$			
332626.0.....	$27_{14,14}\,E$–$26_{14,13}\,E$	0.8	5.0	
332953.3.....	$27_{13,14}\,E$–$26_{13,13}\,E$	0.9	3.7	
332958.3.....	$27_{13,15}\,A$–$26_{13,14}\,A$	1.2	7.0	
332958.3.....	$27_{13,14}\,A$–$26_{13,13}\,A$			
332977.4.....	$27_{13,15}\,E$–$26_{13,14}\,E$	0.7	4.2	
333409.4.....	$27_{12,15}\,E$–$26_{12,14}\,E$	0.7	3.4	
333419.2.....	$27_{12,16}\,A$–$26_{12,15}\,A$	1.3	7.2	
333419.2.....	$27_{12,15}\,A$–$26_{12,14}\,A$			
333435.2.....	$27_{12,16}\,E$–$26_{12,16}\,E$	0.9	5.9	
333449.3.....	$31_{0,31}\,A$–$30_{1,30}\,A$	3.2	13.2	
333449.3.....	$31_{1,31}\,A$–$30_{1,30}\,A$			
333449.3.....	$31_{0,31}\,A$–$30_{0,30}\,A$			
333449.3.....	$31_{1,31}\,A$–$30_{0,30}\,A$			
333449.4.....	$31_{2,30}\,E$–$30_{1,30}\,E$			
333449.4.....	$31_{1,31}\,E$–$30_{2,29}\,E$			
333449.4.....	$31_{1,31}\,E$–$30_{2,29}\,E$			
333449.4.....	$31_{2,30}\,E$–$30_{1,30}\,E$			
333593.2.....	$27_{6,21}\,E$–$26_{6,20}\,E$	2.1	10.4	
333602.0.....	$27_{4,23}\,A$–$26_{4,22}\,A$	2.6	21.4	
333972.4.....	$15_{6,10}\,E$–$14_{5,9}\,E$	0.8	4.9	
334017.2.....	$27_{11,16}\,E$–$26_{11,15}\,E$	1.7	12.5	
334109.2.....	$15_{6,10}\,A$–$14_{5,9}\,A$	0.7	3.8	
334031.5.....	$27_{11,17}\,A$–$26_{11,16}\,A$	2.1	12.9	
334031.8.....	$27_{11,16}\,A$–$26_{11,15}\,A$			

TABLE 21—*Continued*

ν (MHz)	J_{K_-,K_+}	T_R^* (K)	$\int T_R^* dv$ (K km s^{-1})	Notes
334044.0.....	$27_{11,17}\,E$–$26_{11,16}\,E$	1.2	6.2	
334851.0.....	$27_{10,17}\,E$–$26_{10,16}\,E$	0.8	3.0	
334867.0.....	$27_{10,18}\,A$–$26_{10,17}\,A$	0.7	2.8	
334872.8.....	$27_{19,17}\,A$–$26_{10,16}\,A$	1.1	4.2	
334877.5.....	$27_{10,18}\,E$–$26_{10,17}\,E$	1.1	3.3	
336028.1.....	$27_{9,19}\,A$–$26_{9,18}\,A$	1.7	12.6	
336032.4.....	$27_{9,19}\,E$–$26_{9,18}\,E$			
336351.5.....	$27_{4,23}\,E$–$26_{4,21}\,E$	2.9	17.0	
336354.9.....	$26_{1,25}\,E$–$25_{1,24}\,E$			
336368.2.....	$27_{6,22}\,A$–$25_{1,24}\,A$	1.4	5.7	
336373.8.....	$26_{5,21}\,A$–$25_{5,20}\,A$	2.0	7.8	
336889.2.....	$26_{0,26}\,E$–$25_{0,25}\,E$	2.0	7.1	
336918.1.....	$26_{6,20}\,A$–$25_{6,19}\,A$	2.1	7.1	
337489.7.....	$27_{8,20}\,E$–$26_{8,19}\,E$	<2.1	<10.7	5
337503.4.....	$27_{8,20}\,A$–$26_{8,19}\,A$	1.4	6.2	
338355.8.....	$27_{8,19}\,A$–$26_{8,18}\,A$	...	...	6
338396.4.....	$27_{7,21}\,E$–$26_{7,20}\,E$	...	...	7
339129.3.....	$13_{7,7}\,E$–$12_{6,7}\,E$	0.9	4.9	
339152.8.....	$13_{7,6}\,E$–$12_{6,6}\,E$	0.8	4.5	
339186.0.....	$13_{7,7}\,A$–$12_{6,6}\,A$	0.9	6.6	
339196.4.....	$13_{7,6}\,A$–$12_{6,7}\,A$	0.7	3.3	
341722.4.....	$29_{6,24}\,E$–$28_{6,23}\,E$	<3.4	<21.8	8
341732.3.....	$29_{4,26}\,A$–$28_{4,25}\,A$	<3.3	<18.6	9
341862.6.....	$27_{5,23}\,A$–$26_{4,22}\,A$	2.2	21.6	10
341870.3.....	$27_{3,24}\,E$–$26_{6,20}\,E$	1.1	5.7	
341918.1.....	$29_{5,24}\,E$–$28_{5,23}\,E$	2.2	12.6	
341927.5.....	$29_{4,26}\,A$–$28_{3,25}\,A$	3.2	21.7	
342162.5.....	$28_{13,16}\,E$–$28_{12,17}\,E$	0.8	5.5	
342166.8.....	$28_{13,13}\,E$–$28_{12,16}\,E$			
342230.1.....	$29_{6,24}\,E$–$28_{5,23}\,E$	<3.2	<46.8	11
342238.5.....	$29_{4,26}\,A$–$28_{3,25}\,A$			
342342.3.....	$30_{4,26}\,E$–$29_{5,25}\,E$	...	...	12
342350.1.....	$30_{2,28}\,A$–$29_{3,27}\,A$	2.5	15.4	
342351.7.....	$30_{5,26}\,E$–$29_{5,25}\,E$			
342358.5.....	$30_{4,26}\,E$–$29_{3,26}\,E$	2.6	13.3	
342359.4.....	$30_{3,28}\,A$–$29_{3,27}\,A$			
342366.3.....	$30_{2,28}\,A$–$29_{2,27}\,A$	1.6	6.8	
342367.9.....	$30_{5,26}\,E$–$29_{4,26}\,E$			
342375.6.....	$30_{3,28}\,A$–$29_{2,27}\,A$	1.1	5.3	13
342506.7.....	$11_{8,4}\,E$–$10_{7,4}\,E$	0.7	3.7	
342525.3.....	$11_{8,3}\,E$–$10_{7,3}\,E$	0.8	2.9	14
342572.4.....	$11_{8,4}\,A$–$10_{7,3}\,A$	1.1	4.2	
342572.4.....	$11_{8,3}\,A$–$10_{7,4}\,A$			
343148.3.....	$31_{3,29}\,E$–$30_{4,27}\,E$	3.7	13.0	
343148.4.....	$31_{4,28}\,E$–$30_{4,27}\,E$			
343148.5.....	$31_{3,29}\,E$–$30_{3,28}\,E$			
343148.7.....	$31_{4,28}\,E$–$30_{3,28}\,E$			
343152.8.....	$31_{1,30}\,A$–$30_{2,29}\,A$	4.1	19.1	
343153.0.....	$31_{1,30}\,A$–$30_{2,29}\,A$			
343153.1.....	$31_{1,30}\,A$–$30_{1,29}\,A$			
343153.3.....	$31_{1,30}\,A$–$30_{1,29}\,A$			
343435.4.....	$28_{0,28}\,E$–$27_{6,21}\,E$	1.7	8.9	
343443.9.....	$28_{4,24}\,A$–$27_{4,23}\,A$	1.8	11.4	15
343731.8.....	$27_{7,20}\,E$–$26_{7,19}\,E$	1.2	4.2	
343757.9.....	$27_{7,20}\,A$–$26_{7,19}\,A$	<2.8	<15.0	16
344029.6.....	$32_{0,32}\,A$–$31_{1,31}\,A$	3.2	16.7	
344029.6.....	$32_{1,32}\,A$–$31_{1,31}\,A$			
344029.6.....	$32_{0,32}\,A$–$31_{0,31}\,A$			
344029.6.....	$32_{1,32}\,A$–$31_{0,31}\,A$			
344029.6.....	$32_{2,31}\,A$–$31_{1,31}\,A$			
344029.6.....	$32_{1,32}\,A$–$31_{1,31}\,A$			
344029.6.....	$32_{2,31}\,A$–$31_{2,30}\,A$			
344029.6.....	$32_{1,32}\,A$–$31_{2,30}\,A$			

TABLE 21—*Continued*

ν (MHz)	J_{K_-,K_+}	T_R^* (K)	$\int T_R^* dv$ (K km s^{-1})	Notes
344759.0.....	$28_{15,13}\,A$–$27_{15,12}\,A$	...	...	17
344759.1.....	$28_{15,14}\,A$–$27_{15,13}\,A$			
344763.6.....	$28_{15,13}\,E$–$27_{15,12}\,A$			
344913.3.....	$20_{13,7}\,E$–$20_{12,8}\,E$	1.3	11.3	
344922.2.....	$20_{13,8}\,E$–$20_{12,9}\,E$	0.8	7.1	
345068.6.....	$28_{14,14}\,E$–$27_{14,13}\,E$	1.4	9.5	
345069.0.....	$28_{14,14}\,A$–$27_{14,13}\,A$			
345069.0.....	$28_{14,15}\,A$–$27_{14,14}\,A$			
345095.3.....	$28_{14,15}\,E$–$27_{14,14}\,E$	0.7	5.9	
345461.6.....	$28_{13,15}\,E$–$27_{13,14}\,E$	0.3	0.8	
345466.9.....	$28_{13,16}\,A$–$27_{13,15}\,A$	0.8	2.6	
345466.9.....	$28_{13,15}\,A$–$27_{13,14}\,A$			
345975.1.....	$28_{12,16}\,E$–$27_{12,15}\,E$	0.9	4.5	
345985.3.....	$28_{12,17}\,A$–$27_{12,16}\,A$	1.6	9.6	
345985.4.....	$28_{12,16}\,A$–$27_{12,15}\,A$			
346000.9.....	$28_{12,17}\,E$–$27_{12,16}\,E$	1.8	9.3	
347478.4.....	$27_{1,26}\,E$–$26_{1,25}\,E$	1.8	7.8	
347494.0.....	$27_{5,22}\,A$–$26_{5,21}\,A$	1.6	5.5	
347604.6.....	$28_{10,18}\,E$–$27_{10,17}\,E$	1.3	5.5	
347617.0.....	$28_{10,19}\,A$–$27_{10,18}\,A$	1.4	6.6	
347628.3.....	$28_{10,19}\,E$–$27_{10,18}\,E$	2.2	10.0	
347628.4.....	$28_{10,18}\,A$–$27_{10,17}\,A$			
348050.0.....	$28_{4,24}\,E$–$27_{4,23}\,E$	1.3	5.3	
348066.0.....	$28_{6,23}\,A$–$27_{6,22}\,A$	1.2	4.9	
348909.5.....	$28_{9,20}\,E$–$27_{9,19}\,E$	3.9	19.5	18
348915.0.....	$28_{9,20}\,A$–$27_{9,19}\,A$			
349048.5.....	$28_{9,19}\,E$–$27_{9,18}\,E$	1.1	4.5	
349065.7.....	$28_{9,19}\,A$–$27_{9,17}\,A$	0.8	3.3	
350442.3.....	$28_{8,20}\,E$–$27_{8,20}\,E$	1.8	23.8	
350457.6.....	$28_{8,21}\,A$–$27_{8,20}\,A$			
350919.6.....	$27_{0,27}\,E$–$26_{0,26}\,E$	<2.8	<25.9	19
350947.3.....	$27_{6,21}\,A$–$26_{6,20}\,A$	2.1	10.1	
350998.1.....	$28_{7,22}\,E$–$27_{7,21}\,E$	2.0	10.3	
351015.8.....	$27_{7,22}\,A$–$27_{7,21}\,A$	1.3	6.4	
351517.3.....	$29_{3,26}\,E$–$28_{3,25}\,E$	0.7	1.6	
351529.1.....	$29_{5,25}\,A$–$28_{5,24}\,A$	0.9	4.7	20
352283.0.....	$30_{6,25}\,E$–$29_{6,24}\,E$	1.3	6.1	
352292.6.....	$30_{4,27}\,A$–$29_{4,26}\,A$	1.2	5.9	
352404.9.....	$30_{5,25}\,E$–$29_{5,24}\,E$	1.1	4.1	
352414.2.....	$30_{3,27}\,A$–$29_{3,26}\,A$	1.1	5.0	
352912.6.....	$31_{4,27}\,E$–$30_{5,26}\,E$	1.4	22.5	
352918.0.....	$31_{5,27}\,E$–$30_{5,26}\,E$			
352920.2.....	$31_{2,29}\,A$–$30_{3,28}\,A$			
352922.0.....	$31_{4,27}\,E$–$30_{4,26}\,E$			
352925.6.....	$31_{3,29}\,A$–$30_{3,28}\,A$			
352927.4.....	$31_{5,27}\,E$–$30_{4,26}\,E$			
352929.6.....	$31_{2,29}\,A$–$30_{2,28}\,A$			
352935.0.....	$31_{3,29}\,A$–$30_{2,28}\,A$			
353402.0.....	$29_{0,29}\,E$–$28_{0,28}\,E$	1.7	8.9	
353410.6.....	$29_{4,25}\,A$–$28_{4,24}\,A$	2.1	10.9	
353724.0.....	$32_{3,30}\,E$–$31_{4,28}\,E$	4.6	17.6	
353724.1.....	$32_{4,29}\,E$–$31_{4,28}\,E$			
353724.1.....	$32_{3,30}\,E$–$31_{3,29}\,E$			
353724.2.....	$32_{4,29}\,E$–$31_{3,29}\,E$			
353728.4.....	$32_{1,31}\,A$–$31_{2,30}\,A$	5.1	27.8	
353728.5.....	$32_{2,31}\,A$–$31_{2,30}\,A$			
353728.6.....	$32_{1,31}\,A$–$31_{1,30}\,A$			
353728.7.....	$32_{2,31}\,A$–$31_{1,30}\,A$			
353794.0.....	$11_{5,7}\,E$–$10_{3,8}\,E$	2.6	21.3	
354608.0.....	$33_{0,33}\,A$–$32_{1,32}\,A$	3.6	19.6	
354608.0.....	$33_{1,33}\,A$–$32_{1,32}\,A$			
354608.0.....	$33_{0,33}\,A$–$32_{0,32}\,A$			
354608.0.....	$33_{1,33}\,A$–$32_{0,32}\,A$			
354608.4.....	$33_{2,32}\,E$–$32_{1,32}\,E$			

TABLE 21—*Continued*

ν (MHz)	J_{K_-,K_+}	T_R^* (K)	$\int T_R^* dv$ (K km s^{-1})	Notes
354608.4.....	$33_{1,33}\,E$–$32_{1,32}\,E$			
354608.4.....	$33_{2,32}\,E$–$32_{2,31}\,E$			
354608.4.....	$33_{1,33}\,E$–$32_{2,31}\,E$			
354742.4.....	$12_{8,5}\,E$–$11_{7,5}\,E$	0.7	3.4	
354759.1.....	$12_{8,4}\,E$–$11_{7,4}\,E$	0.9	4.9	
354805.7.....	$12_{8,5}\,A$–$11_{7,4}\,A$	0.9	3.8	
354805.7.....	$12_{8,4}\,E$–$11_{7,5}\,A$			
356297.1.....	$29_{20,9}\,A$–$28_{20,8}\,A$	1.2	5.3	
354297.1.....	$29_{20,10}\,A$–$28_{20,9}\,A$			
356426.0.....	$28_{19,10}\,E$–$28_{19,9}\,E$	0.8	4.7	
354427.4.....	$28_{19,11}\,E$–$28_{19,10}\,E$			
356539.8.....	$29_{18,11}\,A$–$28_{18,10}\,A$	1.7	7.2	
356539.8.....	$29_{18,12}\,E$–$28_{18,11}\,E$			
356928.6.....	$29_{16,13}\,A$–$28_{16,12}\,A$	0.9	5.5	
356928.6.....	$29_{16,14}\,A$–$28_{16,13}\,A$			
356937.7.....	$29_{16,13}\,E$–$28_{16,12}\,E$	0.9	5.0	
357989.8.....	$29_{13,16}\,E$–$28_{13,15}\,E$	...	...	21
357995.6.....	$29_{13,17}\,A$–$28_{13,16}\,A$	...	...	21
357995.6.....	$29_{13,16}\,A$–$28_{13,15}\,A$			
357995.6.....	$28_{1,27}\,A$–$27_{1,26}\,E$			
358364.3.....	$28_{7,21}\,E$–$27_{7,20}\,E$	2.9	12.9	
358392.3.....	$28_{7,21}\,A$–$27_{7,20}\,A$	2.4	11.1	
358565.8.....	$29_{12,17}\,E$–$28_{12,16}\,E$	2.2	7.2	
358576.6.....	$29_{12,18}\,A$–$28_{12,17}\,A$	4.9	28.2	
358576.6.....	$29_{12,17}\,A$–$28_{12,16}\,A$			
358591.6.....	$29_{12,18}\,E$–$28_{12,17}\,E$	4.7	24.2	22
359335.6.....	$29_{11,18}\,E$–$28_{11,17}\,E$	1.8	8.8	
359350.6.....	$29_{11,19}\,A$–$28_{11,18}\,A$	3.2	20.3	
359352.0.....	$29_{11,18}\,A$–$28_{11,17}\,A$			
359362.3.....	$29_{11,19}\,E$–$28_{11,18}\,E$	1.8	8.9	
359543.0.....	$29_{4,25}\,E$–$28_{4,24}\,E$	5.0	31.1	
359558.0.....	$29_{6,24}\,A$–$28_{6,23}\,A$	5.0	33.0	
359815.4.....	$20_{4,26}\,A$–$29_{5,25}\,A$	1.4	7.4	

NOTES.—(1) Noisy part of spectrum, parameters unreliable. (2) Blend with SO at 329385.5. (3) Blend with $^{13}CH_3OH$ at 330252.8. (4) Blend of $HCOOCH_3$ lines at 332329.2 and 332334.0. (5) Blend with CH_3OH at 337490.5. (6) Blend with CH_3OH at 338344.6. (7) Blend with CH_3OH at 338404.6. (8) Blend with CH_3CCH at 341715.1 and CH_3CH_2CN at 341703.7 and 341710.6. (9) Blend with CH_3CCH at 341734.6 and CH_3CH_2CN at 341735.0. (10) Blend with CH_3CH_2CN at 341852.7. (11) Blend with $^{34}SO_2$ at 342208.9. (12) Blend with $^{34}SO_2$ at 342332.1. (13) Blend with CH_2CHCN at 342374.9. (14) Blend with HCOOH at 342521.2. (15) Blend with CH_2CHCN at 343445.9. (16) Blend with CH_3OCH_3 lines at 343753.3–343755.1. (17) Blend with *U* line at 344773. (18) Blend with CH_3CN at 348911.4. (19) Blend with CH_3OH at 350905.1. (20) Blend with CH_3CH_2CN at 351531.6. (21) Blend with SO_2 at 357962.9 and 358013.1. (22) Blend with CH_3OH at 358605.8.

six lines of $H_2{}^{13}CO$. The rotation temperature of $H_2{}^{13}CO$ is not well determined because the lines are affected by blending (but see Mangum & Wootten 1993 for a discussion of H_2CO in Orion and elsewhere). The main isotopomer shows signs of all velocity components, but the ^{13}C and ^{18}O isotopomers exhibit the compact ridge component.

H_2CS.—Eleven transitions of thioformaldehyde were detected in our band, but no isotopomers were found. The line velocity and width indicate a hot core origin, but wings are present. Rotation temperature and column density agree well with B87 and S94. T91 finds, with a larger beam and for lower excitation lines, a lower column density and

TABLE 22

TRANSITIONS OF CH_3OCH_3

ν (MHz)	$J_{K-,K+}$	T_R^* (K)	$\int T_R^* dv$ (K km s^{-1})	Notes
328853.3.....	$10_{3,8}\,EA$–$9_{2,7}\,EA$	2.1	17.8	
328853.4.....	$10_{3,8}\,AE$–$9_{2,7}\,AE$			
328856.7.....	$10_{3,8}\,EE$–$9_{2,7}\,EE$			
328860.0.....	$10_{3,8}\,AA$–$9_{2,7}\,AA$			
330405.4.....	$16_{2,15}\,EA$–$15_{1,7}\,EA$	<2.0	<8.0	1
330405.4.....	$16_{2,15}\,AE$–$15_{1,7}\,AE$			
330406.5.....	$16_{2,15}\,EE$–$15_{1,7}\,EE$			
330407.6.....	$16_{2,15}\,AA$–$15_{1,7}\,AA$			
337180.8.....	$31_{3,28}\,AE$–$31_{0,31}\,AE$	...	...	2
337180.8.....	$31_{3,29}\,EA$–$31_{0,31}\,EA$			
337186.7.....	$31_{3,29}\,EE$–$31_{0,31}\,EE$	...	...	2
337192.6.....	$31_{3,28}\,AA$–$31_{0,31}\,AA$			
337420.9.....	$21_{2,19}\,AA$–$20_{3,18}\,AA$	2.8	11.7	
337421.3.....	$21_{2,19}\,EE$–$20_{3,18}\,EE$			
337421.8.....	$21_{2,19}\,AE$–$20_{3,18}\,AE$			
337421.8.....	$21_{2,19}\,EA$–$20_{3,18}\,EA$			
337712.4.....	$7_{4,4}\,EA$–$6_{3,3}\,EA$	<3.3	<25.9	3
337722.3.....	$7_{4,4}\,EE$–$6_{3,3}\,EE$	2.4	11.3	
337723.0.....	$7_{4,4}\,AE$–$6_{3,3}\,AE$			
337730.7.....	$7_{4,4}\,AA$–$6_{3,3}\,AA$	3.0	4.6	
337731.9.....	$7_{4,3}\,EA$–$6_{3,3}\,EA$			
337732.2.....	$7_{4,3}\,EE$–$6_{3,3}\,EE$			
337770.6.....	$7_{4,4}\,EA$–$6_{3,4}\,EA$	0.9	2.5	
337778.0.....	$7_{4,4}\,EE$–$6_{3,4}\,EE$	2.5	11.1	
337779.5.....	$7_{4,3}\,AE$–$6_{3,4}\,AE$			
337787.2.....	$7_{4,3}\,AA$–$6_{3,4}\,AA$	2.9	12.0	
337787.9.....	$7_{4,3}\,EE$–$6_{3,4}\,EE$			
337790.1.....	$7_{4,3}\,EA$–$6_{3,4}\,EA$			
339491.7.....	$19_{1,18}\,AA$–$18_{2,17}\,AA$	3.2	14.7	
339491.7.....	$19_{1,18}\,EE$–$18_{2,17}\,EE$			
339491.8.....	$19_{1,18}\,AE$–$18_{2,17}\,AE$			
339491.8.....	$19_{1,18}\,EA$–$18_{2,17}\,EA$			
340609.2.....	$10_{3,7}\,AE$–$9_{2,8}\,AE$	3.6	29.3	
340609.3.....	$10_{3,7}\,EA$–$9_{2,8}\,EA$			
340612.6.....	$10_{3,7}\,EE$–$9_{2,8}\,EE$			
340615.9.....	$10_{3,7}\,AA$–$9_{2,8}\,AA$			
342608.1.....	$19_{0,19}\,AE$–$18_{1,18}\,AE$	4.1	19.3	
342608.1.....	$19_{0,19}\,EA$–$18_{1,18}\,EA$			
342608.1.....	$19_{0,19}\,EE$–$18_{1,18}\,EE$			
342608.2.....	$19_{0,19}\,AA$–$18_{1,18}\,AA$			
343753.3.....	$17_{2,16}\,EA$–$16_{1,15}\,EA$	<2.8	<15.0	4
343753.3.....	$17_{2,16}\,AE$–$16_{1,15}\,AE$			
343754.2.....	$17_{2,16}\,EE$–$16_{1,15}\,EE$			
343755.1.....	$17_{2,16}\,AA$–$16_{1,15}\,AA$			
344358.0.....	$19_{1,19}\,EA$–$18_{0,18}\,EA$	2.5	<24.3	5
344358.0.....	$19_{1,19}\,AE$–$18_{0,18}\,AE$			
344358.1.....	$19_{1,19}\,EE$–$18_{0,18}\,EE$			
344358.2.....	$19_{1,19}\,AA$–$18_{0,18}\,AA$			
344512.2.....	$11_{3,9}\,EA$–$10_{2,8}\,EA$	4.3	36.3	
344512.2.....	$11_{3,9}\,AE$–$10_{2,8}\,AE$			
344515.4.....	$11_{3,9}\,EE$–$10_{2,8}\,EE$			
344518.6.....	$11_{3,9}\,AA$–$10_{2,8}\,AA$			
349803.0.....	$11_{2,9}\,AE$–$10_{1,10}\,AE$	1.8	30.1	
349803.0.....	$11_{2,9}\,EA$–$10_{1,10}\,EA$			
349806.1.....	$11_{2,9}\,EE$–$10_{1,10}\,EE$			
349809.2.....	$11_{2,9}\,AA$–$10_{1,10}\,AA$			
356442.9.....	$25_{1,24}\,AE$–$24_{4,21}\,AE$	1.2	4.7	
356442.9.....	$25_{1,24}\,EA$–$24_{4,21}\,EA$			
356443.3.....	$25_{1,24}\,EE$–$24_{4,21}\,EE$			
356443.6.....	$25_{1,24}\,AA$–$24_{4,21}\,AA$			
356567.2.....	$8_{4,5}\,EA$–$7_{3,4}\,EA$	2.2	11.6	
356575.3.....	$8_{4,5}\,AE$–$7_{3,4}\,AE$	5.9	24.5	
356576.0.....	$8_{4,5}\,EE$–$7_{3,4}\,EE$			
356582.8.....	$8_{4,5}\,AA$–$7_{3,4}\,AA$	4.9	30.1	
356586.8.....	$8_{4,4}\,EE$–$7_{3,4}\,EE$			
356587.0.....	$8_{4,4}\,EA$–$7_{3,4}\,EA$			
357459.4.....	$18_{2,17}\,EA$–$17_{1,16}\,EA$	4.6	25.1	
357459.4.....	$18_{2,17}\,AE$–$17_{1,16}\,AE$			
357460.2.....	$18_{2,17}\,EA$–$17_{1,16}\,EA$			
357461.0.....	$18_{2,17}\,EA$–$17_{1,16}\,EA$			
358447.4.....	$5_{5,0}\,EA$–$4_{4,0}\,EA$	9.6	83.2	
358449.4.....	$5_{5,1}\,AE$–$4_{4,0}\,AE$			
358449.4.....	$5_{5,0}\,AE$–$4_{4,1}\,AE$			
358451.4.....	$5_{5,1}\,EA$–$4_{4,1}\,EA$			
358451.9.....	$5_{5,0}\,EE$–$4_{4,0}\,EE$			
358454.0.....	$5_{5,1}\,EE$–$4_{4,1}\,EE$			
358456.5.....	$5_{5,1}\,AA$–$4_{4,0}\,AA$			
358456.5.....	$5_{5,0}\,AA$–$4_{4,1}\,AA$			
359381.6.....	$12_{3,10}\,EA$–$11_{2,9}\,EA$	5.3	43.6	
359381.6.....	$12_{3,10}\,AE$–$11_{2,9}\,AE$			
359384.6.....	$12_{3,10}\,EE$–$11_{2,9}\,EE$			
359387.7.....	$12_{3,10}\,AA$–$11_{2,9}\,AA$			

NOTES.—(1) Blend with $^{13}CH_3OH$ at 330408.4. (2) Blend with ^{33}SO at 337195.0. (3) Blend with CH_3OH ($v_t = 1$) at 337707.6. (4) Blend with $HCOOCH_3$ at 343757.9. (5) Blend with SO at 344310.6.

lower rotation temperature component, pointing to the extended ridge as origin. The other surveys would, due to smaller beam size and because they contain higher excitation lines, not be sensitive to this component.

HNCO.—Thirteen lines of isocyanic acid and one line of deuterated isocyanic acid were detected. While the $K_a = 0$ lines show both hot core and plateau components, the $K_a > 0$ lines are confined to the hot core component. (See § 4.2 for a more detailed discussion.)

HCOOH.—Eight lines of formic acid are detected in our band. The values of rotation temperature and column density are too insecure to make meaningful comparisons with other studies. The velocity structure of this line is dominated by the compact ridge component.

H_2CCO.—Two lines of ketene were detected, not enough to determine a rotation temperature reliably. This species has been seen previously by S85, B87, T91, and S94, so its presence in Orion is well established. The frequency errors are too large to allow a determination of the lines' origin on the basis of the line velocity.

NH_2CHO.—Formamide is detected in this survey. The rotation temperature fit, which is based on only three lines, gives a higher rotation temperature than the T91 results, while it is much lower than S94, but all data have large error bars. Different beam sizes could also play a role: T91 samples the largest, coolest region, while S94 have the smallest beam and pick out the warmest gas. The column density is consistent with B87, T91, and S94 estimates. Due to the weakness of the lines, the line velocity is difficult to determine, but it appears to point to a compact ridge origin.

$HCOOCH_3$.—Methyl formate shows 133 spectral features consisting of 211 partly blended lines. It accounts for 22% of all spectral features. In spite of this plethora of lines, all observed lines have their origin in one of two narrow energy ranges, either between 70 and 80 K or around 250 K,

TABLE 23

TRANSITIONS OF CH_2CHCN

ν (MHz)	J_{K_-,K_+}	T_R^* (K)	$\int T_R^* dv$ (K km s^{-1})	Notes
CH_2CHCN:				
327160.1.....	$34_{3,31}$–$33_{3,30}$	1.7	10.8	
327552.4.....	$36_{0,36}$–$35_{1,35}$	1.2	5.5	
327882.0.....	$35_{2,34}$–$34_{2,33}$	0.7	...	1
329191.7.....	$36_{1,36}$–$35_{1,35}$	1.2	4.5	
329462.3.....	$36_{0,36}$–$35_{0,35}$	<1.3	<7.2	2
332385.0.....	$35_{8,28}$–$34_{8,27}$	1.6	10.1	
332385.0.....	$35_{8,27}$–$34_{8,26}$			
332401.7.....	$35_{9,27}$–$34_{9,26}$	0.3	1.1	
332401.7.....	$35_{9,26}$–$34_{9,25}$			
332419.0.....	$35_{7,29}$–$34_{7,28}$	0.9	4.2	
332419.0.....	$35_{7,28}$–$34_{7,27}$			
332453.6.....	$35_{10,25}$–$34_{10,24}$	0.3	1.1	
332453.6.....	$35_{10,26}$–$34_{10,25}$			
332532.3.....	$35_{11,24}$–$34_{11,23}$	...	...	3
332532.3.....	$35_{11,25}$–$34_{11,24}$			
332533.2.....	$35_{6,30}$–$34_{6,29}$			
332534.8.....	$35_{6,29}$–$34_{6,28}$			
332775.7.....	$35_{5,31}$–$34_{5,30}$	<0.4	<0.8	4
333047.3.....	$35_{4,32}$–$34_{4,31}$	0.5	3.7	
333764.6.....	$35_{4,31}$–$34_{4,30}$	<0.9	<7.0	5
337039.7.....	$36_{2,35}$–$35_{2,34}$	0.7	4.1	
338213.5.....	$37_{1,37}$–$36_{1,36}$	0.5	1.7	
338447.9.....	$37_{0,37}$–$36_{0,36}$	...	...	6
340047.4.....	$36_{1,35}$–$35_{1,34}$	...	...	7
341563.8.....	$36_{3,34}$–$35_{3,33}$	1.1	3.2	
341882.0.....	$36_{8,29}$–$35_{8,28}$	0.8	6.4	8
341882.0.....	$36_{8,28}$–$35_{8,27}$			
341894.2.....	$36_{9,28}$–$35_{9,27}$	1.2	8.6	8
341894.2.....	$36_{9,27}$–$35_{9,26}$			
342052.9.....	$36_{6,31}$–$35_{6,30}$	1.3	10.8	
342055.2.....	$36_{6,30}$–$35_{6,29}$			
342317.6.....	$36_{5,32}$–$35_{5,31}$	1.6	12.1	1
342375.6.....	$36_{5,31}$–$35_{0,30}$	...	...	9
342585.5.....	$36_{4,33}$–$35_{4,32}$	0.5	2.2	1
343446.5.....	$36_{4,32}$–$35_{4,31}$	...	...	10
346184.9.....	$37_{2,36}$–$36_{2,35}$	1.3	11.2	1
346943.1.....	$36_{3,33}$–$35_{3,32}$	...	...	11
347232.0.....	$38_{1,38}$–$37_{1,37}$	0.5	3.0	
347434.2.....	$38_{0,38}$–$37_{0,37}$	0.9	3.9	
347759.0.....	$36_{2,34}$–$35_{2,32}$	0.8	6.3	
348991.4.....	$37_{1,36}$–$36_{1,35}$	1.1	6.4	
351379.0.....	$37_{8,30}$–$36_{8,29}$	0.7	4.2	
351379.0.....	$37_{8,29}$–$36_{8,28}$			
351386.3.....	$37_{9,28}$–$36_{9,27}$	0.5	3.8	
351386.3.....	$37_{9,29}$–$36_{9,28}$			
351430.1.....	$37_{7,31}$–$36_{7,30}$	1.1	13.6	
351430.2.....	$37_{7,39}$–$36_{7,29}$	1.1	13.6	
351434.0.....	$37_{10,27}$–$36_{10,26}$			
351434.0.....	$37_{10,28}$–$36_{10,27}$			
353120.6.....	$37_{4,34}$–$36_{4,33}$	0.9	6.6	
353147.2.....	$37_{4,33}$–$36_{4,32}$	0.5	5.4	
353241.5.....	$4_{4,1}$–$3_{3,0}$	0.7	3.6	
353241.5.....	$4_{4,0}$–$3_{3,1}$			
356421.7.....	$39_{0,39}$–$38_{0,38}$	1.2	5.8	
356908.6.....	$18_{2,16}$–$17_{1,17}$	0.7	3.2	
$CH_2CHCN(v_{11}=1)$:				
334073.1.....	$35_{4,32}$–$34_{4,31}$	1.2	7.8	
334894.5.....	$35_{4,31}$–$34_{4,30}$	1.4	16.4	
356911.1.....	$39_{1,39}$–$38_{1,38}$	0.4	1.2	
$CH_2CHCN(v_{15}=1)$:				
351450.9.....	$37_{3,35}$–$36_{3,34}$	0.5	4.9	
356973.1.....	$39_{1,39}$–$38_{1,38}$	1.6	14.1	

NOTES.—(1) Very broad feature, possible blend with *U* lines. (2) Blend with HNCO at 329459.9. (3) In the wing of SO_2 at 332505.2. (4) Blend with NH_2D at 332780.9, 332781.8, and 332782.4. (5) Blend with CH_3CH_2CN at 333767.7. (6) Blend with wings of CH_3OH at 338442.3 and 338456.5. (7) Blend with $C^{33}S$ at 340052.7. (8) Blend with ghost. (9) Blend with $HCOOCH_3$ at 342375.6. (10) Blend with $HCOOCH_3$ at 343443.9. (11) Blend with CH_3CH_2CN at 346947.3.

which limits the use of this molecule as a temperature indicator. The rotation temperature derived between these two point clusters is 98 K, in agreement with the compact ridge value of S94. The column densities agree well with S94. Line velocity and width are also consistent with a compact ridge origin of this molecule. A lower excitation component was found by T91.

CH_3OCH_3.—Dimethylether is found in 25 line groups, mostly consisting of the unresolved or only marginally resolved *AA*, *EE*, *AE*, and *EA* lines of a transition. The rotation temperature we derive is higher than B87 and J84, but close to the T91 and S94 results. Our column density is higher than all of them except S94, which again might be a consequence of our small beam compared with previous studies. Again, the velocity structure suggests the compact ridge as the source of this molecule.

CH_3CH_2CN.—Ethyl cyanide (propionitrile) is detected in 72 spectral features, consisting of 110 partly blended lines. The lines are mostly due to *a*-type transitions, but a few weaker *b*-type transitions are detected as well. There are two groups of lines, one with level energies around 100 K and one with level energies between 300 and 400 K. The rotation temperature and column densities are in agreement with S94. The line velocities and widths indicate a hot core origin of this molecule. The frequencies of vibrationally or torsionally excited transitions are not available.

CH_2CHCN.—Vinyl cyanide is detected in 44 spectral features, consisting of 60 partly blended lines, again mostly *a*-type transitions. Most of the lines have level energies between 300 and 500 K, but one *b*-type transition with a level energy of 40 K is observed. The derived rotation temperature is 96 K. Three lines of the $v_{11}=1$ (in-plane CCN bend, 342 K above ground) and two lines of the $v_{15}=1$ (out-of-plane CCN bend at 486 K above ground) vibrationally excited transitions are found. Frequencies of transitions in the other vibrationally excited or in torsionally excited states are not available. The line velocities are consistent with the lines' originating from the hot core.

CH_3CHO.—Some of the *U* lines coincide with lines of acetaldehyde, which has been detected previously by T91 and ZM93. However, the frequencies are very uncertain, and the relative line strength of the possible CH_3CHO features together with the absence of some intrinsically strong lines do not give a consistent picture. Moreover, both T91 and ZM93 find very low rotation temperatures (<10 K), which would result in very low line strengths of the lines in the frequency range of our survey. Thus, we believe that acetaldehyde was not found in our survey.

TABLE 24

TRANSITIONS OF CH_3CH_2CN

ν (MHz)	J_{K_-,K_+}	T_R^* (K)	$\int T_R^* dv$ (K km s^{-1})	Notes
328001.1.....	$36_{4,32}$–$35_{4,31}$	1.2	9.7	
328754.8.....	$37_{3,35}$–$36_{3,34}$	1.2	10.9	
329234.8.....	$36_{3,33}$–$35_{3,32}$	2.2	24.1	
331439.5.....	$38_{2,37}$–$37_{2,37}$	1.1	9.7	
331484.5.....	$37_{12,25}$–$36_{12,24}$	1.6	11.8	
331484.5.....	$37_{12,26}$–$36_{12,25}$			
331488.3.....	$37_{11,26}$–$36_{11,25}$			
331487.3.....	$37_{11,27}$–$36_{11,26}$			
331523.3.....	$37_{10,28}$–$36_{10,27}$	0.9	8.6	
331523.3.....	$37_{10,27}$–$36_{10,26}$			
331605.6.....	$37_{9,29}$–$36_{9,28}$	1.3	12.5	
331605.6.....	$37_{9,28}$–$36_{9,27}$			
331662.3.....	$37_{2,35}$–$36_{2,34}$	1.2	10.3	
331748.5.....	$38_{1,37}$–$37_{1,36}$	2.2	41.2	
331756.4.....	$37_{8,30}$–$36_{8,29}$			
331756.4.....	$37_{8,29}$–$36_{8,28}$			
332014.7.....	$37_{7,31}$–$36_{7,30}$	<2.5	<26.1	1
332020.6.....	$37_{7,30}$–$36_{7,29}$			
332428.0.....	$37_{6,32}$–$36_{6,31}$	1.6	12.1	
332687.7.....	$19_{4,15}$–$18_{3,16}$	0.7	3.0	
333108.8.....	$38_{2,37}$–$37_{1,36}$	...	...	2
333265.9.....	$39_{1,39}$–$38_{1,38}$	1.6	13.0	
333274.7.....	$39_{0,39}$–$38_{0,38}$	...	...	3
333753.4.....	$14_{5,10}$–$13_{4,9}$	0.7	3.9	
333767.7.....	$14_{5,9}$–$13_{4,10}$	<0.9	<7.0	4
333921.6.....	$37_{5,32}$–$36_{5,31}$	...	...	5
335321.4.....	$9_{6,4}$–$8_{5,3}$	...	...	6
335321.4.....	$9_{6,3}$–$8_{5,4}$			
336613.9.....	$20_{4,17}$–$19_{3,16}$	1.4	8.3	7
337347.6.....	$38_{3,36}$–$37_{3,35}$	3.6	36.3	8
337445.9.....	$37_{4,33}$–$36_{4,32}$	2.2	17.2	
339968.2.....	$38_{3,36}$–$37_{2,35}$	2.5	27.1	9
340149.1.....	$39_{1,38}$–$38_{1,37}$	3.2	22.5	10
340151.3.....	$35_{3,33}$–$34_{2,32}$			
340576.0.....	$38_{9,30}$–$37_{9,29}$	2.2	20.3	
340576.0.....	$38_{9,29}$–$37_{9,28}$			
340808.3.....	$38_{18,20}$–$37_{18,19}$	2.4	20.4	
340808.3.....	$38_{18,21}$–$37_{18,20}$			
340916.5.....	$38_{19,19}$–$37_{19,18}$	0.9	5.9	
340916.5.....	$38_{19,20}$–$37_{19,19}$			
340972.7.....	$38_{4,35}$–$37_{3,34}$	2.0	18.3	
341025.6.....	$38_{7,32}$–$37_{7,31}$	1.7	10.8	
341033.9.....	$38_{7,31}$–$37_{7,30}$	2.5	25.1	
341468.7.....	$38_{6,33}$–$37_{6,32}$	1.7	9.2	
341603.2.....	$38_{6,32}$–$37_{6,31}$	2.0	14.5	
341678.5.....	$40_{0,40}$–$39_{1,39}$	<2.5	<29.1	11
341703.7.....	$40_{1,40}$–$39_{1,39}$	2.8	16.2	12
341710.6.....	$40_{0,40}$–$39_{0,39}$			
341735.9.....	$40_{1,40}$–$39_{0,39}$	...	...	13
341852.7.....	$38_{5,38}$–$37_{5,33}$	...	...	14
342652.0.....	$15_{5,11}$–$14_{4,10}$	0.4	3.3	
342677.7.....	$15_{5,10}$–$14_{4,11}$	0.5	3.3	
343194.6.....	$38_{5,33}$–$37_{5,32}$	...	...	15
344867.3.....	$38_{8,30}$–$37_{7,31}$	0.9	11.3	
346356.2.....	$29_{8,21}$–$29_{7,22}$	1.1	6.1	
346356.9.....	$29_{8,22}$–$29_{7,22}$			
346772.1.....	$24_{8,16}$–$24_{7,17}$	0.8	6.4	
346772.1.....	$24_{8,17}$–$29_{7,18}$			
346822.6.....	$23_{8,15}$–$23_{7,16}$	0.5	5.9	
346822.6.....	$23_{8,16}$–$23_{7,17}$			
346874.3.....	$38_{4,34}$–$37_{4,34}$	1.7	15.7	

TABLE 24—*Continued*

ν (MHz)	J_{K_-,K_+}	T_R^* (K)	$\int T_R^* dv$ (K km s^{-1})	Notes
346947.3.....	$9_{8,1}$–$9_{7,2}$	3.2	33.8	16
346947.3.....	$9_{8,2}$–$9_{7,3}$			
346955.4.....	$10_{8,2}$–$10_{7,3}$			
346955.4.....	$10_{8,3}$–$10_{7,4}$			
346962.8.....	$11_{8,3}$–$11_{7,4}$			
346962.8.....	$11_{8,4}$–$11_{7,5}$			
346969.2.....	$12_{8,4}$–$12_{7,5}$			
346969.2.....	$12_{8,5}$–$12_{7,4}$			
346978.7.....	$14_{8,6}$–$14_{7,7}$	2.9	42.6	
346978.7.....	$14_{8,7}$–$14_{7,8}$			
346979.3.....	$15_{8,7}$–$15_{7,8}5$			
346979.3.....	$15_{8,8}$–$15_{7,9}$			
346983.8.....	$38_{3,35}$–$37_{3,34}$			
348260.6.....	$39_{2,37}$–$38_{2,36}$	2.5	25.5	
348344.5.....	$40_{2,39}$–$39_{2,38}$	5.5	66.1	
348553.3.....	$40_{1,39}$–$39_{1,38}$	3.4	46.7	
349492.5.....	$39_{15,24}$–$38_{15,23}$	0.8	4.2	
346492.5.....	$39_{15,25}$–$38_{15,24}$			
349547.0.....	$39_{9,31}$–$38_{9,30}$	2.0	17.0	
346547.0.....	$39_{9,30}$–$38_{9,29}$			
349730.8.....	$39_{8,32}$–$38_{8,31}$	1.6	16.3	
349731.3.....	$39_{8,31}$–$38_{8,30}$			
350039.4.....	$39_{7,33}$–$38_{7,32}$	0.9	8.8	
350050.9.....	$39_{7,32}$–$38_{7,31}$	0.9	10.1	
350139.7.....	$41_{1,41}$–$40_{1,40}$	1.6	22.2	
350145.2.....	$41_{0,41}$–$40_{0,40}$			
351462.9.....	$22_{4,19}$–$21_{3,18}$	0.7	4.9	
351531.6.....	$16_{5,12}$–$15_{4,11}$	...	...	17
351575.9.....	$16_{5,11}$–$15_{4,12}$	1.3	12.4	
352500.7.....	$39_{5,34}$–$38_{5,33}$	1.1	10.1	
353234.9.....	$11_{6,6}$–$10_{5,5}$	0.4	2.6	
353234.9.....	$11_{6,5}$–$10_{5,6}$			
355755.9.....	$39_{3,36}$–$38_{3,35}$	1.8	31.1	
355276.7.....	$39_{4,35}$–$38_{4,34}$	2.1	18.0	
356546.1.....	$40_{2,38}$–$39_{2,37}$	3.3	30.3	
356960.4.....	$41_{1,40}$–$40_{1,39}$	2.6	20.9	
358326.2.....	$40_{12,28}$–$39_{12,27}$	1.4	10.8	
358326.2.....	$40_{12,29}$–$39_{12,28}$			
358402.6.....	$40_{10,31}$–$39_{10,30}$	1.7	10.4	
358402.6.....	$40_{10,30}$–$39_{10,29}$			
358518.6.....	$40_{9,32}$–$39_{9,31}$	2.1	23.6	
358518.7.....	$40_{9,31}$–$39_{9,30}$			
358692.5.....	$40_{18,22}$–$39_{18,21}$	1.8	19.9	
358692.5.....	$40_{18,23}$–$39_{18,22}$			
358720.4.....	$40_{8,33}$–$39_{8,32}$	2.1	25.5	
358721.2.....	$40_{8,32}$–$39_{8,31}$			
359056.1.....	$40_{7,34}$–$39_{7,33}$	2.2	24.9	
359071.9.....	$40_{7,33}$–$39_{7,32}$	1.6	16.3	
359870.1.....	$40_{5,36}$–$39_{5,35}$	2.2	23.6	

NOTES.—Blend with $CH_3CN(v_8 = 1)$ at 332015.8 and 332017.8. (2) Blend with $^{13}CH_3OH$ at 333114.8. (3) Blend with HDS at 333278.5. (4) Blend with CH_2CHCN at 333764.0. (5) Blend with wing of ^{34}SO at 333902.1. (6) Blend with *U* line at 335335.0. (7) Blend with $CH_3OH(v_t = 2)$ at 336605.9. (8) Blend with $HC_3N(v_7^1)$ at 337344.3. (9) Blend with C_2H_5OH at 339977.4. (10) Blend with CH_3OH at 340141.2. (11) Intensity too high based on rotation diagram. (12) Blend with CH_3CCH at 341715.1 and $HCOOCH_3$ at 341722.4. (13) Blend with $HCOOCH_3$ at 341732.3 and CH_3CCH at 341734.6. (14) Blend with $HCOOCH_3$ at 341862.6. (15) Blend with *U* line at 343202. (16) Blend with $HC_3N(v_7^1)$ at 346948.7 and CH_2CHCN at 346942.5. (17) Blend with $HCOOCH_3$ at 351529.1.

TABLE 25

U LINES

ν (MHz)	T_R^* (K)	$\int T_R^* dv$ (K km s^{-1})	Notes
328415.....	1.3	5.3	
330715.....	0.7	1.7	
332789.....	0.7	3.8	1
332799.....	0.7	4.1	
333851.....	0.8	4.2	?
333865.....	1.4	8.9	
334140.....	0.5	1.6	
334278.....	0.5	1.8	
335335.....	0.5	6.2	2
335363.....	0.4	3.0	
335703.....	0.7	4.6	
335742.....	0.7	6.2	3
335840.....	0.5	2.9	
335867.....	0.5	3.3	
336456.....	0.5	2.4	
337744.....	1.1	4.2	
337839.....	0.8	3.3	
339061.....	0.8	5.4	
339138.....	0.4	3.3	?
339527.....	0.9	8.6	
340496.....	2.2	15.9	
340872.....	0.9	4.6	
341095.....	1.2	6.6	?
341472.....	2.2	10.9	?
341482.....	0.9	11.7	?
341499.....	0.3	0.4	
341510.....	0.7	3.0	
342006.....	0.5	2.2	
342129.....	0.7	4.1	
342274.....	0.4	1.6	
342290.....	0.8	3.9	3
342486.....	0.7	4.7	?
343202.....	2.0	21.8	4
343665.....	1.2	7.8	?
344773.....	...	...	5
344788.....	...	...	5
344796.....	...	....	5
347029.....	0.8	3.0	
347047.....	0.4	1.1	?
347446.....	1.1	4.7	
347743.....	0.5	8.4	?
348084.....	0.5	2.4	
348162.....	0.8	7.0	?
348358.....	5.3	87.6	6
348373.....	...	...	6
350170.....	0.7	2.8	
351490.....	0.9	7.2	?
351540.....	1.6	10.8	
353166.....	0.8	5.0	?
353851.....	0.9	7.0	
354129.....	1.3	7.8	
355231.....	0.5	...	7
355851.....	0.4	3.2	1, 8?
356601.....	0.4	1.3	
356644.....	0.8	5.3	
356662.....	0.9	6.4	
358356.....	2.9	14.1	

NOTE.—(1) Blend with NH_2D at 332782.0. (2) Blend with CH_3CH_2CN at 335321.4. (3) Double or multiple peaked structure. (4) Blend with CH_3CH_2CN at 343194.6. (5) Blend with each other, $^{34}SO_2$ at 344808.0, and $HCOOCH_3$ at 344759.1. (6) Blend with each other and SO_2 at 348387.8. (7) Blend of three *U* lines. (8) Blend with wing of $OC^{34}S$ at 355836.0.

3.2.7. *Unidentified Lines*

We found 60 unidentified lines. The large number is partly due to the high sensitivity and small beam size of our survey, since many of them are in the 0.5–2 K range. We suspect that most of the unidentified lines are due to isotopomeric lines of well-known species (e.g., CH_2DOH, $H^{13}COOH$) or to vibrationally or torsionally excited transitions of the main isotopomers. The plethora of lines makes the identification of lines from new molecules very difficult if not impossible. None of the unidentified lines are outstandingly bright, although some reach the 2–5 K level. Some *U* lines are questionable (see next paragraph). For determining the frequencies of *U* lines, a source velocity of 9 km s^{-1} was assumed.

3.2.8. *Known Defects*

Due to the SSB cleaning procedure, there are inevitable defects in the spectrum. These defects occur at the edges of the band, where only one sideband was available for restoration, and in some very crowded areas, where lines from both sidebands are always present. Known defects are marked as "ghost" in Table 2. For some *U* lines, the possibility exists that they are not real, but ghosts, in which case they are marked with a question mark in the table.

4. ANALYSIS

4.1. *Physical Parameters and Integrated Line Fluxes*

LTE rotation temperatures and column densities of the species where they could be determined are listed in Table 26. No attempt to correct for optical depth effects was made. The column densities have been derived from integrated areas corrected to the T_R^* scale. The values agree roughly with those derived in earlier studies, except that we seem to have systematically higher column densities, which is partly a beam size effect. Some values are certainly arti-

TABLE 26

LTE ROTATION TEMPERATURES AND COLUMN DENSITIES

Line	T_{rot} (K)	N (cm^{-2})	Notes
HC_3N	225 ± 200	5.2(15) ± 7.8(15)	
OCS	83 ± 30	1.8(16) ± 1.8(16)	
SO	27 ± 1	6.3(16) ± 0.7(16)	
^{34}SO	67 ± 100	0.4(16) ± 1.1(16)	
CH_3CN	445 ± 36	1.7(15) ± 0.7(15)	
CH_3CCH	65 ± 9	4.3(15) ± 2.2(15)	
SO_2	124 ± 3	7.7(16) ± 0.5(16)	
$SO_2(v_2 = 1)$	98 ± 8	2.3(15) ± 0.5(15)	
$^{34}SO_2$	138 ± 8	1.5(16) ± 0.1(16)	
$^{33}SO_2$	104 ± 18	5.0(14) ± 1.6(14)	
HDO	272 ± 200	0.9(16) ± 1.3(16)	Two lines only
CH_3OH	188 ± 3	7.0(16) ± 0.2(16)	
C_2H_5OH	64 ± 6	1.4(15) ± 0.7(15)	
$H_2{}^{13}CO$	230 ± 105	6.3(14) ± 4.7(14)	
H_2CS	93 ± 19	8.5(14) ± 3.5(14)	
HNCO	160 ± 14	1.3(15) ± 2.3(15)	Entire data set
	36 ± 5	5.7(15) ± 3.5(15)	$K_a = 0$, $K_a = 1$
	277 ± 100	1.3(15) ± 0.8(15)	$K_a = 1$, $K_a = 2$
	190 ± 40	1.2(15) ± 0.6(15)	$K_a = 2$, $K_a = 3$
HCOOH	39 ± 14	2.0(15) ± 3.5(15)	
NH_2CHO	81 ± 13	1.2(14) ± 0.6(13)	
$HCOOCH_3$	98 ± 3	1.5(16) ± 0.1(16)	
CH_3OCH_3	89 ± 5	1.8(16) ± 0.2(16)	
CH_2CHCN	96 ± 5	8.2(14) ± 1.5(14)	
CH_3CH_2CN	99 ± 3	1.3(16) ± 0.2(16)	

NOTE.—The column densities are determined using the main beam brightness line temperature scale.

TABLE 27

INTEGRATED LINE INTENSITIES FOR EACH SPECIES

Line	$\int T_R^* dv$ (K km s^{-1})
CO	6080.5
CS	653.2
SiO	1132.9
HCN	<2632.0
HC_3N	<437.0
OCS	372.0
HCO^+	<1067.0
HCS^+	9.9
SO	<5574.0
U	369.1
CH_3CN	1165.7
CH_3CCH	106.8
SO_2	14276.0
H_2O	727.0
HDS	17.1
NH_2D	5.8
CH_3OH	<3834.0
C_2H_5OH	77.4
H_2CO	474.0
H_2CS	149.3
HNCO	323.0
HCOOH	46.0
CH_2CO	15.9
NH_2CHO	68.6
$HCOOCH_3$	1268.0
CH_3OCH_3	497.0
CH_2CHCN	226.5
CH_3CH_2CN	1095.3

The numbers are integrals over all transitions (including torsionally or vibrationally excited ones) and all isotopomers. A "less than" sign here and in all previous tables means that the values are upper limits, due to line blends. While these blends very often make the integrated intensity for a single line quite uncertain, they do not affect the sum presented in this table very much.

facts of high optical depths, e.g., the low rotation temperature of SO and the high excitation temperature of CH_3CN.

Organic oxygen-bearing molecules (CH_3OCH_3, $HCOOCH_3$, C_2H_5OH, and CH_3OH) show mostly spectral characteristics of compact ridge molecules, while the oxygen-free molecules CH_3CN, CH_2CHCN, and CH_2CH_3CN are dominated by the hot core.

In Table 27 we show for each detected species the total flux, integrated over all transitions and isotopomers. Although $^{12}CO(3–2)$ is by far the strongest single line, SO_2 has, due to the many strong lines it displays, more than twice the integrated flux of CO. Close behind follow SO and, at some distance, CH_3OH and HCN. The heavy organic rotors like $HCOOCH_3$ are not very important coolants, despite their many lines.

4.2. *Radiatively Excited Molecules*

Transitions that are radiatively excited fall in two categories:

1. Transitions in the vibrationally or torsionally excited states that are almost inevitably excited by (mostly IR) radiation, because collisional excitation would require unrealistically high densities. Examples in our survey are transitions of HCN, $H^{13}CN$, HC_3N, CH_3CN, and SO_2, which display transitions from various vibrationally excited levels, and CH_3OH and $^{13}CH_3OH$, which show transitions due to torsionally excited states.

2. Transitions in the vibrational or torsional ground state that are nonetheless excited by IR excitation. One example is HNCO, but this is probably also true for highly excited SO_2 lines and HDO.

For the first category, it is worth noting which molecules are *not* observed in vibrationally excited states: CO and CS, and lines in the stretching vibration states of HCN. All these lines require excitation by IR photons with wavelengths shorter than ≈ 10 μm. It should also be pointed out that the spectra of many vibrationally and torsionally excited molecules are not known, so it is quite possible that many *U* lines are in this category (e.g., CH_3CH_2CN, C_2H_5OH).

The HCN(3–2) line in the (0, 1, 0) mode was detected by Ziurys & Turner (1986), but this is the first detection of HCN in Orion in the (0, 2, 0) mode, ≈ 2000 K above ground. The intensity ratio of the vibrationally excited $H^{13}CN$ and HCN lines suggest a peak optical depth of ≈ 5 for the vibrationally excited HCN line, for an assumed [HCN]/[$H^{13}CN$] ratio of 60.

As an example of the second category, we concentrate the discussion on HNCO. Isocyanic acid is only slightly asymmetric and has the interesting feature that the K_a-ladders are connected by weak *b*-type transitions. According to Churchwell et al. (1986), these transitions are not excited by collisions, but by IR radiation at 330 μm, 110 μm, and 70 μm for the $K_a = 0–1$, $K_a = 1–2$, and $K_a = 2–3$ transitions, respectively. Hence, the rotation temperatures between the ladders are a measure of the far-infrared (FIR) field. We determine rotation temperature of 36 ± 4 K between $K_a = 0$ and $K_a = 1$, and 221 ± 33 K between the $K_a > 0$ components. The latter is a measure of the dust temperature. They agree reasonably well with other determinations of the dust temperature in the hot core on the basis of vibrationally excited lines (see Schilke et al. 1992b and references therein). The first rotation temperature is probably underestimated because HNCO is present in the ambient gas; thus, the beam filling factor of the $K_a = 0$ lines is higher than for the $K_a \geq 1$ lines, which trace the FIR field. Optical thickness effects may also play a role, since it is likely that the dust is optically thin at 330 μm, while it may become optically thick at 110 and 70 μm.

5. CONCLUSIONS

This CSO 325–360 GHz survey covers the atmospheric window at 850 μm almost completely. We have detected 717 resolvable features consisting of 1004 lines, 60 of them unidentified. The number of features per frequency interval is 205 per 10 GHz, somewhat higher than, but comparable with, T91 (167 per 10 GHz), ZM 93 (180 per 10 GHz), and S85 and B86 (170 per 10 GHz). The percentage of unidentified lines in our sample is 8.4%; T91 find 35%, ZM93 find 25%, and S85 and B86 find 5%. The relatively low percentage of unidentified lines is due to recently determined laboratory frequencies of some of the most important molecules. We found 34 species and several isotopomers, among which $^{33}SO_2$ is new. The earlier claims of detection of C_2H_5OH have been strengthened. Although molecules like $HCOOCH_3$, CH_3CH_2CN, and CH_3OCH_3 still dominate

the emission in terms of numbers of lines, their lines are weak, and it is predictable that these heavy organic rotors will lose importance at even higher frequencies. Apart from strong lines from linear rotors like CO, CS, SO, SiO, HCN, and HCO^+, the spectrum is dominated by SO_2 and CH_3OH. The integrated line intensity of all SO_2 lines is twice that of CO, while CO and SO have comparable integrated line intensities.

Lines from the $v_2 = 2$ state of HCN, 2000 K above ground, were detected for the first time, showing that observations with higher frequencies and smaller beams are able to access the very active centers of the star-forming cores.

The CSO is supported by NSF grant AST 93-13929. We would like to thank an anonymous referee and C. M. Walmsley for valuable comments. Special thanks to the maintainers of the JPL catalog, E. Herbst for making various spectoscopy data sets available in digital form, and E. Klisch and G. Winnewisser for providing $^{33}SO_2$ frequencies prior to publication.

REFERENCES

Anderson, T., Crownover, R. L., Herbst, E., & De Lucia, F. C. 1988, ApJS, 67, 135
Anderson, T., Herbst, E., & De Lucia, F. C. 1992, ApJS, 82, 405
———. 1993, J. Mol. Spectrosc., 159, 410
Blake, G. A., Sutton, E. C., Masson, C. R., & Phillips, T. G. 1986, ApJS, 60, 257 (B86)
———. 1987, ApJ, 315, 621 (B87)
Churchwell, E., Wood, D., Myers, P. C., & Myers, R. V. 1986, ApJ, 305, 405
Cummins, S. E., Linke, R. A., & Thaddeus, P. 1986, ApJS, 60, 819
Dickinson, D. F., & Rodriguez Kuiper, E. N. 1981, ApJ, 247, 112
Ellison, B. N., Schaffer, P. L., Schaal, W., Vail, D., & Miller, R. E. 1989, Int. J. Infrared Millimeter Waves, 10, 8
Gérin, M., Viala, Y., Pauzat, F., & Ellinger, Y. 1992, A&A, 266, 463
Gottlieb, C. A., Ball, J. A., Gottlieb, E. W., Lada, C. J., & Penfield, H. 1975, ApJ, 200, L147
Greaves, J. S., & White, G. J. 1991, A&AS, 91, 237
Groesbeck, T. D. 1994, Ph.D. thesis, California Inst. Technol.
Groesbeck, T. D., Phillips, T. G., & Blake, G. A. 1994, ApJS, 94, 147
———. 1996, in preparation
Jewell, P. R., Hollis, J. M., Lovas, F. J., & Snyder, L. E. 1989, ApJS, 70, 833
Johansson, L. E. B., et al. 1984, A&A, 130, 227 (J84)
Kuiper, T. B. H., Zuckerman, B., Kakar, R. K., & Rodriguez Kuiper, E. N. 1975, ApJ, 200, L151
Lovas, F. J. 1992, J. Phys. Chem. Ref. Data, 21, 181
Mangum, J. G., & Wootten, A. 1993, ApJS, 89, 123
Martín-Pintado, J., Bachiller, R., & Fuente, A. 1992, A&A, 254, 315
Mauersberger, R., Henkel, C., & Wilson, T. L. 1988, A&A, 205, 235
Menten, K. M., Melnick, G. J., & Phillips, T. G. 1990, ApJ, 363, 27
Pearson, J. C., Sastry, K. V. L. N., Herbst, E., & De Lucia, F. C. 1994, ApJS, 93, 589
Penzias, A. A., & Burrus, C. A. 1973, ARA&A, 11, 51
Poynter, R. L., & Pickett, H. M. 1985, Appl. Opt., 24, 2235
Serabyn, E., & Weisstein, E. W. 1995, ApJ, 451, 238
Schilke, P., Benford, D. J., Hunter, T. H., Lis, D. C., Phillips, T. G., & Serabyn, E. 1996a, in preparation
Schilke, P., Güsten, R., Schulz, A., Serabyn, E., & Walmsley, C. M. 1992b, A&A, 261, L5
Schilke, P., Walmsley, C. M., Pineau des Forêts, G., & Flower, D. R. 1996b, A&A, in press
Schilke, P., Walmsley, C. M., Pineau des Forêts, G., Roueff, E., Flower, D. R., & Guilloteau, S. 1992a, A&A, 256, 595
Sutton, E. C., Blake, G. A., Masson, C. R., & Phillips, T. G. 1985, ApJS, 58, 341
Sutton, E. C., Peng, R., Danchi, W. C., Jaminet, P. A., Sandell, G., & Russell, A. P. G. 1994, ApJS, 97, 455 (S94)
Turner, B. E. 1989, ApJS, 70, 539
———. 1991a, ApJS, 76, 617 (T91)
———. 1991b, ApJ, 376, 573
Turner, B. E., & Bally, J. 1987, ApJ, 321, L77
Wilson, T. L., & Matteucci, F. 1992, A&A Rev., 4, 1
Wootten, A., Loren, R. B., & Bally, J. 1984, ApJ, 277, 189
Ziurys, L. M. 1987, ApJ, 321, L81
Ziurys, L. M., & McGonagle, D. 1993, ApJS, 89, 155 (ZM93)
Ziurys, L. M., & Turner, B. E. 1986, ApJ, 300, L19